Analysis of the influence of influenza virus infection on tumour progression and $CD8^+$ T cell immunity

Dissertation

Zur Erlangung des akademischen Grades *doctor rerum naturalium*

Dr. rer. nat.

Der Fakultät für Biologie der Universität Duisburg-Essen

Vorgelegt von

Philine M. Steinbach

(M. Sc. Medizinische Biologie)

aus Gelsenkirchen

Essen, September 2023

Die der vorliegenden Arbeit zu Grunde liegenden Experimente wurden am Institut für Medizinische Mikrobiologie des Universitätsklinikums Essen, Universität Duisburg-Essen, unter der Leitung von Dr. Torben Knuschke durchgeführt.

Teilergebnisse der vorliegenden Arbeit wurden veröffentlicht:

Steinbach P, Pastille E, Kaumanns L, Adamczyk A, Sutter K, Hansen W, Dittmer U, Buer J, Westendorf AM, Knuschke T. Influenza virus infection enhances tumour-specific CD8+ T-cell immunity, facilitating tumour control. PLoS Pathog. 2024 Jan 25;20(1):e1011982. doi: 10.1371/journal.ppat.1011982.

Betreuung:	Dr. Torben Knuschke
Erstgutachter:	Prof. Dr. Jan Buer
Zweitgutachter:	Prof. Dr. Matthias Gunzer
Drittgutachter:	Prof. Dr. Matthias Tenbusch
Vorsitzende des Prüfungsausschusses:	Prof. Dr. Katharina Fleischhauer
Tag der mündlichen Prüfung:	28.02.2024

“Interesting reaction… But what does it mean?”

Jack Skellington

The Nightmare Before Christmas

Table of contents

Zusammenfassung/Summary

Zusammenfassung

Trotz intensiver Forschung zählt Krebs zu den häufigsten Todesursachen weltweit, mit stetig steigenden Inzidenzen. Ebenso stellen Infektionen mit dem Influenza A Virus (IAV) eine erhebliche Bedrohung für die globale Gesundheit dar. Sowohl Influenza als auch Krebs sind einzeln betrachtet gut erforscht. Trotzdem sind die gegenseitigen Wechselwirkungen der beiden Krankheiten noch immer nicht vollständig verstanden. Daher ist es von großer Bedeutung, den Einfluss von Infektionen auf den Verlauf einer Tumorerkrankung und die Modulation der Tumorumgebung zu untersuchen, um neue Strategien für zukünftige Therapien zu entwickeln.

Um den gegenseitigen Einfluss einer IAV Infektion und Krebs zu untersuchen, wurden B16 Melanomzellen, bzw. CT26 kolorektale Krebszellen subkutan in Mäuse transplantiert, die daraufhin intranasal mit IAV infiziert wurden. Entgegen der Erwartung war das Tumorwachstum nach einer IAV Infektion signifikant langsamer, als bei nicht-infizierten Mäusen. Dies deutet auf eine Modulation der antitumoralen Antwort durch die Infektion hin. Die Depletion von natürlichen Killerzellen und Makrophagen zeigte, dass diese Populationen des angeborenen Immunsystems für den antitumoralen Effekt entbehrlich sind. $CD8^+$ T Zellen hingegen trugen entscheidend zur Einschränkung des Tumorwachstums bei, wie entsprechende Depletionsversuche zeigten. Durchflusszytometrische Analysen zeigten, dass tumorspezifische $CD8^+$ T Zellen nach IAV-Infektion ein stärker aktiviertes und proliferierendes Profil im Tumor aufwiesen. Dies wird durch die vermehrte Expression von Aktivierungs- (CD43, Granzym B) und Proliferationsmarkern (Ki67) deutlich. Zusätzlich waren hemmende Marker, die einen dysfunktionalen Zustand der T Zelle widerspiegeln, in Tumoren von infizierten Mäusen verringert, verglichen mit nicht-infizierten Mäusen.

Weitere Analysen ergaben, dass die Migration dieser tumorspezifischen $CD8^+$ T Zellen dabei eine Rolle zu spielen scheint. Um dies zu überprüfen, wurde ein adoptiver Zelltransfer von genetisch markierten tumorspezifischen $CD8^+$ T Zellen durchgeführt. Die Zellen wurden in Empfängermäuse transferiert, die sowohl einen Tumor trugen als auch mit IAV infiziert waren. Dieser Versuch bestätigte die Migration der tumorspezifischen $CD8^+$ T Zellen nicht nur in den Tumor, sondern auch in die infizierte Lunge, in der wegen der Infektion ein stark proinflammatorisches Milieu

herrschte. Diese starke Migration war nach dem Transfer in nicht-infizierte Mäuse nicht nachweisbar. Die Anwendung des Lymphozyten-Migrationsinhibitor FTY720 zeigte zudem, dass eine *de novo* Infiltration des Tumors durch $CD8^+$ T Zellen für den IAV-induzierten antitumoralen Effekt notwendig ist.

Zusammenfassend zeigt die vorliegende Arbeit, dass eine Influenzavirus Infektion einen potenziell schützenden Einfluss auf Krebs haben kann, indem sie die antitumorale $CD8^+$ T Zell Antwort effektiv verstärkt.

Summary

Currently, cancer is one of the leading causes of death worldwide and incidences continuously increase even further. Likewise, influenza A virus (IAV) infections are a substantial threat to global health. Although both diseases are highly studied individually, the interactions of immune responses towards cancer and infections are still not fully understood. Therefore, it is important to study the impact of infections on tumour development and the modulation of the tumour microenvironment, in order to derive new strategies for future therapies.

To investigate the mutual influence of IAV and cancer, B16 melanoma or CT26 colorectal cancer cells were subcutaneously transplanted into mice, which were then intranasally infected with IAV. Unlike expected, tumour growth was significantly slower upon IAV infection compared to non-infected mice, indicating a modulation of the anti-tumour response by the infection. Depletion of natural killer cells and macrophages demonstrated that these cells of the innate immune system are dispensable for the observed antitumoural effect whereas diminished inhibition of tumour growth correlated with $CD8^+$ T cell depletion, indicating the importance of this population. Flow cytometric analysis indeed indicated that tumour-specific $CD8^+$ T cells had an enhanced activation and proliferation phenotype upon IAV infection, as indicated by increased expression of the activation or proliferation markers CD43, granzyme B and Ki67. At the same time, inhibitory receptors reflecting T cell exhaustion were decreased on $CD8^+$ T cells in tumours of infected mice compared to those of non-infected mice.

Subsequent analysis revealed, that the migration of those tumour-specific $CD8^+$ T cells seems to be important. The adoptive cell transfer of congenically marked tumour-derived $CD8^+$ T cells into recipient IAV infected tumour-bearing mice verified the migration of tumour derived $CD8^+$ T cells into the tumour as well as into the infected lung, where a strong pro-inflammatory milieu prevailed. At the same time, this elevated migration of the transferred $CD8^+$ T cells was not detectable in non-infected tumour-bearing mice. Further, the application of the lymphocyte egress inhibitor FTY720 demonstrated, that *de novo* infiltration of the tumour by $CD8^+$ T cells is necessary for the IAV induced antitumoural effect. In summary, this study shows what potentially protective influence an IAV infection can have during cancer by effectively enhancing the antitumour $CD8^+$ T cell response.

1 Introduction

Every day, we are facing multiple immunological challenges, not only in form of pathogens, encountering our bodies from outside (“non self”), but also in form of malignant cells (“altered self”). The immune system has hence evolved to fight this enormous variety of foreign invaders, forming an intricate network to eliminate these kinds of challenges.

1.1 The immune system

The human immune system comprises two stages of immune responses: The evolutionary older innate immediate immune response, followed by a long-lasting adaptive immune response.

1.1.1 Innate and adaptive immune system

The first line of defence against pathogens is carried out by the innate immune system, which comprises barriers like the closed surface of the human skin and mucous membranes, supported by chemical barriers like the low pH in the stomach as well as cellular and humoral immune responses. Cellular components are phagocytic macrophages, dendritic cells (DCs), mast cells, natural killer (NK)-cells and neutrophil, basophil and eosinophil granulocytes. Antibodies form the humoral part of the innate immune system. Further soluble factors are interferons (IFNs) along with the complement system, chemokines and cytokines [1].

The innate immune system does not act in a specific manner. When a pathogen overcomes the physical barriers, tissue resident immune cells of the respective area of infection sense this pathogen, become activated and release cytokines. This leads to vasodilation, and therefore local temperature increase, and inflammation which in turn recruits further immune cells [2]. These immune cells recognise pathogen-associated molecular patterns (PAMPs) *via* pattern recognition receptors (PRRs). PRRs comprise for example nucleotide-binding oligomerization domain (NOD)-like receptors, retinoic acid-inducible gene I (RIG-I)-like receptors or Toll-like receptors (TLRs). TLRs are expressed on the cell membrane (TLR1,2,4,5 and 6) or in the cytosol (TLR3,7,8 and 9). TLR binding triggers mostly MyD88-dependent signalling, which *via* NF-κB or IRFs subsequently leads to the release of pro-inflammatory cytokines such as type I IFNs [3].

IFNs are produced by immune cells but also by virus-infected cells among others. There are three types of IFNs: type I, II and III. Type I IFNs are further divided into subtypes, including IFN-α and IFN-β which are the best described type I IFNs. Type II IFN is IFNγ and type III IFNs are different IFNλ subtypes. IFN-α and IFN-β both bind to IFN-alpha-receptor (IFNAR), whereas IFNγ and IFNλ target individual receptors, IFNγ-receptor and IFNλ-receptor respectively. IFNs act *via* the Janus kinase-signal transducer and activator of transcription proteins (JAK-STAT) pathway, causing an antiviral status of the infected cell and neighbouring cells. IFN-α is produced by leukocytes in general but the main producers in infection are plasmacytoid DCs. IFN-β is mainly produced by fibroblasts and IFNγ solely by NK-cells and T cells [4-6].

Upon infection, epithelial cells further produce chemokines such as CC-chemokine ligand (CCL)-2 to recruit additional cells of the immune system. Following phagocytosis, DCs and macrophages can present foreign antigens on their major histocompatibility complex (MHC) class II as professional antigen presenting cells (APCs). Infected cells can present foreign antigens *via* their MHC I.

The innate immune response reacts to an invading pathogen within a few hours. A response specific to the pathogen by the adaptive immune response develops over days but is then long-lasting, because it can form an immunological memory. The adaptive immune system consists of B and T cells and their effector molecules.

In human adults, a primary B cell repertoire is produced in the bone marrow. Naïve B cells leave the bone marrow and circulate *via* the bloodstream until they enter lymphoid organs in a chemokine-driven manner. There they are activated by follicular T helper cells. In the second phase of a B cell response, some of these activated B cells migrate into B cell follicles for maturation. The centre of these B cell follicles is the germinal centre (GC). Here, antigen-activated B cells undergo affinity maturation *via* somatic hypermutation, selection for adequate antigen binding and finally differentiation into effector B cells (plasma cells) or memory B cells [7]. Memory B cells are long-lived and express the same B cell receptor (BCR) as their parent cells. Plasma cells are short-lived and survive only for a few days. They secrete their BCRs, which are then called antibodies. This antibody production is highly efficient: Estimates go up to 2,000 antibody molecules per second [2].

T cells can either directly kill infected or malignant cells as cytotoxic T lymphocytes (CTLs) or regulate further immunologic reactions as T helper cells or anti-inflammatory regulatory T cells (Tregs). T cells are further characterised in the following section.

1.1.2 T cell immunology

As one central part of the adaptive immune system, T cells play an important role in immune reactions to both, cancer and infections. They are divided into T helper cells which are positive for cluster of differentiation (CD)4 and CTL which are positive for CD8.

1.1.2.1 T cell activation

For full T cell activation, three signals are necessary (Figure 1-1):

Signal 1: Stimulation of the T cell receptor (TCR),
Signal 2: Co-stimulation and
Signal 3: Cytokines.

T cells require APC-mediated antigen presentation to their TCR because they cannot bind antigens directly (signal 1). Co-stimulation (signal 2) is required for survival and cytokine stimulation (signal 3) is required for differentiation. Co-stimulation occurs through CD3 and CD28 on T cells. These are triggered by CD80 and CD86 on APCs and binding enables TCR signalling [8, 9]. When this second signal of co-stimulation is missing, T cells become anerg, which is a state of non-responsiveness to prevent auto-reactivity. The third signal of cytokine stimulation can also be performed by other immune cells including $CD4^+$ T cells, which are therefore also called helper T cells (T_H).

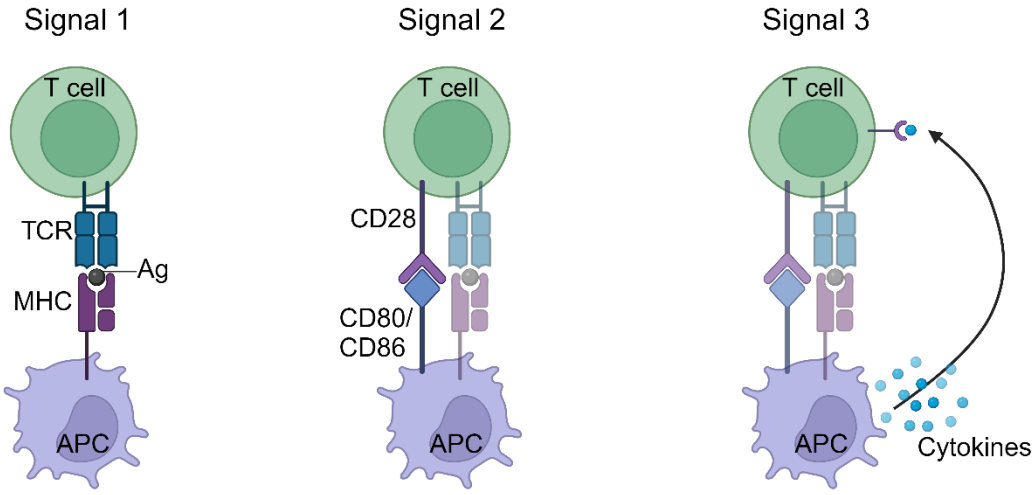

Figure 1-1 T cell activation by antigen-presenting cells.

T cell activation requires three signals: TCR-stimulation (signal 1), co-stimulation (signal 2) and cytokine stimulation (signal 3). These enable antigen-specificity, survival and differentiation respectively. Figure originally from [10], adapted.

For $CD4^+$ T cell activation, presentation *via* MHC II-molecules on APCs like DCs, macrophages or B cells is required [1]. Depending on the cytokine exposition, naïve $CD4^+$ T cells (T_H0) can differentiate into different $CD4^+$ T cell subsets, which are defined by their respective cytokine expression. Most prominent are the T_H1, T_H2, Tregs, T_H9, T_H17 and follicular T helper cell (T_fH) subsets. The pro-inflammatory T_H1 cells are defined by production of IFNγ and further pro-inflammatory cytokines, supporting CTL, macrophage and NK-cell function. T_H2 cells assist B cell differentiation and are characterised by Interleukin (IL)-4 and IL-10 production among others. Tregs have anti-inflammatory properties and express CD25 as well as the transcription factor Forkhead box P3 (FoxP3). These $CD4^+$ $CD25^+$ $FoxP3^+$ Treg cells account for about 10 % of peripheral $CD4^+$ T cells [11]. Tregs often release IL-10 and transforming growth factor-β (TGF-β). Either Tregs can develop in the thymus (natural Tregs) or in the periphery from T_H0 cells (induced Tregs). T_H17 cells act pro-inflammatory and characteristically produce high amounts of IL-17. An overview of different T cell subsets, their functions and cytokines are summarized in Table 1.

Table 1 $CD4^+$ T cell subset characterizations.

$CD4^+$ T cell subset	Lineage-inducing cytokines	Function	Secreted cytokines
T_H1	IL-12, IFNγ	Cellular immune responses ↑; Macrophage activation; CTL proliferation↑; Protection against intracellular pathogens	IFNγ, IL-2, TNF-α
T_H2	IL-4	Humoral response ↑; B cell activation; Protection against extracellular pathogens	IL-4, IL-5, IL-6, IL-13
T_H17	TGF-β, IL-6	Protection at and maintenance of mucosal surfaces; Enhancement of neutrophil responses; Involvement in auto-immune reactions	IL-17A, IL-17F, IL-21, IL-22, IL-26
TfH	IL-6, IL-21	Formation + function of GC; B cell promotion (antibodies + memory B cell formation)	IL-6, IL-10, IL-12, IL-21
T_H9	TGF-β, IL-4	Protection against helminth infections and other inflammatory scenarios	IL-9, IL-10
T_H22	IL-6, TNF-α	Protection against microbes in the skin	IL-13, IL-22, TNF-α
Tregs	TGF-β1, IL-2	Immunosuppression	IL-10, TGF-β, IL-35, IL-9

$CD8^+$ T cells are CTLs and require antigen presentation *via* MHC I-molecules. Upon successful activation, CTLs release cytotoxins: perforin and granulysin which have lytic properties and permeabilize the target cell membrane and granzymes which activate the caspase cascade, resulting in target cell apoptosis. This target cell apoptosis is

additionally achieved in a Fas-mediated manner, so by direct cell-cell interaction. CTLs can be directed against malignant or virus-infected cells; MHC I-molecules can present foreign antigens of either origin. Therefore, almost all body cells express MHC I so that they can be potentially targeted by CTLs. The effector functions are explained in more detail in the following section.

1.1.2.2 T cell effector functions

Following successful stimulation, a T cell focuses on a specific target cell based on the antigen expression of the target cell. As indicated in section 1.1.2.1, there are three classes of effector T cells: CTLs which are $CD8^+$ and T_H1 and T_H2 cells which are both $CD4^+$. T_H1 cells activate macrophages to initiate phagocytosis and B cells to initiate production of different immunoglobulin G (IgG) subclasses, i.e. certain types of antibody subtypes. T_H2 cells induce B cell differentiation to produce all other types of immunoglobulins. When binding to the MHC:peptide complex, the TCR molecules and co-receptors cluster at that site. This clustering evokes a polarization of the T cell. This leads to the release of effector molecules towards the target cell which makes the T cell effects highly specific for the respective target cell and thereby does not affect surrounding cells [1]. As previously mentioned, CTLs act *via* cytotoxins. Since they are stored in granules, these cytotoxins act only after their release. Perforins polymerize and finally form pores into target cell membranes. With the loss of an intact membrane integrity, extracellular substances like water and salts enter the cell, leading to rapid cell death [12]. Granzymes belong to the family of serine proteases. They activate apoptosis in the target cell when reaching the cytoplasm by cleavage of proteins there. Granzyme B for example can cleave CPP-32, which is a caspase and therefore initiates an apoptosis pathway [13]. The apoptotic target cells are phagocytosed by nearby phagocytic cells, and therefore usually do not cause an inflammation. CTLs and T_H1 cells also express Fas ligand (FasL). FasL binds Fas on the target cell. This ligation leads to caspase activation, i.e. induces target cell apoptosis. Also activated lymphocytes express Fas so that the immune reaction can be terminated *via* this pathway once the pathogen is cleared [14].

Activated effector T cells show a distinct activation profile. One example is the dynamic expression of CD43, which is a transmembrane protein involved in co-stimulation of T cells [15, 16]. Therefore, increased CD43 expression mirrors T cell activation, similar to Granzyme B expression [17]. Proliferation is marked for example by expression of Ki67, a marker which is present in proliferating cells but absent in resting cells [18].

When an infection is cleared, 90 – 95 % of T cells die by apoptosis and the remaining 5 – 10 % of $CD4^+$ or $CD8^+$ T cells can develop into memory T cells to enable a faster recurrence in re-infection [19]. On the other hand, in a chronic infection or cancer, CTLs are driven into an exhausted status, to prevent immunopathology by an overshooting immune response [20, 21]. This state is explained in more detail in the following.

1.1.2.3 T cell exhaustion

Exhausted T cells develop upon overstimulation by constant TCR triggering. This observation was first made in chronic lymphocytic choriomeningitis virus (LCMV) infection but has since been seen in many further infections and diseases such as human immunodeficiency virus (HIV), hepatitis B virus (HBV) or hepatitis C virus (HCV) infection or in cancer [22]. T cell exhaustion is a step-wise process. Firstly, cells lose their capacity to highly proliferate and to produce cytokines. Cytokine production loss is successive. For example, tumour necrosis factor (TNF) production is lost at an intermediate stage and IFNγ production is diminished at a later exhaustion step (reviewed in [23]). The progressive loss of function results in different stages of T cell exhaustion: progenitor, intermediate, effector and terminally exhausted T cells, which stop proliferation and then also co-express inhibitory receptors [24, 25]. In parallel, exhausted T cells show epigenetic reprogramming throughout their exhaustion progress, driven by expression of the transcription factor Thymocyte Selection Associated High Mobility Group Box (TOX) [26]. This challenges therapeutic manipulation of T cell exhaustion [27, 28]. Exhausted T cells are dysfunctional, but not fully inert and may still contribute to virus or tumour control. However, they are strongly limited in their efficacy so that an immune balance can be re-established [20, 24]. Figure 1-2 describes this process and the change in expression patterns. T cells with a high expression of Programmed Cell Death Protein 1 (PD-1) in combination with T cell immunoglobulin mucin-3 (TIM-3) expression have been described to be highly dysfunctional T cells, whereas T cells with an intermediate PD-1 expression, lacking TIM-3 have been attributed more functional [29].

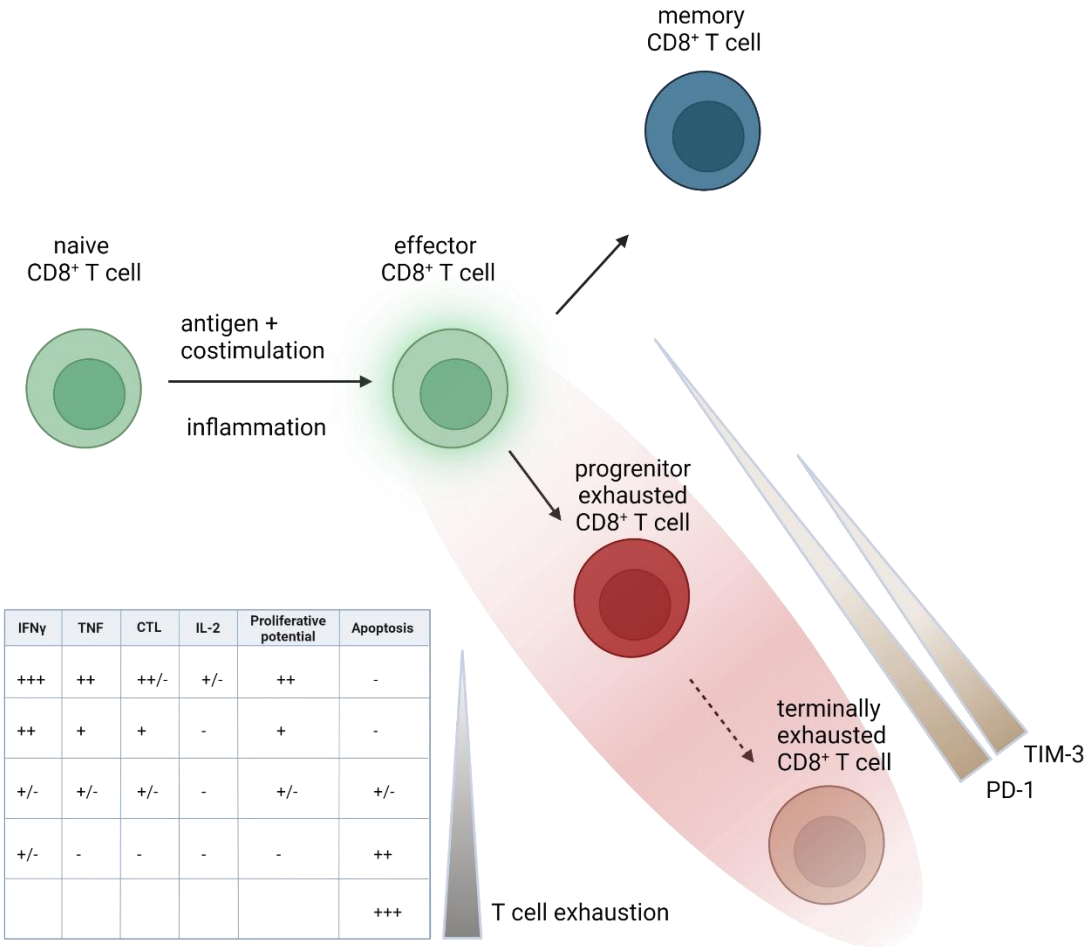

IFNγ	TNF	CTL	IL-2	Proliferative potential	Apoptosis
+++	++	++/-	+/-	++	-
++	+	+	-	+	-
+/-	+/-	+/-	-	+/-	+/-
+/-	-	-	-	-	++
					+++

Figure 1-2 T cell exhaustion.

When a naïve CD8⁺ T cell is initially primed by antigen and co-stimulation it differentiates into an effector T cell. In an acute infection, the antigen is cleared over time and memory CD8⁺ T cells form. In a chronic infection, the antigen persists or even accumulates. This drives the T cell into different stages of dysfunction. IFNγ and TNF production decrease as well as the cytotoxic and proliferative potential. Figure originally from [23], adapted.

Exhausted T cells resemble the previously mentioned anerg T cells that arise when co-stimulation during T cell activation is absent. Both statuses are characterised by non-responsiveness but differ in the development of the T cell: Exhausted T cells arise from previously activated effector T cells whereas the dysfunctional state of anergy arises in naïve T cells. Therefore, the two statuses are two different phenomena. Both were long thought to be irreversible statuses, but an increasing number of studies finds that terminally exhausted T cells can be re-activated under specific conditions [30].

1.2 Tumour immunology

A tumour forms as a result of a malignant cell that escapes the immune system. A malignant cell is defined by uncontrolled growth [31]. The following sections deal with the formation of a tumour and cancer and how the immune system reacts to this challenge.

1.2.1 Tumour and cancer development

Cancer development requires multiple steps. When a cell gains mutations and proliferates in an uncontrolled manner, it becomes malignant. Most malignant cells are recognised and cleared by the immune system, but if a malignant cell evades the immune system, it can proliferate to finally form a tumour. Any abnormal proliferation is referred to as tumour [32]. Therefore, a tumour can *per se* be benign, for example skin warts, or malignant if it invades other tissues. The latter one is referred to as cancer. Since all kinds of dividing cells can mutate, there is a wide variety of types of resulting cancers. Mutated epithelial cells form carcinomas (90 % of human cancers), solid tumours of connective tissues are called sarcomas, blood-forming cells can rise to leukaemia and cancer from cells of the immune system are referred to as lymphomas [33].

In 2000, Hanahan and Weinberg defined eight hallmarks of cancer:

- Genome instability and mutation,
- sustained proliferative signalling,
- growth suppressor evasion,
- cell death resistance,
- replicative immortality,
- inducing/accessing vasculature,
- tumour promoting inflammation,
- invasion and metastasis activation.

In 2011, they added two further hallmarks:

- deregulation of cellular metabolism and
- avoiding immune destruction.

Finally, in 2022, Hanahan proposed the two characteristics of

- non-mutational epigenetic reprogramming and
- polymorphic microbiomes

and the two hallmarks of

- unlocking phenotypic plasticity and
- senescent cells [34-36].

As described above, a tumour is initiated as the result of a genetic alteration in a single cell, leading to an exceptionally high proliferative capacity of this cell. Throughout tumour progression, further mutations accumulate within this tumour population. Cells with mutations that bring a selection advantage become predominant in the tumour population. Advantages can include faster growth or improved immune evasion. Tumours may for example secrete perforin-degrading enzymes [37] or down-regulate MHC I expression to avoid antigen presentation to $CD8^+$ T cells. However, the lack of MHC I may lead to killing by NK-cells [33].

1.2.2 Melanoma

Melanoma is a type of skin cancer that arises from melanocytes. It is not the most abundant but the most aggressive type of skin cancer. Melanocytes are the pigment-producing cells of the skin. Many risk factors can be considered in this regard but the most common cause for abnormal development of melanocytes is exposure to ultraviolet (UV) light. Incidences have been increasing over the last decades [38], presumably due to more intense UV light exposure on holidays [39]. Although incidences still rise, death rates start declining as treatment options and especially awareness and therefore early recognition improve [40].

1.2.3 Immune response towards melanoma

For an effective immune response, the immune system has to recognize the tumours. Since the malignant cells derive from physiological body cells, the immune system has to be able to recognize them as “altered self”. Tumours often develop a tumour microenvironment (TME) of immunosuppressive nature to evade immune mechanisms.

The melanoma TME is highly heterogeneous. Despite the malignant tumour cells, a variety of immune cells infiltrate the TME, including cells of the innate immune system, like macrophages, dendritic cells or NK-cells, as well as B and T cells of the adaptive immune system but also soluble factors like cytokines, chemokines and interferons [41]. These cells can be of pro-inflammatory nature, like CTLs, or immunosuppressive, like Tregs. The high lymphocyte infiltration characterizes melanoma as an immunogenic tumour [42]. T cells migrate into the tumour as tumour-infiltrating

lymphocytes (TILs). The specific TME differs in individual patients. In this context, a higher TIL-density correlates with better clinical outcome [41, 43]. Additionally, the TME comprises non-immunogenic cells like fibroblasts or endothelial cells [44]. All these different cell types and the molecules and paracrine factors released make the TME an intricate network with both pro- and anti-inflammatory properties and interactions. This results in a complexity of the TME which is still not fully understood to date [42]. This dense intertwining however shows that the immune responses can be altered by another immunologic challenge like an infection.

The TME can act suppressive on immune cells including T cells for example by upregulating inhibitory signalling. Tumour cells can upregulate PD-L1, the ligand for PD-1 on T cells. Blocking this ligation is one therapeutic option, which is often used in melanoma treatment, among other therapy options. Based on their gatekeeping function in immune response, PD-1 and other inhibitory receptors are referred to as “immune checkpoints”. The therapy based on blocking these receptors is therefore called “immune checkpoint blockade” (ICB). For PD-1 it can be directed either against PD-1 on T cells or its ligand PD-L1 on tumour cells [45].

1.3 Virus

Viruses are obligate intracellular pathogens because they are not able to replicate on their own. All viruses consist of at least nucleic acids, either RNA or DNA, proteins and partly lipids. Upon entry into the host cell, viral proteins interact with the host cell replicative system to produce new virions. Some viruses kill the host cells as part of their viral replication (cytolytic cycle) and some only change the function of the cells (lysogenic cycle), which both can consequently cause diseases.

1.3.1 Influenza virus

The influenza virus is one of the most common pathogens of the respiratory tract, infecting 10 % of the global population annually [46] and leading to up to 650,000 annual deaths [47]. Transmission occurs *via* droplets, usually of >5 µm, or smear infection [48]. After a short incubation time of 1-2 days, infection causes respiratory symptoms including cough, rhinitis and a sore throat. Further symptoms are fever, muscle and joint pain, malaise and headache [47, 48]. In severe courses, the influenza virus itself or a bacterial superinfection can lead to pneumonia, which may develop to a sepsis and organ failure. Patients may die from these complications (e.g. in the severe season 2012/13) whereas in years with mild seasons (e.g. season 2013/14), no excess influenza-associated mortality was detected in Germany [49]. A vaccine is available but the high variability of the influenza virus impels annual renewing of vaccination. Different mechanisms of vaccines are available. The most widely used vaccine in western countries is an inactivated one [50].

Influenza viruses belong to the family of Orthomyxoviridae. They comprise four types: Influenza A (IAV), B, C and D. The seasonal epidemics each year are caused by type A and B. Worldwide pandemics have only been caused by type A. Examples are the “Spanish flu” (subtype H1N1) 1918/1919, the “Asian flu” (subtype H2N2) 1957/1958, the “Hong Kong flu” (subtype H3N2) 1968/1969 and the “Swine flu” (subtype H1N1) 2009/2010. Influenza C virus causes only mild symptoms in humans, and influenza D virus infects mainly cattle but so far not humans [51].

The influenza virus genome consists of 8 negative sense RNA segments that encode for 11 viral genes, which in turn encode for 13 proteins due to different splicing [52]. The proteins and their roles are listed in Table 2 in the next section. The segmented nucleocapsid lies within a viral envelope. In this viral envelope, there are glycosylated surface proteins: hemagglutinin (H or HA) which is required for binding to sialic acids

(SA) on the target cell and neuraminidase (N or NA), needed for the release of newly produced virions. The structure is depicted in Figure 1-3. Based on the receptor expression alveolar epithelial cells (AEC) act as the primary target cells. Infection hence causes alveolar epithelial injury, which can impair the functionality of gas exchange.

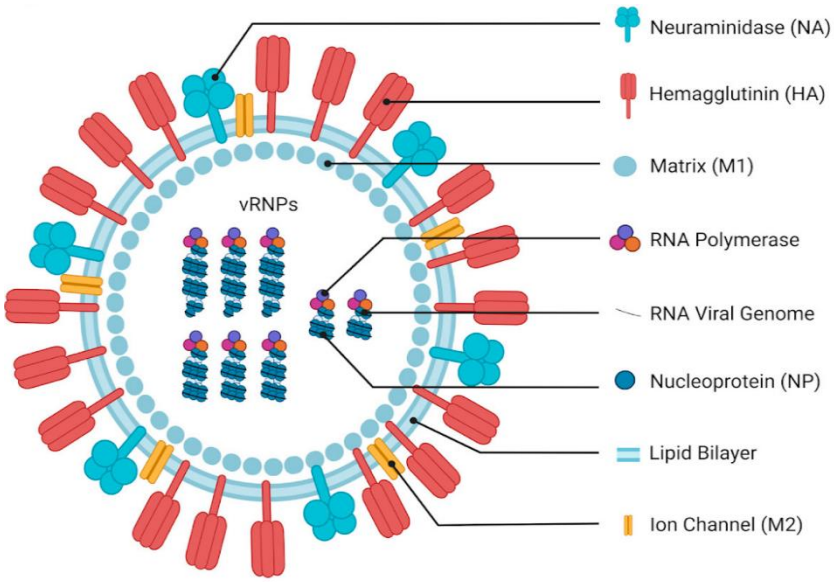

Figure 1-3 Schematic structure of an influenza virion.

Influenza A viruses comprise 8 RNA segments which form the viral genome. These are surrounded by an inner surface envelope, formed by the M1 protein and a lipid bilayer which forms a viral envelope. Figure adapted from [53].

To date, 18 different HA and 11 different NA subtypes are known [54], enabling large antigenic variations. Human influenza viruses comprise H1, H2, H3 and N1 and N2, the remaining subtypes are mostly avian influenza viruses [55]. The respective HA and NA expression define the Influenza A subtype. If an individual is infected with more than one influenza subtype at the same time, the different HA and NA proteins can re-assort in different combinations. This is referred to as antigenic shift. Antigen alteration by point mutations of the viral genome due to bad fidelity of RNA transcription is referred to as antigenic drift. These high variations enforce an annual adaption of the influenza vaccine.

1.3.2 Influenza A virus infection route

During an influenza A virus infection the host cells are invaded and the host cell machinery is undermined by the incoming influenza virus, to produce new virions. The processes of host cell entry and virus replication are described in more detail in the following and depicted in Figure 1-4.

Host cell entry begins with interaction of viral HA with sialic acids expressed on distinct host cells. The virus enters *via* receptor-mediated endocytosis into an endosomal vesicle. The acidic milieu in the endosome leads to a conformational change resulting in fusion of viral and endosomal membrane. The low pH promotes further conformational changes resulting in an acidification of the viral core. This in turn enables a first exposition of viral proteins to the host cell cytoplasm. The proteins exposed to the cytoplasm contain nuclear localization signals so that translocation into the nucleus can occur using the host cell nuclear import machinery [56]. Although untypical for RNA-viruses, influenza genome replication occurs in the host cell nucleus. The viral journey from cell-membrane binding until translocation into the nucleus takes about 1 h [51].

In the host cell nucleus, viral transcription and replication takes place. Nuclear export of the newly produced viral mRNAs is orchestrated by both, cellular proteins and viral components. The different proteins assemble subsequently. Initial budding structures form, the membrane starts budding and encloses the nucleocapsids that are then released to the surface. Table 2 explains in detail which steps of infection are performed by which virally encoded proteins.

Host specificity of different influenza viruses is determined by the capability to bind to different sialic acids in the initial step of cell binding. Sialic acids are linked to carbohydrates in glycoproteins. In different sialic acids, these linkages are at different positions. Depending on the specificity of the HA protein, influenza virus binds either to α(2,3) (avian and equine viruses) or α(2,6) (human) sialic acids. Swine influenza viruses can bind both types, therefore avian and human influenza viruses can mix in swine to highly infectious pathogenic viruses [52].

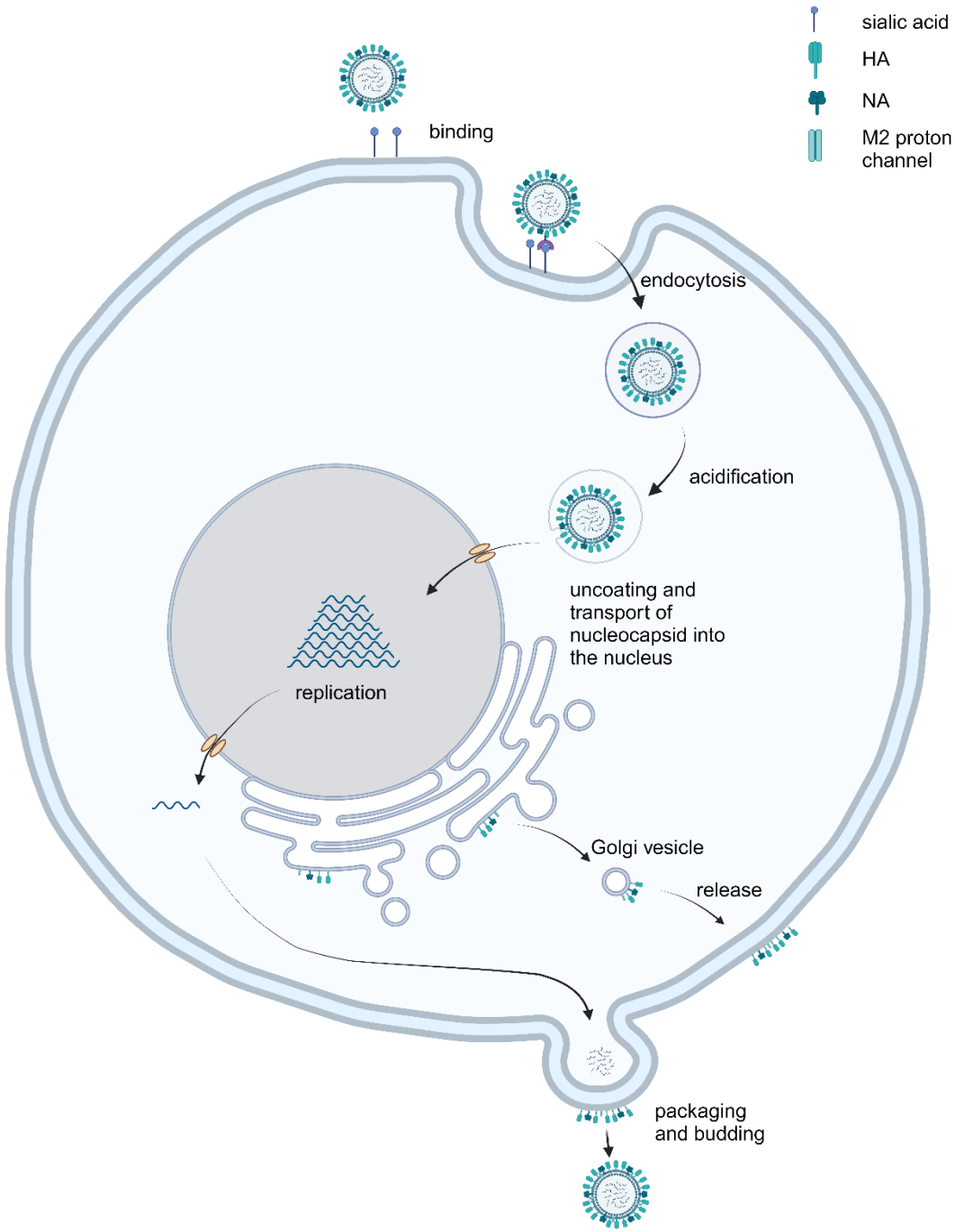

Figure 1-4 Influenza virus life cycle.

The influenza virus can bind *via* its HA proteins to sialic acids on the cell membrane of the target cell. The virus then enters *via* receptor-mediated endocytosis into an endosome with an acidic pH. The low pH enables conformational changes so that fusion peptides are exposed and the M2 ion channel opens, both of which are required for translocation of viral ribonucleoprotein (vRNP) into the host cell cytoplasm. The viral proteins have nuclear localization signals and therefore enter the nucleus. In the nucleus, the viral genome is transcribed and replicated. vRNPs are exported from the nucleus presumably *via* nuclear pores [52]. Finally, viral particles are formed and the newly formed virions leave the cell by budding. The budding enables that the host cell membrane is used for the virus envelope. HA = hemagglutinin, NA = neuraminidase. Figure originally from [51], adapted.

Table 2 IAV proteins and their functions in pathogenesis.

Table adapted from [57].

IAV Protein	Primary viral function
NP	–Nucleocapsid protein which provides virion structure
	–Mediates genome replication through RNA binding activity
NS1	–Antagonises host IFN response
	–Mediates vRNA synthesis, mRNA splicing and translation
NS2 (NEP)	–Mediates export of viral RNA from the nucleus to the cytoplasm
PA	–Part of the RNA polymerase complex, required for RNA synthesis
PB1	–Part of the RNA polymerase complex, required for RNA synthesis
PB2	–Part of the RNA polymerase complex, required for RNA synthesis
PA-X	–Impairs cellular host gene expression
PB1-F2	–Intrinsically induces apoptosis
PB1-N40	–Currently unclear
NA	–Cleaves sialic acid to release viral progeny
HA	–Mediates host cell entry by binding membrane receptors
M1	–Provides structure and stability to the virion
M2	–Ion channel which aids viral assembly and budding

1.3.3 Immune response towards influenza infection

Most influenza infections are mild, meaning that they are resolved by the immune system and severe tissue damage is prevented by the simultaneously initiated tissue repair and regeneration. In severe cases, an exuberant host response can be detrimental for the host. Bronchiolitis and alveolar edema seem to be linked to an excess of pro-inflammatory cytokines, the so-called “cytokine storm”, rather than to the virus infection itself (reviewed in [58] and [59]). This excess cytokine release is mainly coordinated by the influenza target cells, the AECs [60]. After AEC infection, the virus can spread to further cells, including alveolar macrophages among others. During the viral life cycle, the infected cells die by apoptosis and necrosis. Infected and dying cells release pro-inflammatory cytokines and chemokines leading to an acute inflammation. In consequence, the blood flow increases and further leukocytes are recruited. As these cells again release cytokines and chemokines, a self-amplifying circle arises. Finally, the cytokine storm leads to the above described tissue damages. Multi-organ dysfunctions occur when the inflammatory cytokines and chemokines spill into the

circulation and therefore become systemic [61]. For example, the severity of the 1918 "Spanish flu" pandemic was determined by the severity of the cytokine storm [61, 62].

IAV infection causes strong innate and adaptive immune responses. The receptors of the innate immune system recognizing IAV infection are PRRs like RIG-I and TLR 3 & 7. The resulting signalling leads to an antiviral state of the infected and surrounding cells as described in section 1.1.1. Especially type I IFNs (IFNα and β) but also type III IFNs (IFNλ) are important to create antiviral responses [63]. Interferons induce the expression of Interferon stimulated genes (ISGs) that can target different steps of influenza virus replication, such as the nuclear import which is inhibited by MxA [64, 65].

For an adaptive response, APCs activate T cells in the draining lymph nodes [66]. This is mainly performed by DCs. The extent to which also alveolar macrophages migrate upon influenza infection is under debate [67]. DCs have been observed to leave the respiratory tract within the first 24 h after infection [68]. Supported by cytokines including IFNs, IL-2 or IL-12, naïve and memory $CD8^+$ T cells proliferate and differentiate into CTLs [69]. A switch in chemokine expression then enables migration to the lung at the site of infection: CCR7 expression is down-regulated and CXCR3 and CCR4 expressions are upregulated [69]. In the lung, CTLs lead to target cell lysis by release of perforin and granzymes, induce target cell apoptosis *via* FasL and additionally produce pro-inflammatory factors including IFNγ [70-72]. Like in tumours, a high $CD8^+$ T cell abundance correlates with a better outcome for the patient [73]. Expression of MHC II on epithelial cells and DCs also activates $CD4^+$ T cells, although $CD4^+$ T cell contribution to *in vivo* influenza virus clearance is modest compared to $CD8^+$ T cells [74, 75]. When naïve $CD4^+$ T cells differentiate into T_H1 cells they also express antiviral cytokines and further enhance CTLs. T_H2 cells support B cell driven immune responses but T_H1 responses are stronger than T_H2 responses in influenza infection [76]. For immune homeostasis, anti-inflammatory Tregs play an important role, restricting T_H1-responses and producing IL-10 [77, 78]. The specific T cell response is achieved within a few days upon infection [79] as depicted in Figure 1-5.

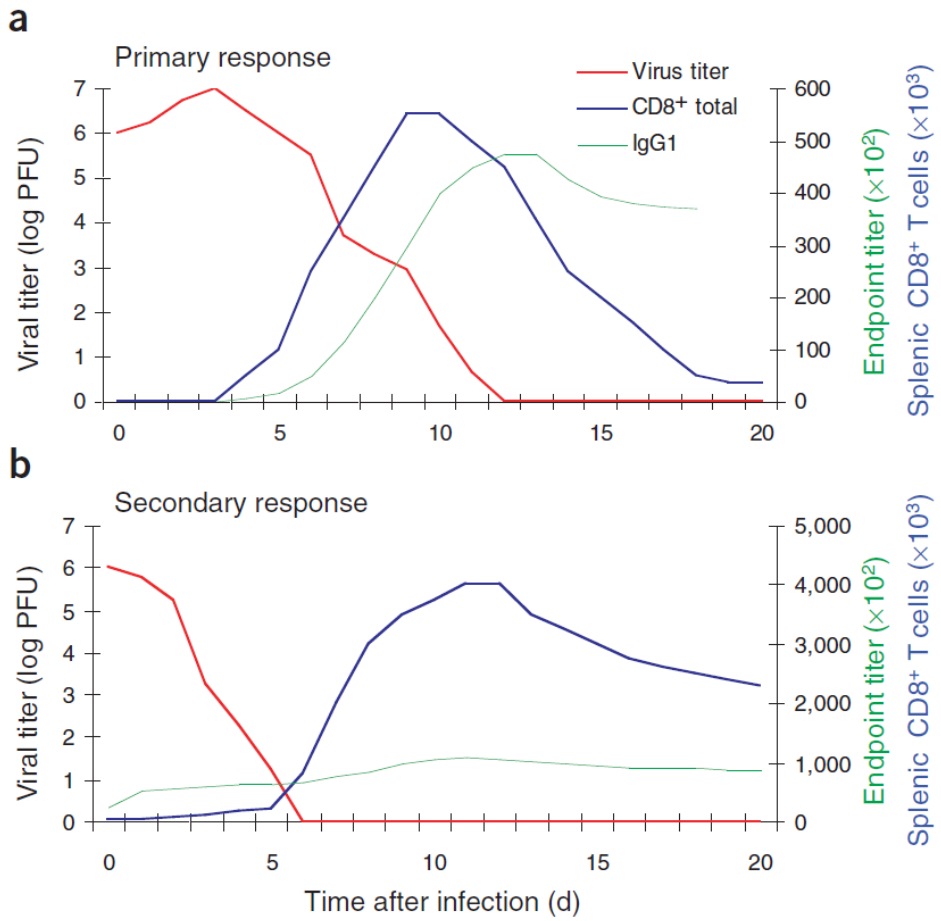

Figure 1-5 Primary and secondary response to an IAV infection.

An IAV infection provokes both antibody and T cell responses that enable viral clearance. The responses differ in primary (a) or secondary (b) infections. Immune responses are stronger in secondary infections, resulting in earlier viral clearance. PFU = Plaque Forming Units. Figure from [59].

Cells of the adaptive immune system can then stay as memory cells, however specific for epitopes of the respective strain. For heterosubtypic immunity, B cells seem to be crucial [80]. Memory $CD8^+$ T cells can reside in lymphoid tissues or non-lymphoid tissues [59]. This enables a more rapid T cell response in secondary infections, although the lungs still show high viral titres for up to 48 h after infection [81]. With the help of the faster T cell response, clearance is then achieved much earlier (Figure 1-5).

1.4 Aim of the study

The current trend of increasing melanoma rates without increasing death rates shows the clear success of melanoma and tumour research and the high potential of further advances in this field. Therefore, it is highly important to study the impact of infections on tumour development in order to optimize therapeutic strategies.

IAV causes a respiratory infection, triggering a strong inflammatory response in the lungs. It is often assumed that an influenza virus infection increases tumour progression and weakens the immune response. However, the extent to which the immune reactions triggered by IAV and melanoma influence each other has not been examined in detail.

Both tumour and influenza infection elicit effector T cell responses. In addition to this T cell response, influenza infection results in an excessive host immune response in the lung by the innate immune system, including high expression of IFNs. Alveolar macrophages are activated and NK-cells are recruited to the lung to fight virally infected cells, directly interact with the virus and activate $CD8^+$ T cell effector functions. However, how these immunological processes influence an anti-tumour immune response is still elusive.
Hence, the aim of the present study was to uncover mutual interactions and to understand the associated principles in order to be able to use the findings for future cancer therapies.

To explore the reciprocal effects of both IAV and cancer, we conducted experiments involving the transplantation of B16 melanoma or CT26 colorectal cancer cells subcutaneously in mice. Subsequently, these mice were subjected to IAV infection by administering the virus through intranasal application. One possibility to assess to what extent the anti-tumour effect is mediated immunologically is by treatment of mice with antibodies that deplete certain cell populations. The phenotype of $CD8^+$ T cells was determined using flow cytometry. To further highlight how $CD8^+$ T cells may be effectively activated, genetically marked $CD8^+$ T cells were adoptively transferred into infected and non-infected tumour-bearing mice and the application of the egression inhibitor FTY720 was included in the study.

Results obtained in this thesis will support our understanding how IAV infection modulates the anti-tumoural immune response and will reveal new possibilities for future treatment strategies.

2 Materials and Methods

2.1 Materials

All materials listed in the tables are in alphabetical order.

2.1.1 Media and Buffers

Table 3 Media and buffers

Buffer/Medium	Ingredients or manufacturer
1 × PBS-buffer pH 7.0	8 g/L NaCl 0.2 g/L KCl 1.44 g/L [Na_2HPO_4 * 2 H_2O] 0.2 g/L [KH_2PO_4]
ACK-buffer for erythrocyte lysis pH 7.2-7.4	8.3 g/L [NH_4Cl] 1 g/L [KHCO3] 200 µL/L EDTA
Dulbecco's Modified Eagle Medium (DMEM)	Gibco, Fisher Scientific Inc, Schwerte, Germany
DMEM complete (DMEMc)	DMEM 10 % FCS (v/v) 1 % Penicillin-Streptomycin (v/v) 3.6 % L-Glutamine (v/v)
FACS-buffer	1 × PBS-buffer 2 % (v/v) FCS 2 mM EDTA
Freezing medium for long-time cell storage	FCS 10 % (v/v) DMSO
Iscove's Modified Dulbecco's Medium (IMDM), GlutaMAX™	Gibco, Fisher Scientific Inc, Schwerte, Germany
IMDM complete (IMDMc)	IMDM 10 % heat-inactivated FCS (v/v) 2.5 mM β-Mercaptoethanol 100 µg/mL Penicillin/Streptomycin
Influenza medium	DMEMc 0.05 % BSA 0.2 µg/mL Trypsin

	0.1 mg/mL Gentamycin
Lung Digestion Medium	IMDM + 5 % FCS 5.6 % Collagenase D (v/v) 3.5 % DNase (v/v)
Roswell Park Memorial Institute (RPMI)	Gibco, Fisher Scientific Inc, Schwerte, Germany
RPMI complete (RPMIc)	RPMI 10 % heat-inactivated FCS (v/v), 1 % L-Glutamine 1 % Penicilline/Streptomycin
TBE-buffer	89 mM Tris 89 mM boric acid 2.53 mM EDTA

2.1.2 Enzymes and nucleic acids

Table 4 Enzymes and nucleic acids

Enzyme/nucleic acid	Manufacturer
Gene Ruler 100 bp ladder Plus	Thermo Fisher Scientific, Braunschweig, Germany
GoTaq Hot Start Polymerase	Promega, Mannheim, Germany
GoTaq 5x flexi reaction buffer	Promega, Mannheim, Germany
Collagenase D	Merck KGaA, Darmstadt, Germany
Deoxyribonuclease I (DNase I)	Merck KGaA, Darmstadt, Germany
Deoxynucleotide Triphosphate (dNTP)	Bio-Budget technologies GmbH, Krefeld, Germany
Maxima SYBR Green/ROX qPCR Master Mix (2x)	Thermo Fisher Scientific, Braunschweig, Germany
Midori Green Advance	Nippon Genetics Europe, Düren, Germany
M-MLV Reverse Transcriptase (H-) Point Mutant	Promega, Mannheim, Germany
Oligo dT Primer	Invitrogen, Karlsruhe, Germany
Proteinase K	Merck KGaA, Darmstadt, Germany

Random Hexamer Primer	Invitrogen, Karlsruhe, Germany

2.1.3 Chemicals

Table 5 Chemicals

Chemical	Manufacturer
2-Mercaptoethanol	Carl Roth GmbH & Co. KG, Karlsruhe, Germany
Ampli Taq 10x Reaktionspuffer	Applied Biosystems, Waltham, USA
AutoMACS Pro Washing Solution	Miltenyi Biotec, Bergisch Gladbach, Germany
AutoMACS Running Buffer	Miltenyi Biotec, Bergisch Gladbach, Germany
Avicel® PH-101	Merck KGaA, Darmstadt, Germany
Brefeldin A (BFA)	Sigma Aldrich, St. Louis, USA
Bovine serum albumin (BSA), Fraction V	BIOMOL GmbH, Hamburg, Germany
Crystal violet	Carl Roth GmbH & Co. KG, Karlsruhe, Germany
Dimethylsulfoxid (DMSO)	Carl Roth GmbH & Co. KG, Karlsruhe, Germany
Ethanol, absolute	Carl Roth GmbH & Co. KG, Karlsruhe, Germany
Ethylenediaminetetraacetic acid (EDTA)	Carl Roth GmbH & Co. KG, Karlsruhe, Germany
FACS Clean Solution	BD Biosciences, Heidelberg, Germany
FACS Flow Sheath Fluid	BD Biosciences, Heidelberg, Germany
FACS Rinse Solution	BD Biosciences, Heidelberg, Germany
Fetal calf serum (FCS)	Sigma-Aldrich, St. Louis, USA
Fixable viability dye eFluor780 (FVD)	eBioscience, San Diego, USA
Gentamicin solution 10 mg/mL	Sigma-Aldrich, St. Louis, USA
Heparin-Natrium-25000-ratiopharm$_C$	Merckle GmbH, Blaubeuren, Germany
Ionomycin	Sigma-Aldrich, St. Louis, USA
LE Agarose	Biozyme Scientific GmbH, Oldendorf, Germany

Matrigel Growth Factor Reduced Basement Membrane Matrix	Corning, Bedford, USA
MML V-RT 5x Puffer	Promega, Mannheim, Germany
Paraformaldehyde (PFA)	Carl Roth GmbH & Co. KG, Karlsruhe, Germany
Penicillin-Streptomycin (10,000 U/mL)	Gibco, Life Technologies, Carlsbad, USA
Phorobol 12-myristate 13-acetate (PMA)	Sigma-Aldrich, St. Louis, USA
QuantiTect Primer Assay Mm_Ifnl_1_SG	Qiagen, Hilden, Germany
Tris	Carl Roth GmbH & Co. KG, Karlsruhe, Germany
Trypan blue	Gibco, Life Technologies, Carlsbad, USA
Trypsin-EDTA solution 10x	Sigma Aldrich, St. Louis, USA
β-Mercaptoethanol	Promega, Mannheim, Germany

2.1.4 Consumables

Table 6 Consumables

Consumable	Manufacturer
96-well PCR plate (0.1 mL)	BIOplastics, Landgraaf, Netherlands
Acella 50 slides	Anvajo GmbH, Dresden, Germany
Cell strainer (40, 70 and 100 µm)	Falcon, Durham, USA
Culture plates (6-, 12-, 24-, 48- and 96- well)	Greiner BioOne, Frickenhausen, Germany
Micro reaction tubes (0.6 mL)	Biozyme Scientific GmbH, Oldendorf, Germany
Micro reaction tubes (1.5 mL)	Sarstedt, Nümbrecht, Germany
Micro reaction tubes (2 mL)	Greiner BioOne, Frickenhausen, Germany
Needle (26G x 13 mm)	BD Biosciences, Heidelberg, Germany
Opti-Seal Optical sealing sheet	BIOplastics, Landgraaf, Netherlands
Petri dish, 92 x 16 mm	Sarstedt, Nümbrecht, Germany

Pipettes (5, 10, 25 mL)	Greiner BioOne, Frickenhausen, Germany
Pipettes tips (10, 200, 1000 µL)	Sarstedt, Nümbrecht, Germany
Round bottom plates (96-well)	Greiner BioOne, Frickenhausen, Germany
Syringe sterile (1 mL, 2 mL, 10 mL)	BD Biosciences, Heidelberg, Germany
Syringe Filcons (30 µm)	BD Biosciences, Heidelberg, Germany
Strips 8 PCR tubes with cap strips (0.2 mL)	Bio-Budget technologies GmbH, Krefeld, Germany
Tubes conical (15 and 50 mL)	Greiner BioOne, Frickenhausen, Germany
Tubes round bottom (1.3 mL) FACS-tubes	Greiner BioOne, Frickenhausen, Germany

2.1.5 Primers

Primer pair sequences for mouse genotyping PCR

Table 7 Primer sequences for transgenic mice

Transgene	Sequence 5'→3'	Annealing Temperature
Rag2$^{-/-}$	GCTATTCGGCTATGACTGGGGAAG GCGATAGAAGGCGATGATGTCCCT GCAGATGGTAACAGCCTTTGTATG AGCAAGTAGC	57 °C

Murine qPCRs

Table 8 Primer sequences for qPCRs

Target gene	Sequence 5'→3'	Annealing Temperature
M1	AGGGCATTTTGGACAAAGCGTCTA TTCTAACCGAGGTCGAAACG	55 °C
Mmp9	CTTCTGGCGTGTGAGTTTCC ACTGCACGGTTGAAGCAAAGA	59 °C

Rps9	CTGGACGAGGGCAAGATGAAGC TGACGTTGGCGGATGAGCACA	58 °C
Tgfβ	ACCTGGGTTGGAAGTGGAT GAAGCGCCCGGGTTGTGTTGGTT	58 °C
Vegf	TTAGAGCTCAACCCAGACACCTGTA CCTGTGAAGCAGGGCCATAA	65 °C

2.1.6 Cell lines

Table 9 Cell lines

Cell line	Mouse background (if applicable)	Tissue	Disease (if applicable)	Organism	Culture Medium
B16F1	C57BL/6J	Skin	Melanoma	*Mus musculus*	IMDMc
CT26	Balb/c	Large intestine, colon	Colon carcinoma	*Mus musculus*	IMDMc
Lewis Lung Carcinoma (LLC)	C57BL/6	Lung	Lung cancer	*Mus musculus*	RPMIc
Madin-Darby canine kidney (MDCK)	-	Kidney	-	*Canis familiaris*	DMEMc

2.1.7 Viruses

Table 10 Viruses

Virus	Strain	Disease
Friend Virus (FV)	FV complex containing B-tropic F-MuLV and polycythemia-inducing SFFV	Leukemia
IAV	mouse-adapted A/Puerto Rico/8/1934 H1N1	Influenza A virus infection

FV stocks were kindly provided by PD Dr. Kathrin Sutter.

2.1.8 Machines

Table 11 Machines

Machine	Manufacturer
AutoMACS (AutoMACS pro)	Miltenyi Biotec, Bergisch Gladbach, Germany
Cell Counter & Spectrometer fluidlab R-300	anvajo GmbH, Dresden, Germany
Centrifuge 5417R	Eppendorf AG, Hamburg, Germany
Centrifuge ThermoScientifc Multifuge^{TM} X3	Thermo Fisher Scientific Inc, Waltham, Massachusetts, USA
ELISA reader Mitras^{2} LB943	Berthold Technologies, Bad Wildbad, Germany
FACS LSR II	BD Biosciences, Heidelberg, Germany
Gel Documentation Imaging Quantum CX5	VILBER LOURMAT Germany GmbH, Eberhardzell, Germany
Gel electrophoresis station PowerPac universal	Bio-Rad, Feldkirchen, Germany
Homogenisator FastPrep24	MP Biomedicals Germany GmbH
Incubator HERA cell 150	Thermo Electron Corporation, Waltham, USA
Luminex MAGPIX	Luminex, Austin, USA
Microscope Binokular Axiovert Z1	Carl Zeiss Microscopy GmbH, Jena, Germany
Microwave	Sharp, Hamburg, Germany
Precision balance AX120	Shimadzu, Kyōto, Japan
qPCR 7500 Fast Real-Time PCR System	Applied Biosystems, Waltham, USA
Spectrophotometer NanoDrop1000	PEQLAB Biotechnologie GmbH, Erlangen, Germany
Thermocycler T3000	Biometra GmbH, Göttingen, Germany
Top-loading balance CP2202S	Sartorius AG, Göttingen, Germany
Vortexer D-6013	Neo Lab, Heidelberg, Germany
Vortexer IKA MS 3 basic	IKA-Werke GmbH & Co. KG, Staufen, Germany

Water bath	GFL, Burgwedel, Germany

2.1.9 Software

Table 12 Software

Software	Distributor
7500 Fast System Software v2.3	Thermo Scientific, Darmstadt, Germany
BioRender	BioRender.com, Ontario, Canada
EndNote X9 v9.3.3	PDFNet SDK from PDF Tron Systems Inc., Vancouver, Canada
FACSDiva™ Software v8.0.1	BD Biosciences, Heidelberg, Germany
FlowJo V10	FlowJo LLC, Ashland, USA
GraphPad Prism 8.4.3	GraphPad Software, Boston, USA
Luminex xPONENT® Software v4.2	Luminex, Austin, USA
Microsoft Office 2016	Microsoft Corporation, Redmond, USA
NanoDrop Software ND-1000 v3.7.1	Thermo Scientific, Darmstadt, Germany

2.1.10 *In vivo* antibodies

All *in vivo* antibodies were purchased from Biozol, Eching, Germany.

Table 13 in vivo antibodies

Target	Clone	Isotype	Application
CD8	YTS 169.4	IgG2b	200 µg i.p. on days 4, 7 and 10
CD4	YTS 191	IgG2b	200 µg i.p. on days 4, 7 and 10
CSF1R	AFS98	IgG2a	200 µg i.p. on days 4, 7 and 10
CXCR3	CXCR3-173	IgG1	200 µg i.p. on days 4, 7 and 10
IFNAR-1	MAR1-5A3	IgG1	200 µg i.p. on days 4, 7 and 10
IFNγ	XMG1.2	IgG1	250 µg i.p. on days 4, 8, 10 and 12

NK1.1	PK136	IgG2a	200 µg i.p. on days 4, 7 and 10

2.1.11 Fluorochromes

Table 14 Fluorochromes

Fluorochrome	Absorption (nm)	Emission (nm)
Alexa Fluor 488 (AF488)	490	525
Allophycocyanin (APC)	650	660
Brilliant Violet (BV510)	405	510
Fluoresceinisothiocyanat (FITC)	494	519
Pacific Blue (PB)	401	452
Phycoerythrin (PE)	496	578
Phycoerythrin-Cyanine 7 (PE-Cy7)	496	786
Peridinin chlorophyll (PerCP)	482	678
Peridinin chlorophyll protein-Cyanine5.5 (PerCP-Cy5.5)	482	690

2.1.12 Flow cytometry antibodies

Except for anti-Granzyme B, all antibodies used for flow cytometry are directed against murine proteins. To measure Granzyme B, an anti-human antibody was used.

Table 15 Flow cytometry antibodies

Epitope	Clone	Label	Dilution	Manufacturer
CCR5	HM-CCR5	PerCP-Cy5.5	1:200	BioLegend
CCR7	4B12	AF488	1:100	BioLegend
CD4	RM4-5	PerCP	1:1200	BD
CD4	RM4-5	PE-Cy7	1:800	Biolegend
CD8a	53-6.7	BV510	1:1600	BioLegend
CD8a	53-6.7	PB	1:200	BD
CD8a	53-6.7	PE	1:800	BD
CD43	1B11	PE-Cy7	1:1000	BioLegend

CXCR3	CXCR3-173	APC	1:1000	eBioscience
CXCR6	SA051D1	PE-Cy7	1:200	BioLegend
Epcam	G8.8	APC	1:500	eBioscience
FOXP3	FJK-16s	FITC	1:150	eBioscience
Granzyme B	GB12	APC	1:100	Invitrogen
Granzyme B	GB12	PE	1:100	Molecular Probes
IFNγ	XMG1.2	BV510	1:300	BioLegend
Ki67	SolA15	APC	1:1000	eBioscience
Ki67	SolA15	PE-Cy7	1:1000	eBioscience
NK1.1	PK136	FITC	1:300	BD
PD1	RMP1-30	PE-Cy7	1:200	BioLegend
THY1.1	OX-7	PE	1:600	BD
TIM3	215008	APC	1:200	R&D Systems

2.1.13 MHC tetramers

Table 16 MHC tetramers

Specificity	Target	Label	Manufacturer
B16 melanoma	gp100	PE	MBL international
IAV	nucleoprotein	PE	MBL international

2.1.14 Commercial kits

Table 17 Commercial kits

Kit	Manufacturer
$CD8^+$ T Cell Isolation Kit, mouse	Miltenyi Biotec, Bergisch Gladbach, Germany
CD8 (TIL) MicroBeads, mouse	Miltenyi Biotec, Bergisch Gladbach, Germany
FoxP3 Staining Buffer Kit	eBioscience, Frankfurt a.M., Germany
RNeasy Fibrous Tissue Kit	Qiagen, Hilden, Germany

2.2 Laboratory animals

2.2.1.1 Laboratory animal facility

The mice were kept in the laboratory animal facility of the Robert Koch Haus at the university hospital Essen under specific pathogen free (SPF) conditions in individually ventilated cages (IVC2). Mice were at least 6 weeks old at the beginning of the experiments. Histological, serological and parasitological tests in sentinel mice were performed every 3 months to exclude microbiological contaminations. Animals were kept in a room with controlled temperature of 21 ± 2 °C and relative humidity of 55 ± 5% at 12-hour light/dark cycles. Water and food were provided *ad libitum*. In experiments that included genetically modified mice, these were co-housed with wildtype mice for at least one week to allow for microbial exchange. All experiments were conducted following the ethical principles and guidelines for scientific experiments and were approved by the State Agency for Nature, Environment and Consumer Protection (Landesamt für Natur-, Umwelt- und Verbraucherschutz, LANUV).

2.2.1.2 C57BL/6 and Balb/c

Female wildtype C57BL/6JOlaHsd (C57BL/6) and Balb/cOlaHsd (Balb/c) mice were purchased from Envigo (Horst, Netherlands).

2.2.1.3 Thy1.1

The thymus cell antigen 1 (*Thy1*) gene encoded protein Thy1 or CD90 was initially discovered as thymocyte antigen, the precursors of T cells in the thymus. Since two alleles of *Thy1* exist: *Thy1.1* and *Thy1.2*, the *Thy1.1* allele can be used as an endogenous marker in adoptive lymphocyte transfers. After cell transfer, lymphocytes from these donor mice can be distinguished by their specific Thy1.1 expression from wildtype host Thy1.1$^-$negative cells *via* flow cytometry. *Thy1.1* mice with a Balb/c background were bred in-house.

2.2.1.4 Rag2$^{-/-}$

Recombination activating gene 2 (*Rag2*) encodes for the RAG2 protein that is involved in the development of T and B cells, in the initiation of V(D)J recombination for the TCRs and BCRs. RAG2 forms a complex with RAG1 and this RAG complex can cleave DNA at recombination signal sequences to form double-strand breaks. In the absence of RAG2, recombination does not occur and B and T cells cannot mature. Therefore,

Rag2 knockout mice lack these lymphocytes. *Rag2*$^{-/-}$ mice in this study had a Balb/c background and were bred in-house.

2.3 Methods

2.3.1 Cell Culture

2.3.1.1 Cell Cultivation

All cell lines were cultivated at 37 °C, 5 % CO_2. Cells were split bi-weekly at a confluence of ~70 %. B16F1, CT26 and MDCK cells are adherent cells. LLC cells grow adherent and in suspension. For adherent cells, medium was removed, the cell layer was washed with PBS (37 °C) and cells were detached with Trypsin-EDTA. A small homogenous cell portion, dependent on confluency, was transferred into a new cell culture flask and cultivated with the respective medium (37 °C). For LLC cells, the supernatant was collected, centrifuged (300 x g, 10 min) and mixed with the detached cells for transfer to the new flask.

2.3.1.2 Thawing and freezing

For storage, cells were kept at -196 °C in liquid nitrogen. For freezing, cells were detached with Trypsin-EDTA as described in section 2.3.1.1, re-suspended in medium, centrifuged (300 x g, 10 min), supernatant was removed and cells were re-suspended in freezing medium. Cells were transferred into cryo-tubes, which were immediately transferred into a Mr. Frosty™ Freezing Container to achieve a cooling rate of -1 °C/min. This cooling rate is important to prevent formation of ice within and cell and thus mechanical damage. Thawing on the other hand was done quickly to reduce stress induced by DMSO in the freezing medium.

2.3.1.3 Cell counting

Cultured cells were counted with a Neubauer cell counting chamber. Cells were stained with trypan blue (Invitrogen), 10 µL cell suspension was added to the counting chamber and living cells were counted with a light microscope. Dead cells were distinguished from live cells with the help of blue staining by trypan blue. Trypan blue can pass the membranes of dead cells but not of living cells, hence dead cells are stained blue and living cells remain unstained. Cell numbers were calculated following formula (1).

$$C = n \times d \times V \times 10^4 \quad (1)$$

C = total cell number, n = mean counted cells per quadrant, d = dilution factor, V = volume of cell suspension

2.3.2 Animal experiments

2.3.2.1 Tumour transplantation and measurement

Mice were shaved on their right flanks one day prior to tumour transplantation. Detached B16F1, CT26 or LLC cells were counted using a Neubauer cell counting chamber. Cells were re-suspended in PBS at 5×10^5 cells/100 µL. Cells were transported on ice and used immediately for tumour cell transplantation. For this, 5×10^5 cells were mixed with 100 µL Matrigel and directly transplanted subcutaneously (s.c.) into the right flank. Once established, tumours were measured in length, width and height with an electric calliper. Mice were re-shaved if required for measuring. Tumour volume was calculated following formula (2)

$$\frac{Length\ [mm] \times Width\ [mm] \times Height\ [mm]}{1000} = Tumour\ volume\ [mm^3] \qquad (2)$$

2.3.2.2 IAV infection

IAV stocks were stored at -80 °C and diluted to the desired concentrations in PBS + 0.3 % BSA. For infection, mice were anesthetized by 100 mg/kg body weight Ketamine and 5 mg/kg bodyweight Xylazine. When mice were fully unconscious, they were infected intranasally (i.n.) with 7.5 PFU total, in form of 50 µL of 150 PFU/mL suspension, if not indicated otherwise. Upon infection, body weight was measured every day or more often if required.

For mock infection, virus was inactivated chemically, as described previously [82]. Briefly, a PR/8/34 stock was treated with 0.1 % β-propiolactone for 24 h at room temperature, followed by dialysis against HNE buffer (5 mM HEPES, 150 mM NaCl, 0.1 mM EDTA, pH 7.4) for 24 h at 4 °C.

2.3.2.3 Friend Virus Infection

Friend Virus was a kind gift by Kathrin Sutter (Institute for Virology, Essen). FV is a complex of two viruses: Friend murine leukaemia virus (F-MulV) and spleen focus forming virus (SFFV). F-MulV is a replication competent gammaretrovirus, whereas SFFV is replication defective but the main pathogenic factor (/component) in FV infection [83]. Stocks were made from spleen homogenates and were stored at -80 °C. The stock was lactate dehydrogenase virus (LDV)-free. For infection, stocks were centrifuged (10,000 × *g*, 5 min) and supernatants were diluted with PBS to the desired concentrations of 20,000 spleen focus-forming units (SFFU). The virus was applied

intravenously (i.v.) into the tail vein. Upon infection, body weight was measured every day.

2.3.2.4 In vivo cell neutralizations

For *in vivo* cell depletion, antibodies according to Table 13 were applied i.p. on days 4, 7 and 10 post tumour transplantation, 200 µg each. As an exception, the IFNγ neutralizing antibody was applied on days 4, 6, 8 and 10 post tumour transplantation, 250 µg each. On day 4 post tumour transplantation, the respective antibodies were applied in the morning and mice were infected at least 5 h post antibody application, to allow for systemic distribution of the antibody before infection.

2.3.2.5 Migration inhibition with Fingolimod

Migration from lymphoid organs was blocked by application of Fingolimod (FTY720). FTY720 diminishes exit from lymphoid organs. Upon application, it gets phosphorylated *in vivo* and in this form leads to the internalization of sphingosine-1-phosphate receptors (S1PRs). These are in turn degraded. S1PRs are required for egress of lymphocytes from lymphoid organs such as lymph nodes. Therefore, the FTY720-induced degradation of the receptor blocks this egress and therefore migration from lymphoid organs. 1 mg/kg body weight FTY720 was applied every second day, starting on the day of infection.

2.3.3 Cell isolation

2.3.3.1 Tumour

After isolation, tumours were weighed and if applicable for the respective experiments, biopsies were taken. Tumours were then mashed through a 70-µm-nylon strainer and washed with FACS-buffer to obtain cell suspensions. Cells were centrifuged (375 × *g*, 5 min, 4 °C), re-suspended in 1 mL ACK-buffer (3 min, RT) for osmosis-based erythrocyte lysis. FACS-buffer was added to dilute ACK-buffer and stop the lysis. Cells were centrifuged again (375 × *g*, 5 min, 4 °C) and finally taken up in FACS-buffer for further analysis. The individual amount of FACS-buffer was dependent on cell pellet size.

2.3.3.2 Lung

Lungs were perfused with PBS (RT) *via* injection into the right heart ventricle prior to lung isolation. To obtain cells from the pulmonary tissues, lungs were digested. For

this, the organs were chopped and incubated with 3 mL lung digestion medium (Table 3) at 37 °C for 45 min. Digested tissues were mashed through a 70-µm-nylon strainer, washed with PBS, centrifuged (375 × *g*, 5 min, 4 °C) and re-suspended in 2 mL ACK-buffer (3 min, RT) to lyse red blood cells. After dilution with FACS-buffer to stop erythrocyte lysis, cell suspensions were centrifuged (375 × *g*, 5 min, 4 °C) and re-suspended in 500 µL FACS buffer for further analysis.

2.3.3.3 Spleen

Cell isolation from spleens was performed *via* mashing through a 70-µm-cell strainer as described for tumour and lung. In the latter case, cells were re-suspended in 2 mL ACK-buffer (3 min, RT) after centrifugation, red blood cell lysis stopped by addition of FACS-buffer, centrifuged (375 × *g*, 5 min, 4 °C) and taken up in FACS-buffer for further analysis.

2.3.3.4 Cell counting from organs

Cells obtained from organs (tumour, lung or spleen) were counted using an anvajo fluidlab automated cell counting instrument. Tumours were diluted 1/10, lungs were diluted 1/10, and spleens were diluted 1/100, each in PBS. Tumour cells were counted using the “viability” programme. Cells from other organs were counted using the “cell counting” programme.

2.3.4 Serum collection and preparation

For serum collection, heart blood was collected directly after the mouse’s sacrifice. The heart was punctured with a 26G needle on a 1-mL-syringe and the blood was transferred into reaction tubes. Blood samples were incubated for 5 h at room temperature and then centrifuged (300 × *g*, 10 min). The serum (supernatant) was transferred into a fresh reaction tube and stored at -20 °C until use.

2.3.5 Magnetic cell separation (MACS)

Cell separation *via* MACS is based on magnetic beads. Target cells are bound by specific antibodies, which are in a next step bound by the magnetic bead. A magnetic column then enables separation of labelled cell populations. Depending on the kit, this can be either a positive or a negative selection.

For separation *via* MACS, organs were processed to single cell solutions as described in section 2.3.3. General $CD8^+$ T cells were isolated from spleens or lungs using the $CD8a^+$ T Cell Isolation Kit mouse (Miltenyi Biotec) using the deplete_s programme and tumour infiltrating $CD8^+$ T cells were isolated from tumours using the CD8 (TIL) MicroBeads mouse (Miltenyi Bitoec) using the possel_s programme. Kits were used per the manufacturer's instructions.

2.3.6 Flow cytometry *via* Fluorescence Activated Cell Sorting (FACS)

The principle of flow cytometric analysis is based on fluorescently labelled antibodies that stain proteins of interest or cell-associated molecules like DNA on or inside cells.

Flow cytometric analysis enables multi-parameter analysis of single cells. The stained cell suspension is taken up by the instrument and processed through a nozzle to produce a tiny stream so that cells continue individually (Figure 2-1). These individual cells pass a laser beam and a detector measures forward scatter (FSC) and side scatter (SSC). Additionally, a detector measures the emitted fluorescence of the stained molecules. FSC and SSC correlate with cell size and granularity respectively. This enables an easy identification of lymphocytes.

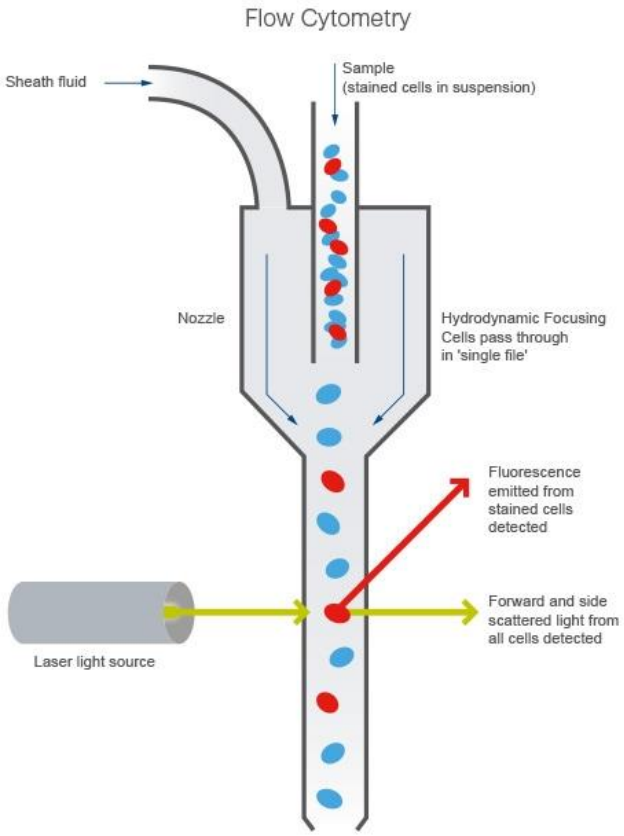

Figure 2-1 Schematic functioning of flow cytometry.

Cells from a sample pass a laser beam individually due to the sheath fluid. The machine measures forward and side light and fluorescence, which is emitted from stained cells. Figure from [84].

For flow cytometry analysis, the desired antibodies were diluted in FACS-buffer for surface staining, according to Table 15. 100 µL single cell suspensions of the different tissues/organs or serum were transferred into 96-well-round bottom plates for staining. After centrifugation (300 × *g*, 5 min, 4 °C), cells were resuspended in 100 µL antibody solution and incubated for 10 min at 4 °C, followed by centrifugation (300 × *g*, 5 min, 4 °C). In case of intracellular staining, cells were fixated and permeabilized with eBioscience™ Foxp3/Transcription Factor Staining Buffer Set (Invitrogen) per the manufacturer's instructions. Antibodies for intracellular staining were diluted in Permeabilization buffer from the same staining buffer set (Invitrogen) and incubated for 30 min at 4 °C. After staining, cells were washed with FACS buffer.

For the measurement, cells were finally resuspended in 150-200 µL FACS buffer depending on the expected cell density.

2.3.7 IAV Plaque Assay

To determine influenza virus titres, MDCK cells were infected with IAV stocks to determine the stock concentration or exposed to supernatants of infected lungs to check for successful infection. For this, detached MDCK cells were counted using a *Neubauer* cell counting chamber and 150,000 MDCK cells were seeded per well in a 12-well-plate in 1 mL DMEMc and incubated at 37 °C, 5 % CO_2 overnight. The next day, the IAV stock solution or lung supernatants were serially diluted 1/100 or 1/10 respectively in OptiMEM + 0.3 % BSA. MDCK cells were washed with PBS and treated with 500 µL virus or lung supernatant dilution (1 h, room temperature). After incubation, cells were sealed with 2 mL Influenza medium supplemented with 3 % Avicel®. Avicel® is a cellulose powder and functions as a sediment to prevent viral distribution *via* the medium so that only cell-to-cell spread is possible. Sealed cells were cultivated for 3 d at 37 °C, 5 % CO_2.

After the incubation, cells were washed with PBS, fixated with 4 % PFA (30 min, room temperature), stained with 0.5 % crystal violet solution (10 min, room temperature), washed with PBS and dried until plaques were counted and PFUs were calculated.

2.3.8 Biopsy preparation

For RNA isolation and for cytokine analysis, supernatants of organ biopsies of 20-60 mg were prepared. The specific weight was measured and biopsies were transferred into a 2-mL-screw cap vessel with 500 µL IMDM and a bead. For biopsy-homogenisation, the following programme was used in a FastPrep-24TM bead-beating grinder:

Bead-beating	4.0 m/s, 20 s
Pause	5 min
Bead-beating	4.0 m/s, 20 s

Biopsy-homogenates were centrifuged (6800 × *g*, 8 min, 4 °C), supernatants were collected and stored at -80 °C.

2.3.9 Cytokine analysis

Absolute cytokine levels were measured *via* Luminex analysis. This assay is based on beads which are colour coded for the specific analyte of interest and pre-bound with "capture antibodies". When the sample is added, the antibodies bind to the analytes. In the next step, biotinylated "detection antibodies" specific for the analytes are added so that the analyte is surrounded by both antibody types. The detection antibodies are bound by added PE-coupled streptavidin. This mixture is then measured in a Luminex analyser, in this work in a Luminex MAGPIX® Instrument. The beads are kept in a monolayer with the help of a magnet and are illuminated by two LEDs: One to determine the analyte and the other to determine the magnitude of PE-derived signal which directly corresponds to its amount.

Via Luminex analysis, the cytokine levels of serum or supernatants of lung or tumour biopsies were determined on a Luminex MAGPIX® instrument following the manufacturer's instructions. Tumour and lung samples were measured undiluted, serum samples were diluted 1:1. Concentrations were calculated with the xPONENT software. Total organ cytokine levels [pg cytokine per g tissue] were calculated with the respective biopsy weight.

2.3.10 Reverse transcriptase real-time Polymerase chain reaction (RT-qPCR)

2.3.10.1 RNA isolation

RNA from biopsy supernatants was isolated using the RNeasy Fibrous Tissue Kit (Qiagen) per the manufacturer's instructions. Briefly, proteins were digested by Proteinase K treatment, centrifuged, supernatants were treated with ethanol and subsequently transferred to a mini spin column, washed and treated with DNase. After further washing steps, RNA was eluted with 21.5 µL RNase-free water.

RNA purity was determined in a NanoDrop 1000 machine. RNA was stored at -80 °C.

2.3.10.2 Reverse transcription

The enzymatic synthesis of DNA from an RNA template is called reverse transcription (RT). The resulting DNA is called complementary DNA (cDNA).

When RNA purity was ensured *via* NanoDrop measurement, 1 or 2 µg RNA per sample were reverse transcribed. For this, RNA was solved in 13 µL RNase-free water, 0.25 µg Oligo(dT) and 1.5 µg random hexamer-primer were added and incubated at

70 °C for 10 min in a thermocycler to allow the primers to bind the RNA. For reverse transcription, retroviral Moloney Murine Leukemia reverse transcriptase (MML V-RT) was used. 4 µL MML V-RT 5× buffer, 10 mmol dNTP mix and 1 µL MML V-RT were added per sample. For cDNA synthesis, samples were incubated at 42 °C for 60 min in a thermocycler. Finally, the synthesis was stopped by a 5-min-incubation at 95 °C. cDNA was stored at -20 °C.

2.3.10.3 Polymerase chain reaction (PCR) and agarose gel electrophoresis

In a PCR, specific gene segments are enriched to produce large amounts of the respective gene segment. For this, the DNA is denatured by hot temperature, resulting in single-stranded DNA. Next, primers that are designed for the specific for the gene of interest bind to the template DNA (annealing) and a DNA polymerase synthesizes new DNA which is complementary to the template DNA (elongation). Denaturation, annealing and elongation require different temperatures; therefore each PCR cycle consists of these three steps.

To test the success of the reverse transcription, the housekeeping gene for Ribosomal Protein S9 (RPS9) was amplified by PCR using the PCR programme in Table 18.

Table 18 RPS9 PCR programme

	Temperature [°C]	Time [min]	Number of cycles
Initial denaturation	94	10	1
Denaturation	94	0.75	30
Annealing	55	0.75	
Elongation	72	1	
Terminal elongation	72	10	1
	4	∞	

The amplified PCR products were tested by agarose gel electrophoresis. In this technique, nucleic acids are separated by size in an electric field. Since DNA is negatively charged, it migrates towards the anode. Different fragments have different velocities, depending on their size, smaller fragments migrate faster.

1 % (w/v) agarose was boiled in 1 × TE-buffer. After boiling, 5 µL Midori Green were added per 100 mL buffer. After casting, the PCR products and a DNA size marker (Gene Ruler 100 bp Ladder Plus) were loaded onto the gel. Visualization was enabled by UV radiation.

2.3.10.4 Real-time SYBR®-Green PCR

To quantify gene expression, cDNA was amplified with primers for the respective target and *Rps9* with Maxima SYBR Green/ROX qPCR Master Mix 2x (Thermo Fisher Scientific) using a 7500 Fast Real-Time PCR System (Thermo Scientific) per the manufacturer's protocol. The respective reaction mixture for quantitative real-time PCR (RT-qPCR) is described in Table 19 and the programme in Table 20.

Table 19 RT-qPCR reaction mix

Component	Concentration/Dilution
cDNA template	1 µL
H_2O	4 µL
Maxima SYBR Green qPCR Master Mix with ROX	10 µL
Primer mix (in H_2O) *Rps9*: forward 900 nM, reverse 50 nM *Ifnλ, M1, Mmp9, Vegf* forward 300 nM, reverse 300 nM *Tgfβ*: forward 50 nM, reverse 900 nM	5 µL

Table 20 RT-qPCR programme

Step		Temperature	Time	Cycles
1	Denaturation	95 °C	10 min	
2	Denaturation	95 °C	15 s	40
	Annealing	AT	30 s	
	Amplification	72 °C	30 s	
3	Melting curve stage	95 °C	15 s	
		60 °C	60 s	
		95 °C	15 s	
		60 °C	15 s	

Relative expression of target genes was determined using formula 3.

$$relative\ expression = \frac{mean\ quantity\ of\ target\ gene}{mean\ quantity\ of\ Rps9} \quad (3)$$

2.3.11 Adoptive cell transfer experiments

Adoptive cell transfers were performed in two different experimental setups.

2.3.11.1 Transfer of endogenously marked tumour CD8$^+$ T cells to follow migration.

In order to follow T cell migration, endogenously marked tumour CD8$^+$ T cells were isolated and transferred into tumour-bearing mice which were infected or not. For this, *Thy1.1*$^+$ mice were used as donor mice, and *Thy1.1*$^-$ Balb/c mice were used as recipient mice. 1×10^5 CT26 tumour cells were transplanted s.c. into *Thy1.1*$^+$ mice. One day later, 1×10^5 CT26 tumour cells were transplanted s.c. into Balb/c mice. 4 days post recipient tumour transplantation Balb/c mice were infected i.n. with IAV (150 PFU). 11 days post donor tumour transplantation, donor mice were sacrificed in order to isolate tumour CD8$^+$ T cells using MACS CD8 (TIL) MicroBeads (Miltenyi Biotec) as described in section 2.3.5. 1.5×10^5 cells were adoptively transferred into recipient mice. Purity was confirmed *via* flow cytometric analysis before i.v. transfer. 2 days post transfer, recipient mice were sacrificed and tumours, lungs and spleens were isolated, processed as described in section 2.3.3, stained, counted and analysed *via* flow cytometry to determine differences in Thy1.1$^+$ cell numbers in the organs of infected or non-infected mice.

2.3.11.2 Transfer of influenza CD8$^+$ T cells

To assess the contribution of CD8$^+$ T cells primed for influenza antigens to tumour growth inhibition, 1×10^5 B16F1 tumour cells were transplanted s.c. into C57BL/6 mice. 7 days post tumour transplantation, i.e. at a time when an adaptive immune response is established, mice adoptively received i.v. 6×10^5 CD8$^+$ T cells isolated from influenza infected lungs 8 days post infection. CD8$^+$ T cell isolation was performed using the MACS CD8a isolation kit (Miltenyi Biotec) as described in section 2.3.5.

2.3.12 Statistical analysis

Data were analysed with GraphPad Prism software. Mann-Whitney test was used for unpaired data. Differences between two or more groups with different factors were calculated using two-way ANOVA, followed by Tukey's multiple comparisons-test. p-values of 0.05 or less were considered indicative of statistical significance (*$p < 0.05$, **$p < 0.01$, ***$p < 0.001$, ****$p < 0.0001$).

3 Results

3.1 The impact of IAV infection on tumour immunology.

Cancer is a central cause of death worldwide; almost every sixth death is caused by cancer [85]. Especially elderly people are affected. So as populations are growing older, the global number of cancer deaths is steadily increasing [86]. Infections can have a significant influence on the course of a tumour disease. Endemic diseases play an important role in this. In this context, influenza viruses appear in seasonal waves; causing millions of deaths every year, again especially elderly people are affected. This leads inevitably to the situation of both challenges affecting the same patient. Both fields are of high interest in ongoing research. However, the combination of both is understudied. It has been shown in previous studies that an influenza infection can have pro- or anti-tumour effects. It can induce anti-tumour properties for lung cancer [87] and during the development of this study, it was shown that in melanoma, an influenza infection can have detrimental effects [88]. Both observations show a clear interaction between the infection and the tumour, although in separate directions. Therefore, it is of urgent need to understand the interactions between this viral respiratory infection and tumour immunology.

3.2 Tumour growth inhibition upon IAV infection.

Initially, the effect of viral influenza infection on tumour growth in general was tested.

3.2.1 IAV infection is associated with restricted tumour growth.

To investigate the direct effect of IAV infection on tumour progression, B16F1 cells were transplanted subcutaneously in the right flank of mice. Tumour sizes were measured and are depicted in Figure 3-1. The tumour growth rate was diminished when tumour bearing mice were infected with IAV, compared to tumours of mice without infection. Interestingly, the effect was more prominent with a medium level of infection (150 PFU) than with a high infection dose (300 PFU) (Figure 3-1 A). Therefore, further experiments were conducted with this moderate infection dose if not indicated otherwise.

The observed tumour growth inhibition was not restricted to B16 melanoma but all tested tumour models showed diminished growth when mice were infected with IAV: CT26 colon cancer and Lewis Lung Cancer (LLC) tumours showed comparable effects (Figure 3-1 B and C respectively). B16 and LLC tumours were transplanted into

C57BL/6 mice, whereas CT26 tumours were transplanted into Balb/c mice, showing that this observation is not restricted to one mouse strain background.

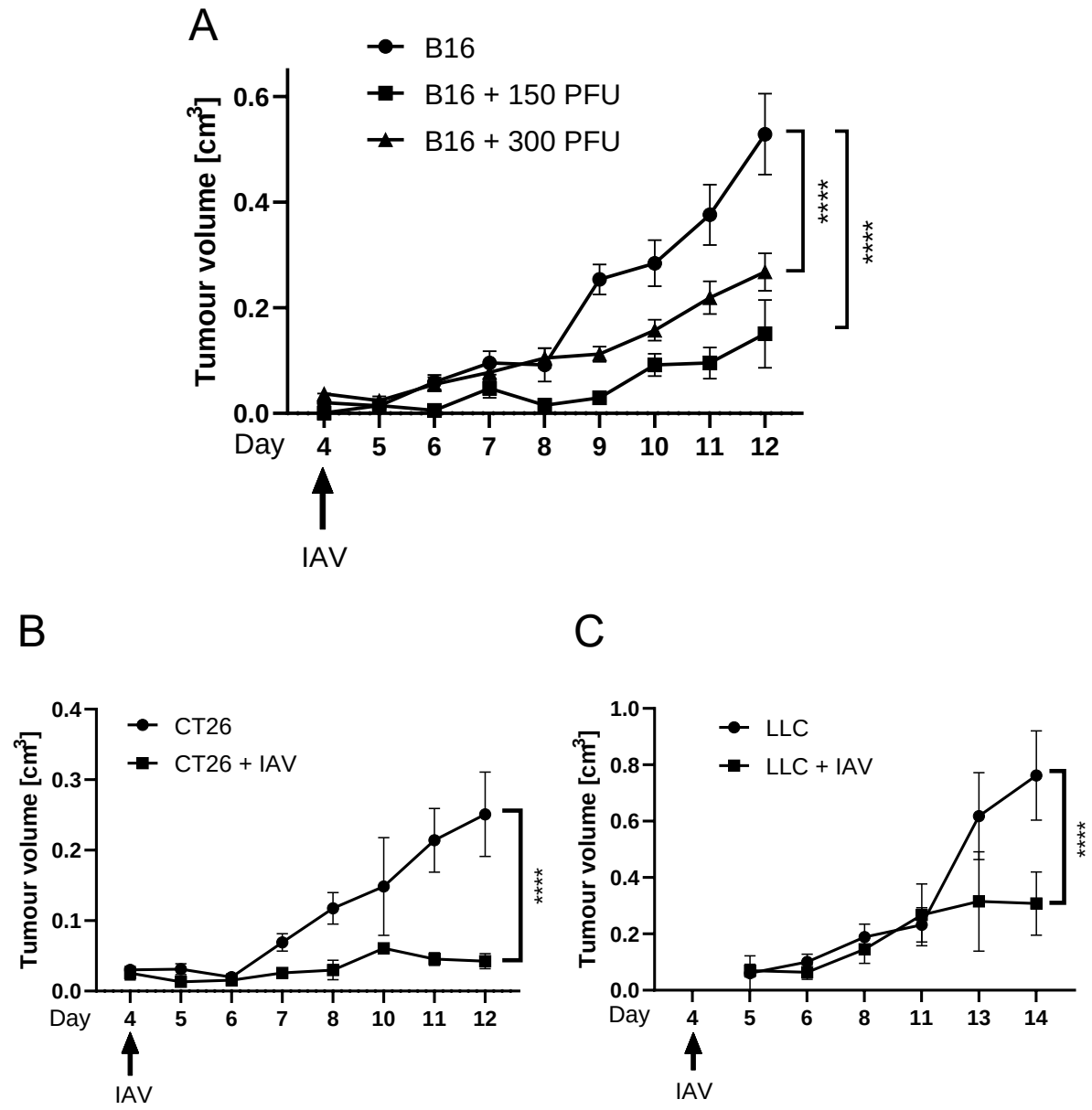

Figure 3-1 IAV infection restricts tumour growth.

Indicated tumour cell lines were transplanted subcutaneously into C57BL/6 mice (B16F1 and LLC, A and C) or Balb/c mice (CT26, B). Mice were intranasally infected with 150 PFU if not indicated otherwise. Tumours were measured and the volume was calculated as described in section 2.3.2.1 following formula (2). Data from 4-7 individual experiments are shown for B16 tumour, from 4 individual experiment for CT26 and from one experiment for LLC. Mean tumour sizes ± SEM are plotted for B16 and CT and ± SD for LLC with respect to experiment numbers. Statistical analysis was performed by 2way ANOVA, followed by Tukey's multiple comparisons test. **** = $p \leq 0.0001$.

To further clarify if the process of infection is required or if treatment with an inactivated virus is sufficient, mice were mock-infected with inactivated virus. However, tumour sizes showed no difference with or without infection with inactivated virus (Figure 3-2), indicating that this attenuated virus is not sufficient for the observed IAV-induced tumour growth inhibition.

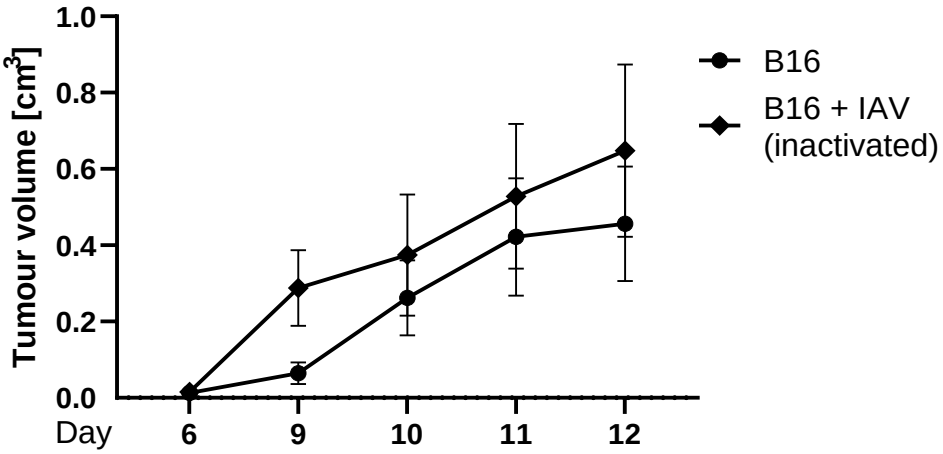

Figure 3-2 Inactivated IAV is not sufficient for tumour growth inhibition.

B16F1 tumour cells were transplanted subcutaneously into C57BL/6 mice. Mice were intranasally (i.n.) treated with 0.05 µg inactivated virus [82]. Tumours were measured and the volume was calculated as described in section 2.3.2.1 following formula (2). Data from 3 individual experiments are shown. Mean tumour sizes ± SEM are plotted.

3.2.2 IAV remains in the infected lungs and is not detectable in the tumour.

Since treatment with the infectious IAV is required to restrict tumour growth, the next step was to test whether the observed tumour growth inhibition is based on spreading of the virus to the tumour. Theoretically, direct cell lysis is possible since it has been described that B16 cells *per se* are susceptible to IAV infection *in vitro* [89]. qPCR analysis targeting the expression of the IAV specific matrix gene *M1* was used to mirror viral infection. Expression levels of *M1* in tumours of infected mice were as low as from non-infected mice (Figure 3-3), indicating the absence of IAV in the tumour in our infection model. Lung viral titres of infected mice were used as a positive control.

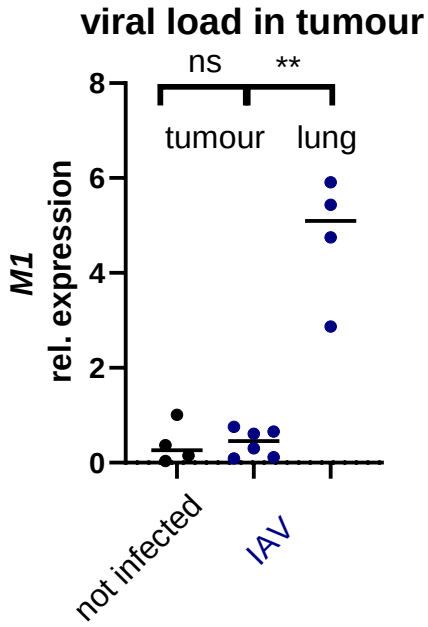

Figure 3-3 IAV is not detectable in tumours.

B16F1 tumour cells were transplanted subcutaneously into C57BL/6 mice. Mice were i.n. infected with IAV 4 days post tumour transplantation. Viral loads were determined by qPCR 12 days post tumour transplantation, which complies with 8 days post infection. Viral *M1* gene expression levels without a tumour were measured 8 days post infection. Relative *M1* expression was calculated with respect to *Rps9* expression. Statistical analysis was performed by Mann-Whitney test. ** = p≤0.01.

3.3 Factors determining angiogenesis are altered in the tumour by a simultaneous IAV infection.

As a tumour grows, it needs further supply of oxygen and nutrition for sustained growth. These are transported *via* the blood. Therefore, the tumour needs to establish blood vessels. The process of new blood vessel formation is called angiogenesis. Angiogenesis begins *in utero* and continues throughout life, following functional requirements for metabolic activity of the respective tissue. It is determined by an interplay between pro- and anti-angiogenetic factors. Inhibiting angiogenesis is therefore one approach in tumour therapy [90]. In the following, levels of angiogenetic factors in tumours of mice with or without infection were determined.

3.3.1 Angiogenetic factors are reduced in tumours of IAV infected mice.

We measured mRNA levels of the angiogenetic factors Vascular Endothelial Growth Factor (VEGF) and Matrix metallopeptidase 9 (MMP9). MMP9 is involved in extracellular matrix breakdown [91]. VEGF is involved in the regulation of blood vessel formation directly [92]. Tumour *Mmp9* mRNA levels show a slight reduction and *Vegf*

mRNA levels are significantly reduced when mice were infected 8 dpi (Figure 3-4). Both tendencies are in agreement with the observation of smaller tumours.

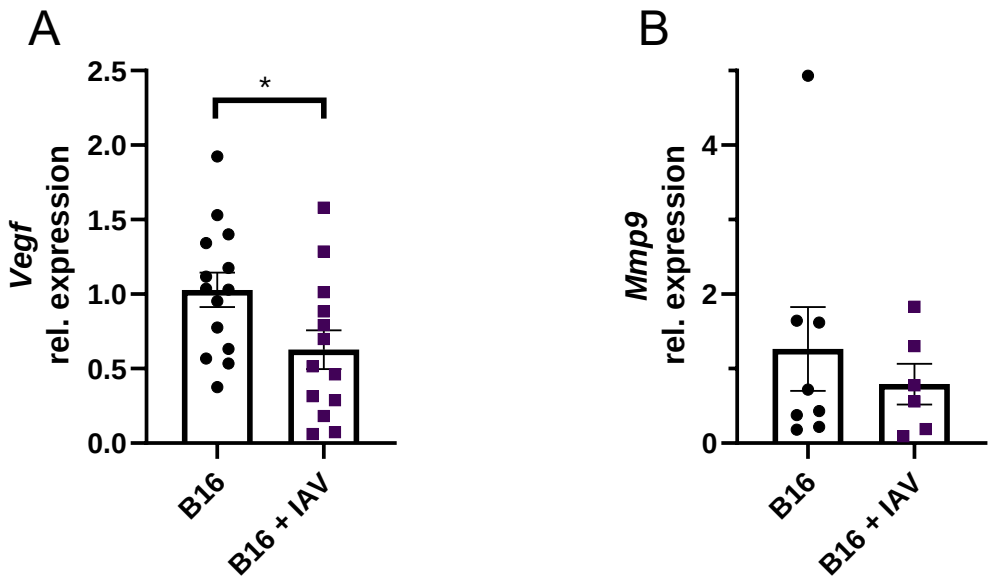

Figure 3-4 Angiogenetic factors show reduced mRNA levels in tumour when mice were infected with IAV.

B16F1 tumour cells were transplanted subcutaneously into C57BL/6 mice. Mice were i.n. infected with IAV 4 days post tumour transplantation. Total RNA was isolated from tumour biopsies 12 days post tumour transplantation. Tumour mRNA expression of *Vegf* (A) and *Mmp9* (B) was measured by qPCR. Relative expression was calculated with respect to *Rps9* expression. Data from 2-4 individual experiments are shown. Mean expression values ± SEM are plotted. Statistical analysis was performed by Mann-Whitney test. * = p≤0.05.

3.4 The contribution of IFNs.

IFNs play important roles in the immunological fight against diseases. They are highly involved in the immune responses, towards both, infections and malignant cells. The benefit however is under debate. A current view is that IFNs initially support anti-tumour responses but eventually contribute to inhibitory feedback mechanisms to avoid hyper-inflammation or resulting tissue damage [93]. For example, type I IFNs can directly affect the growth and proliferation of tumour cells [94]. Both type I IFNs and IFNγ promote tumour-specific $CD8^+$ T cell responses increasing their antigen recognition *via* upregulation of MHC molecules on tumour cells [95]. On the other hand, IFNγ-induced upregulation of immune checkpoints can also drive $CD8^+$ T cells into exhaustion [96]. IFNλ acts similarly to type I IFNs but its receptor IFNLR1 is expressed preferentially on epithelial cells, making IFNλ important in influenza infection but it is also discussed in tumour therapy [97, 98]. The TME contains danger-associated molecular patterns (DAMPs) that can activate TLRs and enforce IFN production.

With respect to the viral side, influenza infection results in an excessive host immune response in the lung by the innate immune system, including high expression of IFN [99].

3.4.1 Type I and type III IFN levels are increased upon infection.

To examine their contribution to tumour development, type I IFN concentrations were firstly determined by ELISA. Tumours showed increased levels of IFNα and IFNβ 8 days after infection (Figure 3-5 A, B). Interestingly, neither IFNα nor IFNβ levels were significantly changed in infected lungs compared to uninfected lungs at day 8 after infection (Figure 3-5 C, D). Type II IFN (IFNγ) concentrations were determined *via* Luminex analysis. The levels were decreased in the tumours of infected mice (Figure 3-5 E) but strongly increased in lungs of infected mice (Figure 3-5 F) 8 days post infection. Relative type III IFN (IFNλ) levels were measured by qPCR. Like absolute type I IFN levels, tumour *Ifnλ* mRNA levels were increased when mice were infected (Figure 3-5 G).

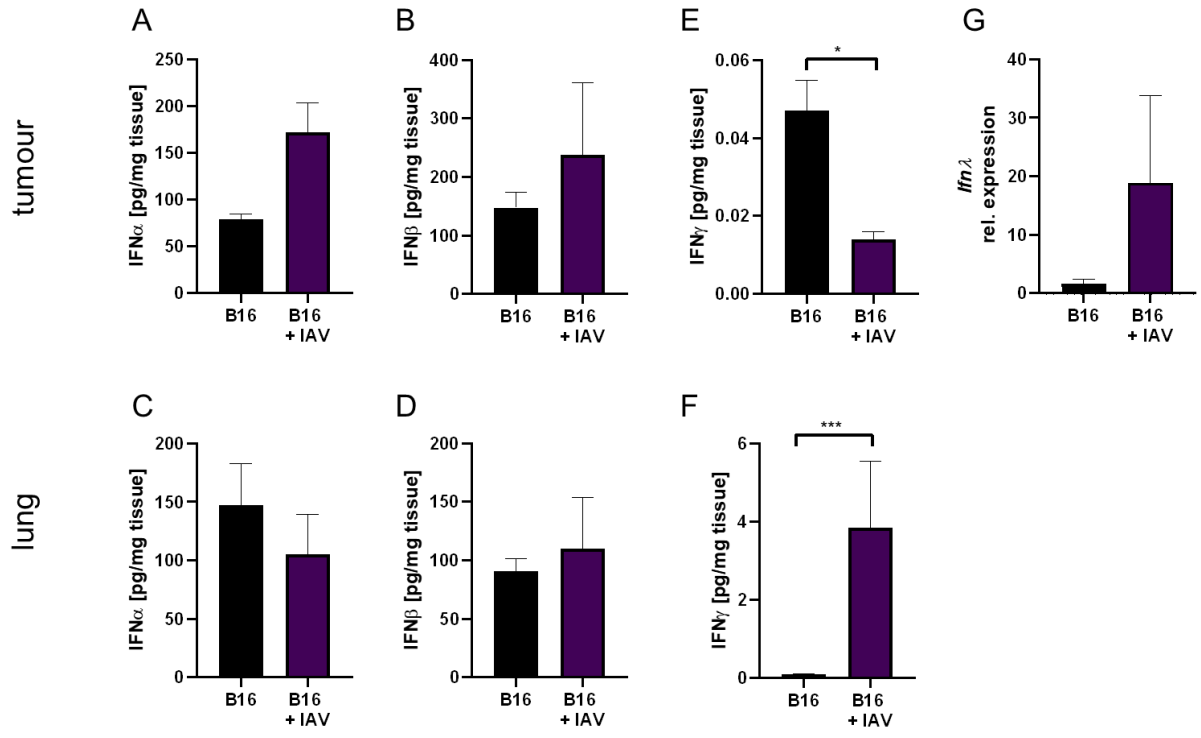

Figure 3-5 IFN levels in tumour and lung.

B16F1 tumour cells were transplanted subcutaneously into C57BL/6 mice. Mice were i.n. infected with IAV 4 days post tumour transplantation. IFN levels were determined by ELISA (IFNα and IFNβ, A-D), Luminex analysis (IFNγ, E-F) or by qPCR (IFNλ, G) 12 days post tumour transplantation. Biopsies were homogenized and supernatants were collected and analysed for IFN levels. Relative *Ifnλ* expression was calculated with respect to *Rps9* expression A, B, E and G show tumour IFN levels and C, D and F show lung IFN levels. Data from 3-4 mice or up to 12 mice

(IFNγ) are shown. Mean levels/expression ± SD or ±SEM (IFNγ) are depicted. Statistical analysis was performed by Mann-Whitney test. * = p≤0.05, *** = p≤0.001.

3.4.2 Type II but not type I IFNs are required for tumour growth inhibition.

That IFN concentration levels were altered in the tumour depending on the infection status of the mice raised the question of their direct impact on influenza infection-induced tumour growth inhibition. To this end, IFNAR was blocked to interrupt type I IFN signalling or IFNγ was neutralized directly using monoclonal antibodies. The experimental setups are depicted in Figure 3-6. Despite the increased levels of IFNα in the tumour, IFNAR blockade did not diminish IAV-induced tumour growth inhibition (Figure 3-6 A). On the other hand, IFNγ seems to be required for the full effect of tumour growth inhibition: Upon IFNγ neutralization, tumours were not significantly smaller in infected mice any more, compared to non-infected mice (Figure 3-6 B). Therefore, IFNγ seems to play an important part in tumour growth inhibition.

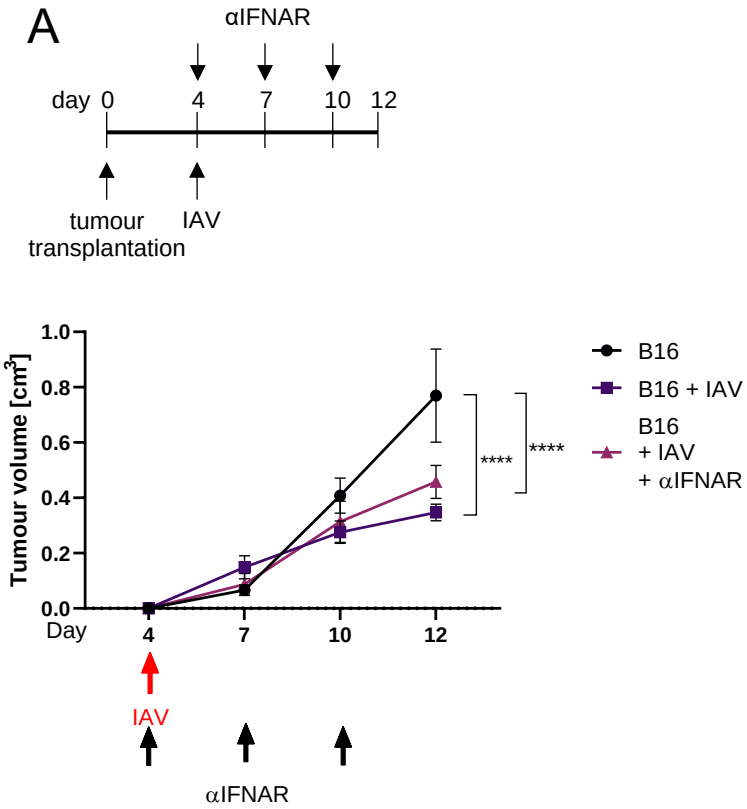

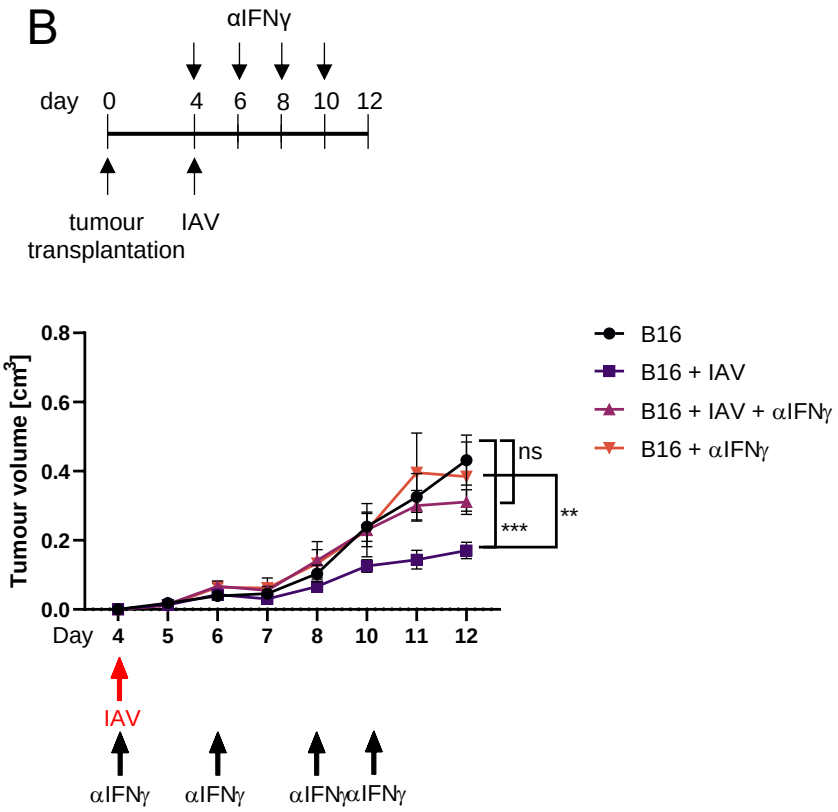

Figure 3-6 Tumour growth inhibition is not affected by IFNAR blockade but by IFNγ blockade.

B16F1 tumour cells were transplanted subcutaneously into C57BL/6 mice. Mice were i.n. infected with IAV 4 days post tumour transplantation. Antibodies were applied i.p. at the indicated days. Tumours were measured and the volume was calculated as described in section 2.3.2.1 following formula (2). A: 200 µg αIFNAR was applied on day 4, 7 and 10 post tumour transplantation. B: 250 µg αIFNγ was applied on day 4, 6, 8 and 10 post tumour transplantation. Data from 2 experiments are shown each. Mean tumour sizes ± SEM are plotted. Statistical analysis was performed by 2way ANOVA, followed by Tukey's multiple comparisons test. ** = p≤0.01, *** = p≤0.001.

3.5 The contribution of different cell types.

To further define the underlying effectors of the observed tumour growth inhibition, the following section focuses on different immune cell populations. Since melanoma is a solid tumour, it is characterized by the infiltration of lymphocytes. Generally, T cells and NK-cells exhibit tumour-limiting functions. However, levels of these cell populations were not altered in the tumour with or without IAV lung infection (Figure 3-7 A-C).

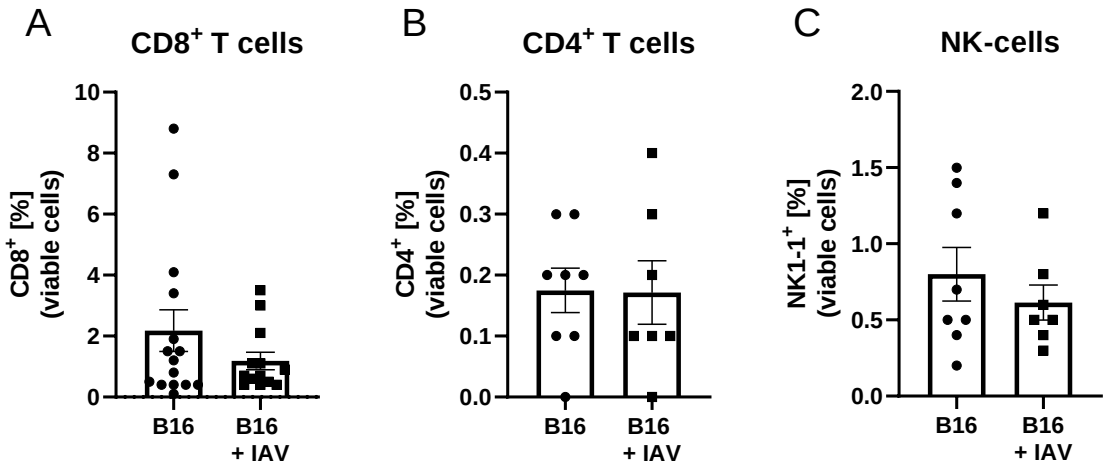

Figure 3-7 Different immune cell populations in the TME.

B16F1 tumour cells were transplanted subcutaneously into C57BL/6 mice. Mice were i.n. infected with IAV 4 days post tumour transplantation. Tumours were analysed 12 days post transplantation *via* flow cytometry. Indicated cell populations were calculated with respect to all viable cells. Data from 2 individual experiments are shown in B and C and from 5 individual experiment in A. Mean frequencies ± SEM are plotted.

3.5.1 NK-cells and macrophages are dispensable for tumour growth inhibition.

An influenza infection induces the activation of alveolar macrophages and NK-cells [100, 101]. Likewise, both cell types are described to have established roles in the TME and therefore in the tumour development [102].

Therefore, their contribution to tumour growth inhibition was assessed by depletion of NK-cells or macrophages in the established model. Macrophage depletion was achieved by antibody-mediated depletion by anti-CSF1R treatment and NK-cell depletion was performed by anti-NK1.1 application, both of which are factors that are required specifically for macrophage and NK-cell development respectively. Neither NK-cell nor macrophage depletion could diminish tumour growth inhibition by IAV infection, indicating that these populations are dispensable for the observed effect on tumour growth (Figure 3-8).

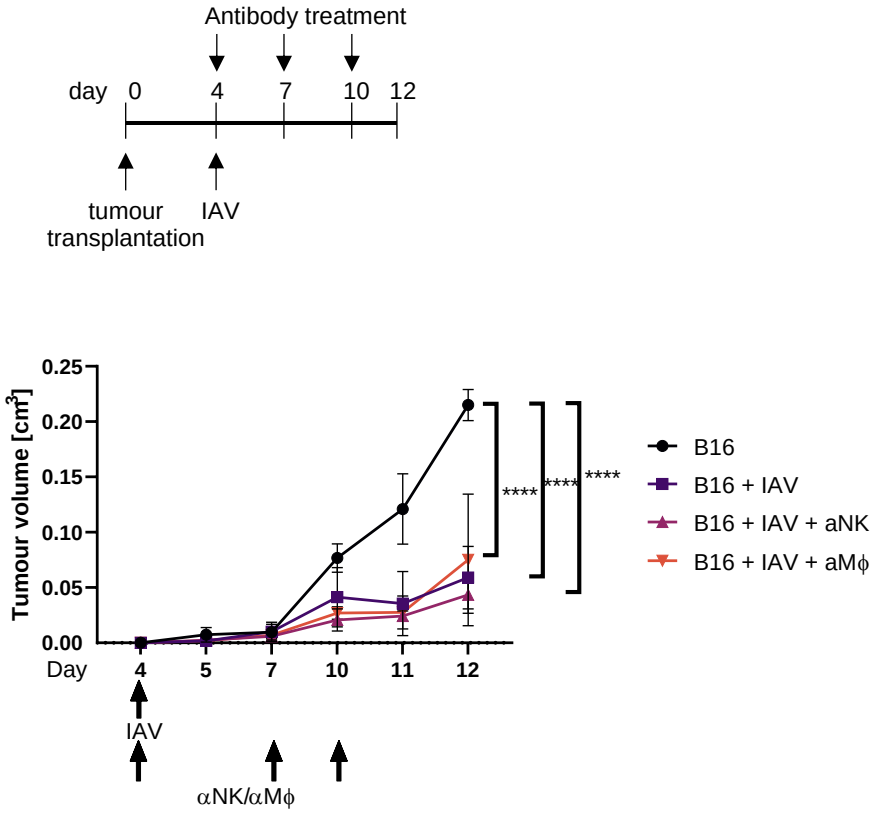

Figure 3-8 Tumour growth inhibition is still present upon NK-cell or macrophage depletion.

B16F1 tumour cells were transplanted subcutaneously into C57BL/6 mice. Mice were i.n. infected with IAV 4 days post tumour transplantation. 200 µg antibodies against CSF1R or NK1.1 were applied i.p. at the indicated days for macrophage or NK-cell depletion respectively. Tumours were measured and the volume was calculated as described in section 2.3.2.1 following formula (2). Data from one experiment are shown. Mean tumour sizes ± SD are plotted. Statistical analysis was performed by 2way ANOVA, followed by Tukey's multiple comparisons test. **** = $p \leq 0.0001$.

3.5.2 CD8⁺ T cells but not CD4⁺ T cells mediate tumour growth inhibition.

Next, the importance of cells of the adaptive immune system was tested. *Rag2*$^{-/-}$ mice lack both, B and T cells (section 2.2.1.4). CT26 tumour growth inhibition by IAV was not as prominent in this experiment as in wildtype mice (Figure 3-9 A), indicating a role of the adaptive immune system in this effect.

Thus, the next approach focused specifically on the contribution of T cells. CD4⁺ or CD8⁺ T cells were depleted in B16 tumour bearing mice starting several hours before infection. The success of both T cell depletions was checked *via* blood analysis throughout the experiment. Upon CD4⁺ T cell depletion, tumours still showed a growth inhibition in IAV infection compared to tumours of non-infected mice (Figure 3-9 B). Hence, CD4⁺ T cells are not responsible for this control. However, when comparing tumour sizes of non-infected mice with those of infected mice with or without

CD8$^+$ T cell depletion, only infected mice show significantly smaller tumours. Upon depletion of CD8$^+$ T cells, tumours of infected mice were not significantly smaller any more (Figure 3-9 B). Therefore, CD8$^+$ T cells seem to be required for the observed tumour growth inhibition by IAV infection.

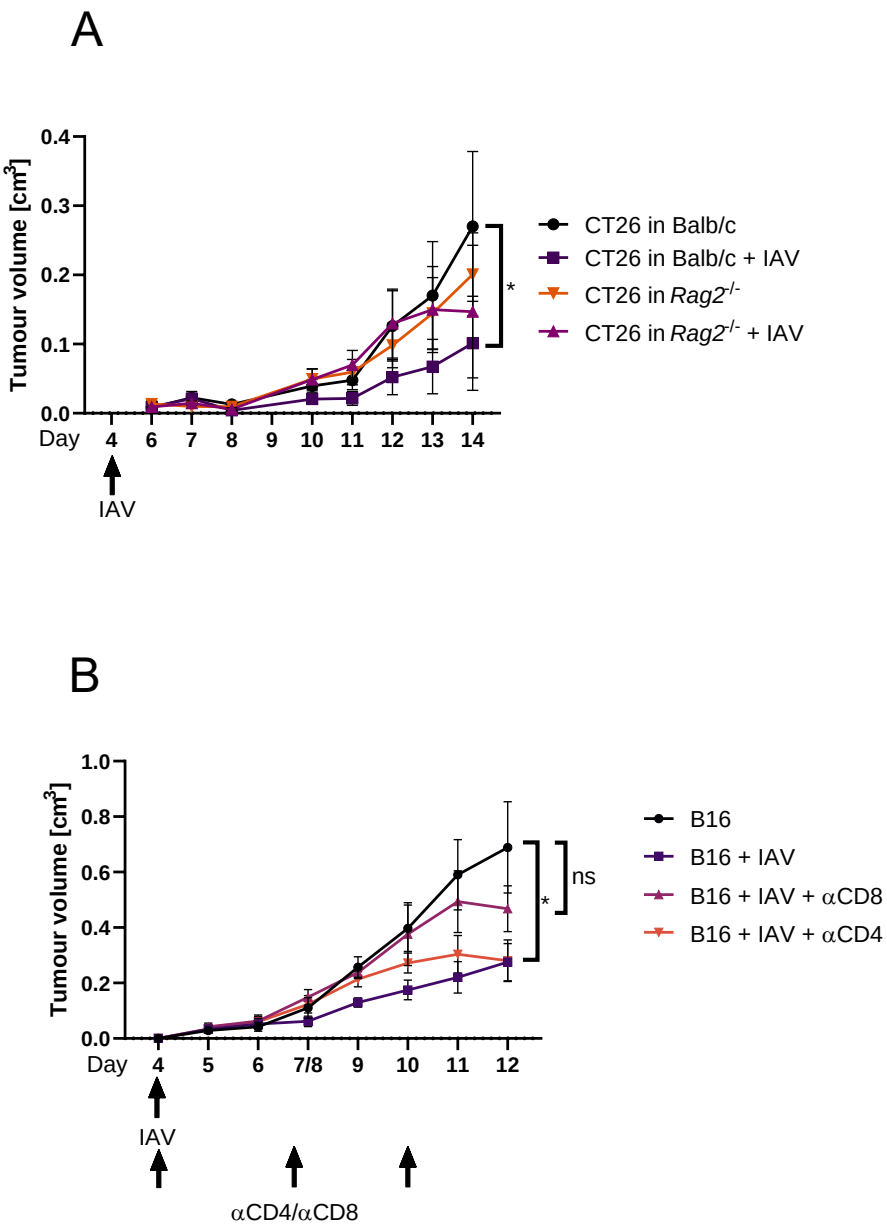

Figure 3-9 CD8$^+$ T cells are required for tumour growth inhibition.

CT26 tumour cells were transplanted subcutaneously into *Rag2*$^{-/-}$, Balb/c or B16F1 tumour cells into C57BL/6 mice. Mice were i.n. infected with IAV 4 days post tumour transplantation. A: CT26 tumour transplantation in *Rag2*$^{-/-}$ or Balb/c mice. B: B16 tumour transplantation in C57BL/6 mice. 200 µg antibodies were applied i.p. at the indicated days. Tumours were measured and the volume was calculated as described in section 2.3.2.1 following formula (2). Data from 2 individual experiments are shown. Mean tumour sizes ± SEM are plotted. Statistical analysis was performed by 2way ANOVA, followed by Tukey's multiple comparisons test. * = p≤0.05.

3.6 Defining the role of T cells.

After showing that $CD8^+$ T cells are required for tumour growth inhibition, the following section provides a more detailed characterization of this population.

3.6.1 $CD8^+$ T cells show a stronger activated phenotype in the tumour upon IAV infection.

The cytotoxicity of CTLs is directed against infected or tumour cells and is achieved by different means. Once the T cell is presented with an antigen from a malignant or infected cell *via* its TCR, it secretes cytokines such as TNFα or IFNγ, which have anti-tumour and anti-viral effects. CTLs can also release cytotoxic granules containing cytolytic proteins or proteases such as perforin or granzymes. Granzymes cleave proteins inside the target cell and finally lead to its apoptosis. Generally, the expression of these substances mirrors the activation of $CD8^+$ T cells. Yet another marker for activation is CD43 which is involved in ligand-receptor engagement for co-stimulatory pathways for T cell activation by APCs [103].

In IAV infected mice, the $CD8^+$ T cell population was slightly decreased in the tumour (Figure 3-7 in section 3.5). However, these $CD8^+$ T cells in the tumour were stronger activated as the populations of CD43 and Granzyme B expressing $CD8^+$ T cells were increased (Figure 3-10 A and B). Higher levels of Ki67, which is present during the active phase of the cell cycle, indicate increased proliferation. In this regard, more $CD8^+$ T cells in the tumour showed a proliferating phenotype when mice were infected compared to tumours of non-infected mice. PD-1 can likewise act as an activation marker, although with this marker, a caution has to be paid since sustained high PD-1 expression can also indicate exhaustion. In general, the population of PD-1 expressing $CD8^+$ T cells was increased in tumours of infected mice compared to tumours of non-infected mice (Figure 3-10).

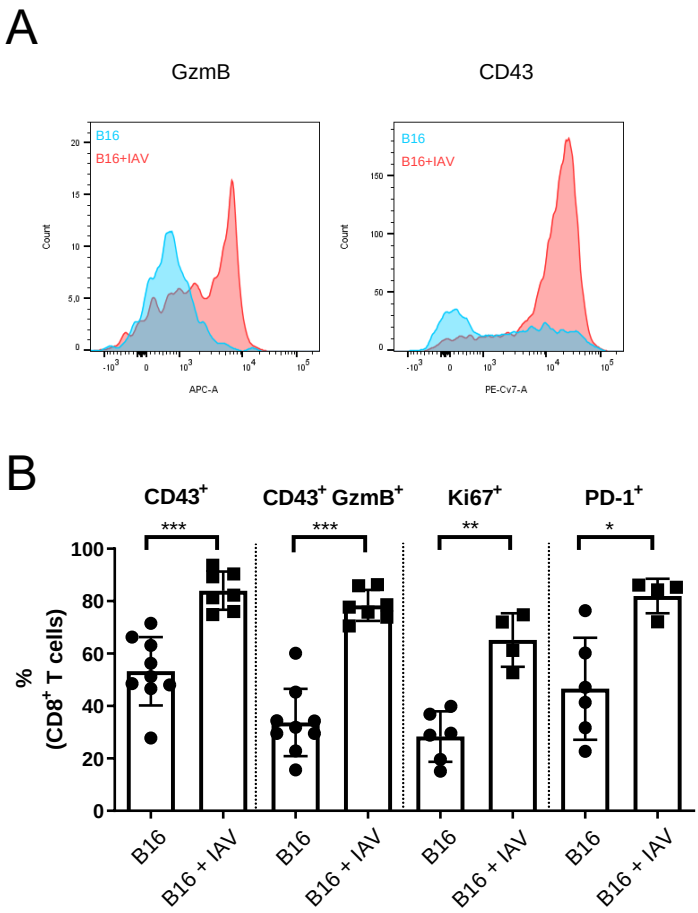

Figure 3-10 CD8⁺ T cells in the tumour are stronger activated upon influenza infection.

B16F1 tumour cells were transplanted subcutaneously into C57BL/6 mice. Mice were i.n. infected with IAV 4 days post tumour transplantation. Tumours were analysed 12 days post transplantation *via* flow cytometry. Indicated cell populations were calculated with respect to all viable CD8⁺ T cells. A: Representative histograms of flow cytometry of CD43 and Granzyme B on CD8⁺ T cells. B: Activation markers on CD8⁺ T cells. Data from 3 (CD43 and CD43 Granzyme B) or 2 (Ki67 and PD-1) individual experiments are shown. Mean population sizes ± SEM are plotted. Statistical analysis was performed by Mann-Whitney test. GzmB = Granzyme B.

3.6.2 Tumour specific CD8⁺ T cells are stronger activated in tumour and lung.

TCRs of CD8⁺ T cells oblige recognition by an MHC I/peptide complex. This requirement can be used to detect tumour specific CD8⁺ T cells by engineering an MHC I tetramer linked to a fluorescent tag. The tetramer consists of four H-2 MHC I molecules, here bound to the B16 melanoma specific peptide gp100. The fluorescent protein allows determining the number and detailed further characterisation of tetramer positive CD8⁺ T cells *via* flow cytometry.

With the help of the described tetramer, this population of tumour specific CD8⁺ T cells was analysed in tumour and lung. An increase in this population in the tumour when mice were additionally infected was observed (Figure 3-11 A). Interestingly, we not

only found some tetramer-specific CD8$^+$ T cells in the lung but this population was significantly even more prevalent upon infection (Figure 3-11 A-D).

Binding the tetramer itself does not rely on functionality of the T cells but the population shows all tetramer-binding T cells, regardless of their activation status. Therefore, these cells were further characterised. Staining for functional markers revealed a stronger activated phenotype of tetramer-specific CD8$^+$ T cells both in the tumour and even more prominent in the lung upon infection compared to the non-infected setup as shown by an increase in CD43$^+$ and Granzyme B$^+$ cells (Figure 3-11 E, F).

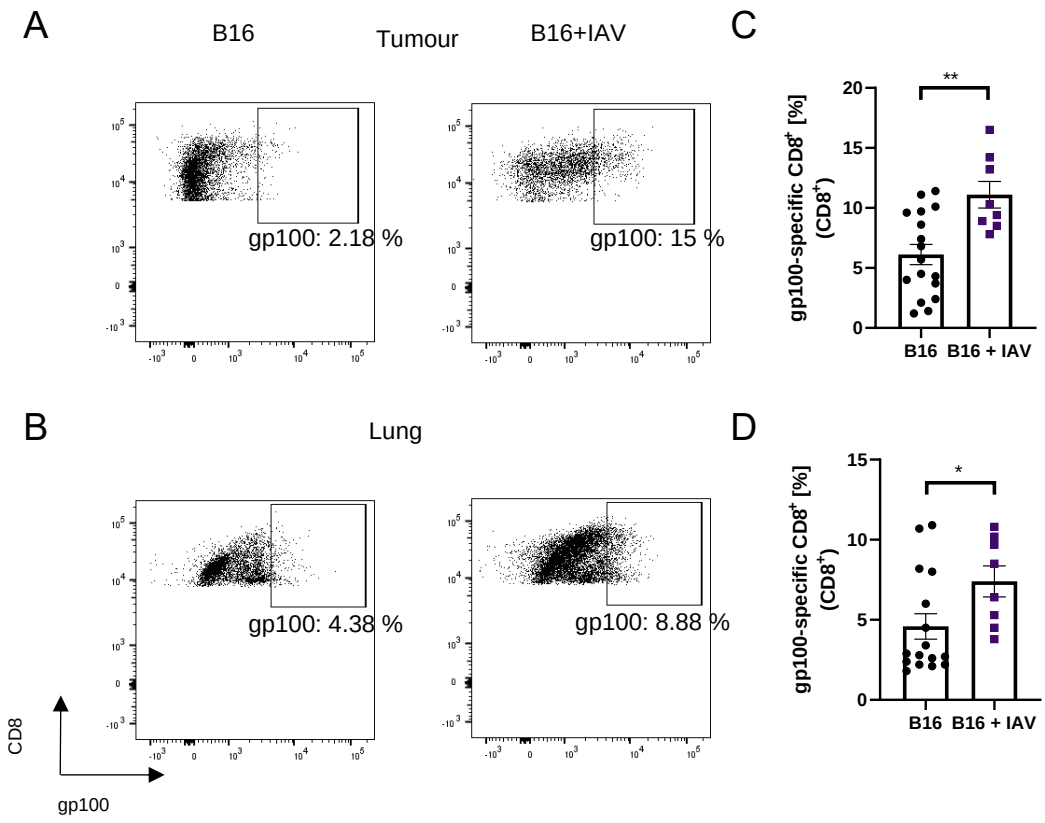

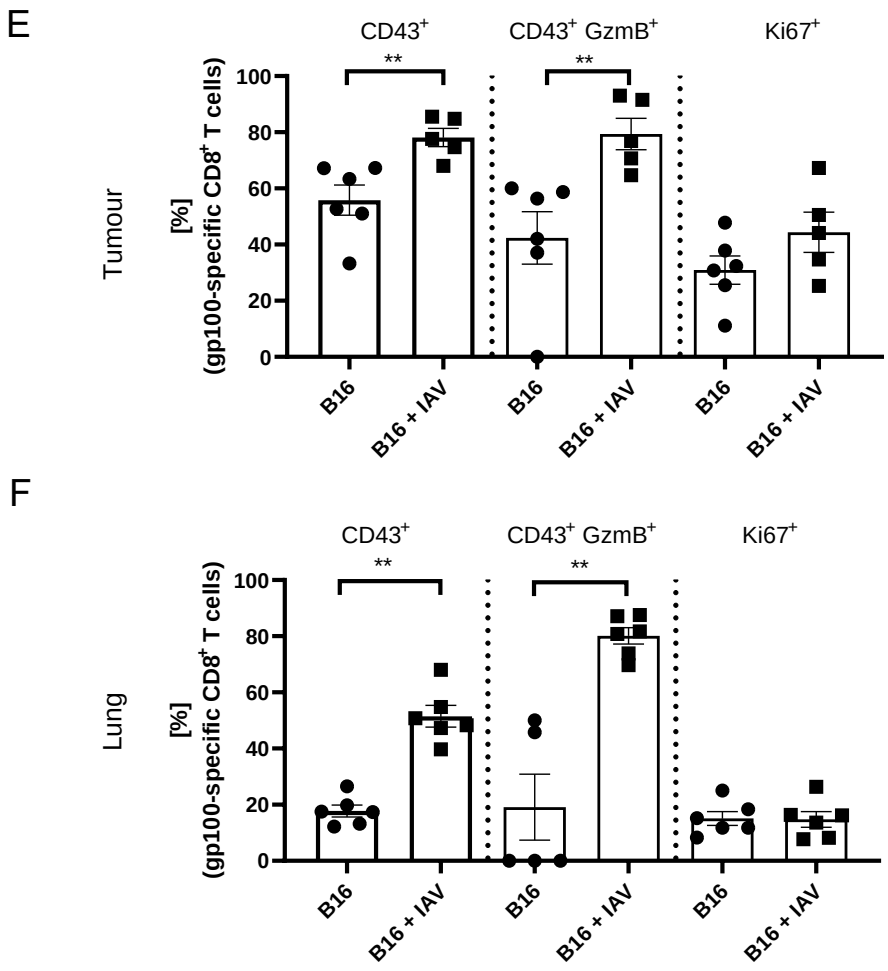

Figure 3-11 gp100-specific CD8⁺ T cells are more abundant and stronger activated upon influenza infection.

B16F1 tumour cells were transplanted subcutaneously into C57BL/6 mice. Mice were i.n. infected with IAV 4 days post tumour transplantation. Tumours were analysed 12 days post transplantation *via* flow cytometry. Indicated cell populations were calculated with respect to all viable CD8⁺ T cells (A-D) or all viable gp100-specific CD8⁺ T cells (E, F). A,B: Representative dot plots showing the gating for gp100-specific CD8⁺ T cells in tumour (A) and lung (B). C,D: Frequencies of gp100-specific CD8⁺ T cells in tumour (C) and lung (D). E,F: Frequencies of indicated activation markers on gp100-specific CD8⁺ T cells in tumour (E) and lung (F). Data from 2-5 individual experiments are shown. Mean frequencies ± SEM are plotted. Statistical analysis was performed by Mann-Whitney test. GzmB = Granzyme B. * = p≤0.05, ** = p≤0.01.

3.6.3 Tumour CD8⁺ T cell exhaustion levels are decreased with lung infection.

In response to prolonged antigen exposure, CD8⁺ T cells experience a progressive loss of effector function. This includes impaired cytokine production and reduced cytotoxicity. This functional decline is associated with the upregulation of co-inhibitory receptors such as PD-1 and TIM3 [104]. Therefore, we looked at the expression of TIM3 and PD-1. Increased expression of the combination of both markers mirrors a highly dysfunctional status of these cells [29]. In non-infected mice, many PD-1^{high} TIM3⁺ CD8⁺ T cells in the tumour and only few PD-1^{int} TIM3⁻ CD8⁺ T cells were found.

In agreement with the stronger activation observed during infection, we also find significantly fewer dysfunctional CD8⁺ T cells in the tumour. These differences were observed for bulk CD8⁺ T cells (Figure 3-12 A, B) as well as for tetramer-specific tumour-specific CD8⁺ T cells (Figure 3-12 C).

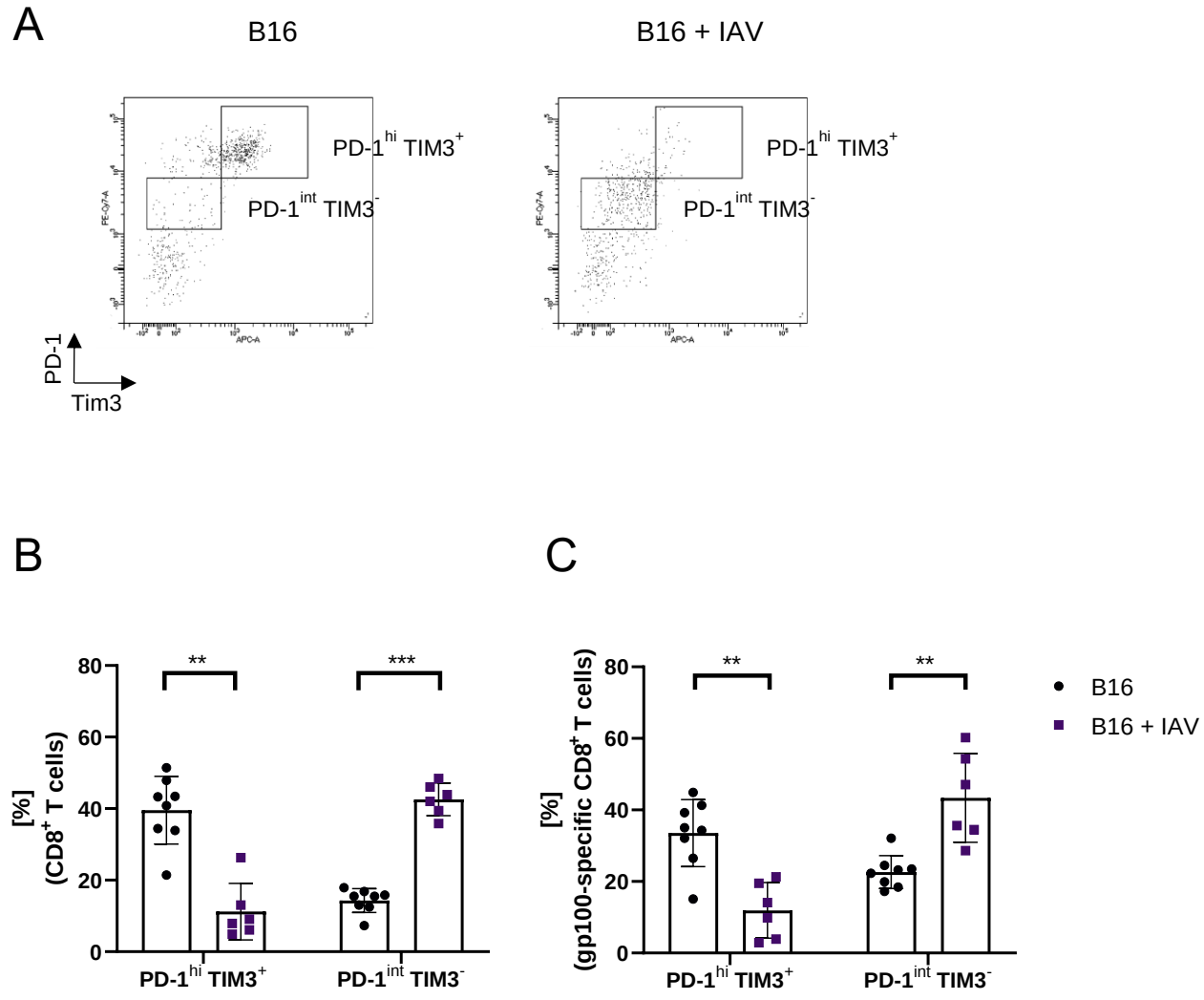

Figure 3-12 CD8⁺ T cells and gp100-specific T cells show a less exhausted phenotype upon influenza infection.

B16F1 tumour cells were transplanted subcutaneously into C57BL/6 mice. Mice were i.n. infected with IAV 4 days post tumour transplantation. Tumours were analysed 12 days post transplantation *via* flow cytometry. A: Representative dot plots of Flow cytometry. B,C: Frequencies of PD-1^{high} TIM3⁺ and PD-1^{int} TIM3⁻ cell populations with respect to all CD8⁺ T cells (B) or gp100-specific CD8⁺ T cells (C) in the tumour. Statistical analysis was performed by Mann-Whitney test. ** = p≤0.01, *** = p≤0.001.

3.6.4 CD4⁺ T cells in the tumour are not affected by Influenza infection.

After characterizing CD8⁺ T cells, we next focused on CD4⁺ T cells. In agreement with the observation that CD4⁺ T cells are not required for tumour growth inhibition, since tumours were still smaller upon infection despite CD4⁺ T cell depletion, differences

were not observed in tumour-derived CD4$^+$ T cells with or without lung infection. Population sizes of CD4$^+$ T cells in general (as shown already in Figure 3-7) and of FOXP3$^+$ Tregs specifically were comparable (Figure 3-13 A, B). Also activation profiles, namely the expression of CD43 and GzmB, did not alter in the tumours of mice with or without additional infection (Figure 3-13 C). In addition to the depletion experiments conducted previously, we conclude that CD8$^+$ T cells, but not CD4$^+$ T cells, have an important role in tumour growth inhibition.

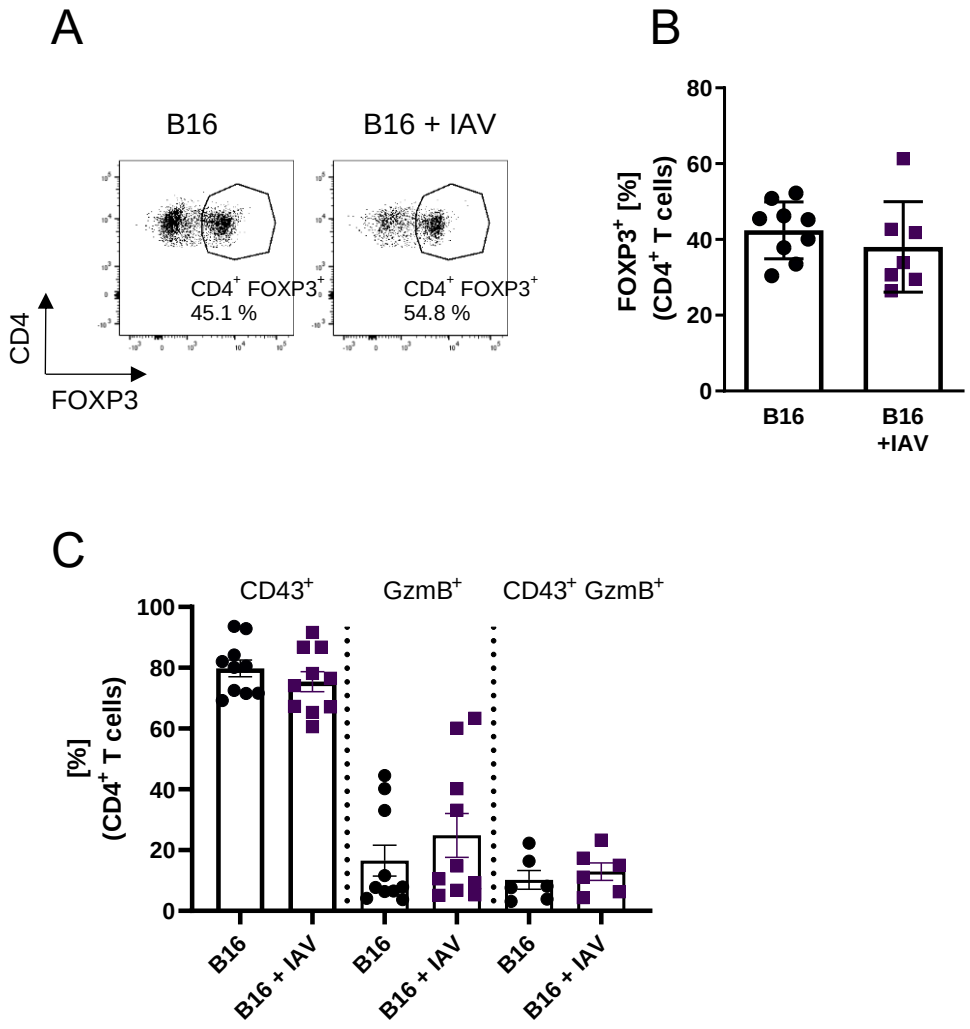

Figure 3-13 Neither regulatory T cells nor CD4$^+$ T cells in general are altered in the tumour upon influenza infection.

B16F1 tumour cells were transplanted subcutaneously into C57BL/6 mice. Mice were i.n. infected with IAV 4 days post tumour transplantation. Tumours were analysed 12 days post transplantation *via* flow cytometry. Indicated cell populations were calculated with respect to all viable CD4$^+$ T cells (B, C) A: Representative dot plots showing the gating for FOXP3$^+$ CD4$^+$ T cells in the tumour. B: Frequencies of FOXP3$^+$ CD4$^+$ T cells in the tumour following the gating in B. C: Frequencies of indicated activation markers on CD4$^+$ T cells in the tumour. Data from 3 individual experiments are shown. Mean frequencies ± SEM are plotted.

3.7 Cytokine and chemokine levels are altered in tumour, serum and lung.

In order to understand why there is an increased activation of tumour-specific $CD8^+$ T cells during an IAV infection, the concentrations of various cytokines and chemokines in the lung, the serum and the tumour were measured next. Absolute cytokine/chemokine levels in tumour, lung and serum were measured by Luminex analysis 8 days post infection, which corresponds to 12 days after tumour cell transplantation.

In the tumour, cytokine levels were generally low. Interestingly, upon infection, many cytokine levels decreased even further. As depicted in Figure 3-14, only few cytokine levels were unchanged, i.e. levels of TNFα. Chemokine levels of CCL5, CXCL10, and cytokines IL-6 and IL-10 were decreased, whereas levels of IL-17 were slightly increased. Overall, the cytokine/chemokine milieu in the tumour was only slightly affected by the IAV infection.

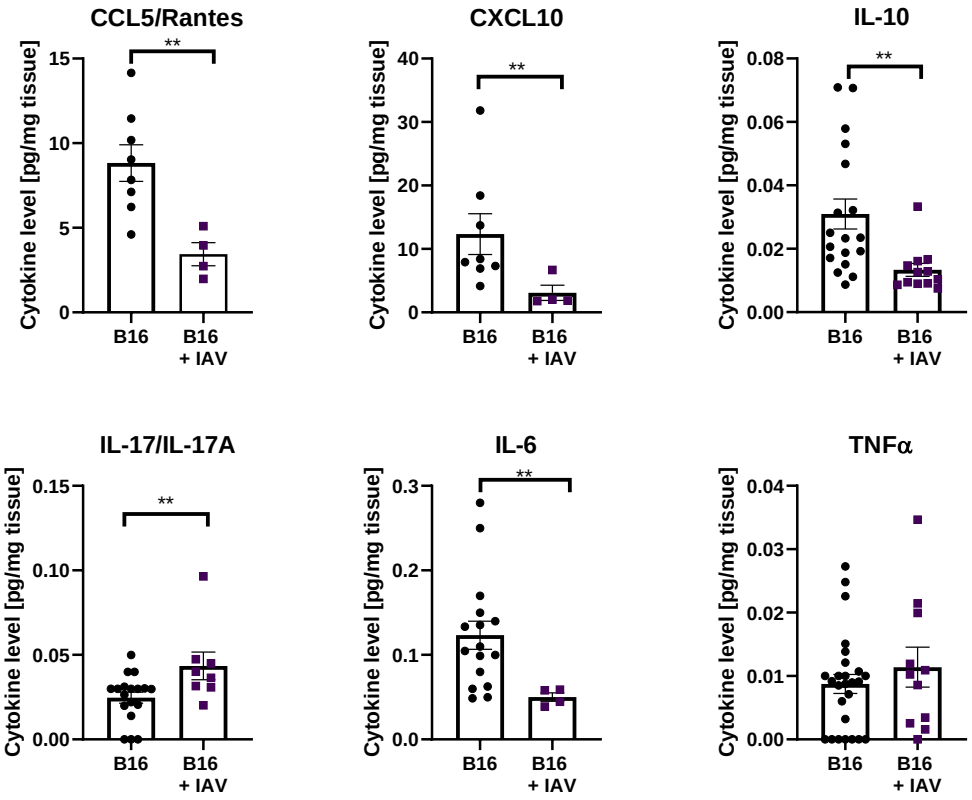

Figure 3-14 Cytokine and chemokine levels in the tumour are mostly decreased upon influenza infection.

B16F1 tumour cells were transplanted subcutaneously into C57BL/6 mice. Mice were i.n. infected with IAV 4 days post tumour transplantation. Tumours were analysed 12 days post transplantation, corresponding with 8 days post

influenza infection with 150 PFU. Tumour biopsies were homogenized and supernatants were analysed by Luminex. Cytokine levels were normalised to biopsy weight to obtain cytokine level per tissue-mass. Significance was calculated by Mann Whitney t test. ** = p≤0.01.

Also TGFβ plays an important role in regulating immune responses. For example, current studies suggest a role for the IFNα response in positive cross-talk between IFNα and TGFβ signalling [105], whereas other studies observed TGFβ in its more prominent role as an anti-inflammatory factor, in that case limiting IFNα anti-tumour effects [106]. Relative *Tgfβ* levels were determined *via* qPCR in the tumour. *Tgfβ* mRNA levels were slightly decreased in the tumour 8 days post influenza infection (Figure 3-15). This is in agreement with the observation that lung IFNα levels did only slightly increase 8 dpi as seen before (Figure 3-5).

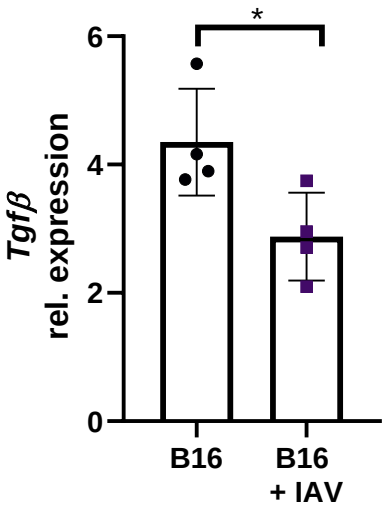

Figure 3-15 *Tgfβ* levels in the tumour are slightly decreased upon influenza infection.

B16F1 tumour cells were transplanted subcutaneously into C57BL/6 mice. Mice were i.n. infected with IAV 4 days post tumour transplantation. Tumours were analysed 12 days post transplantation, corresponding with 8 days post influenza infection with 300 PFU. Tumour biopsies were homogenized, RNA was isolated from the supernatants, transcribed to cDNA and analysed *via* qPCR. Significance was calculated by Mann Whitney t test. * = p≤0.05.

Serum was extracted from cranial blood collected directly after mouse sacrifice. Especially inflammatory cytokines like IFNγ, TNFα or IL-6 showed increased serum levels in mice with infection compared to non-infected mice (Figure 3-16). On the other hand, also the anti-inflammatory cytokine IL-10 was increased when mice were infected. In the immune response this is important to prevent an overshooting immune response.

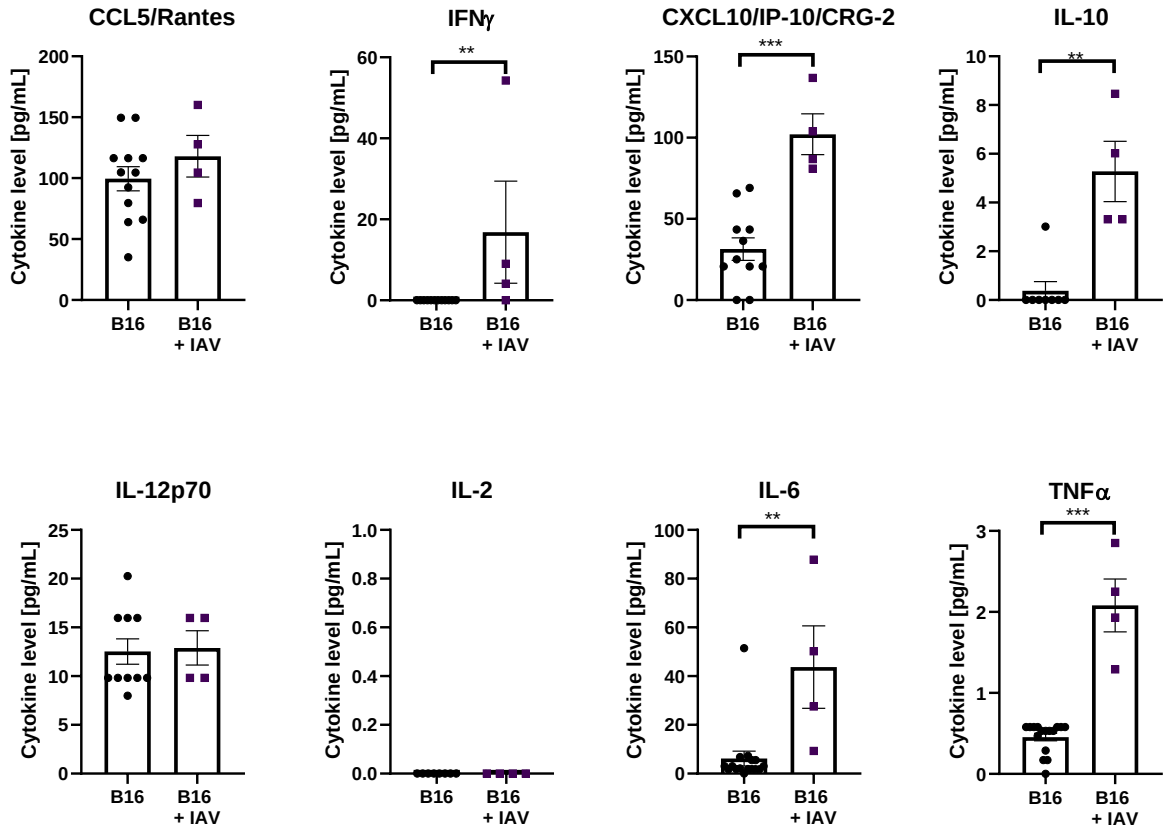

Figure 3-16 Cytokine and chemokine levels in the serum are partly increased upon influenza infection.

B16F1 tumour cells were transplanted subcutaneously into C57BL/6 mice. Mice were i.n. infected with IAV 4 days post tumour transplantation. Serum was analysed 12 days post transplantation, corresponding with 8 days post influenza infection with 150 PFU. Cranial blood was collected immediately after sacrifice and serum was extracted. Significance was calculated by Mann Whitney t test. ** = p≤0.01, **** = p ≤ 0.0001.

In contrast to the general decrease in cytokine and chemokine levels in tumours after IAV infection, a strong increase in mainly pro-inflammatory cytokines in the infected lung could be determined (Figure 3-17). This is not surprising since IAV is an infection of the lung, so local cytokine increase was expected whereas the tumour as a distant organ is affected in the opposite way. Specifically, levels of the chemokines CCL5 and CXCL10 and the cytokines IL-10, IL-6 and TNFα were increased. Levels of IL-12, IL-2 and IL-17 were not or only slightly increased. None of the measured cytokine levels showed a decrease.

One of the chemokines which was increased in the IAV-infected lung was CXCL10. This observation has been described previously for IAV [107].

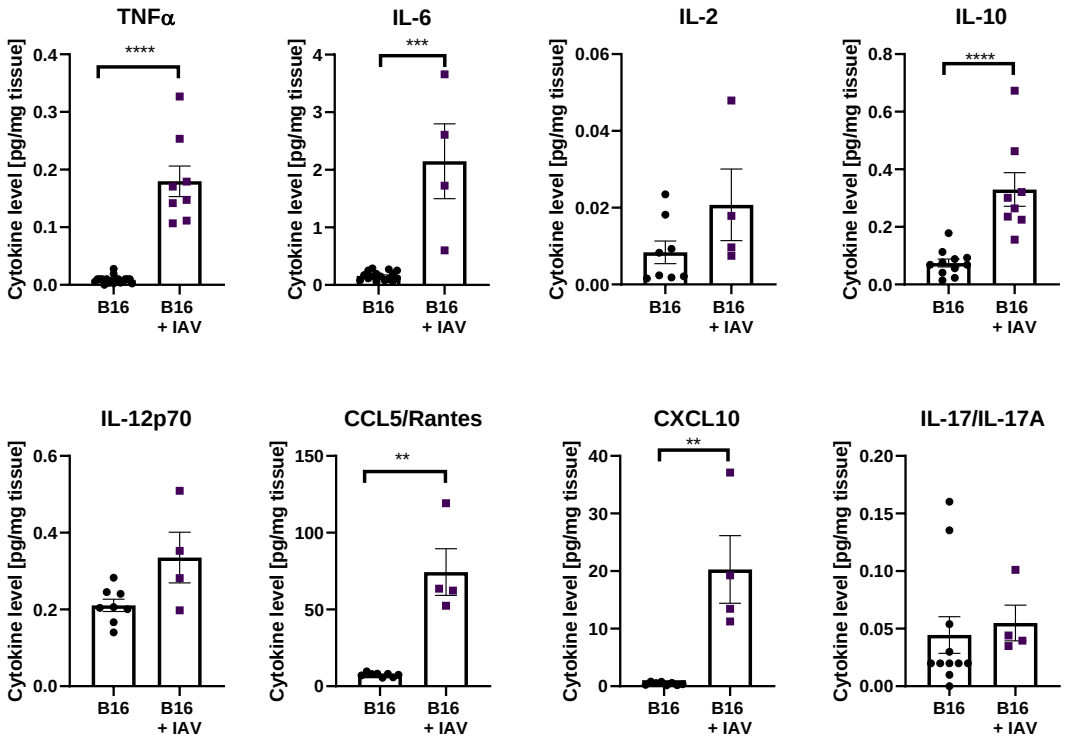

Figure 3-17 Cytokine and chemokine levels in the lung are strongly increased upon influenza infection.

B16F1 tumour cells were transplanted subcutaneously into C57BL/6 mice. Mice were i.n. infected with IAV 4 days post tumour transplantation. Lungs were analysed 12 days post transplantation, corresponding with 8 days post influenza infection with 150 PFU. Lung biopsies were homogenized and supernatants were analysed by Luminex. Cytokine levels were normalised to biopsy weight to obtain cytokine level per tissue-mass. Significance was calculated by Mann Whitney t test. *** = p≤0.001, **** = p ≤ 0.0001.

When directly comparing cytokine levels in tumour and lung, it is obvious that cytokine levels are much higher in the lung than in the tumour. Studying cytokine levels in infected mice reveals a highly pro-inflammatory milieu in the lung and a highly anti-inflammatory milieu in the TME. Although also IL-10 levels are significantly higher in the lung than in the tumour, this might be compensated by the bulk of pro-inflammatory cytokines that are stronger increased in the lung compared to the tumour.

3.8 Migration is required for tumour growth inhibition.

The previously observed overall anti-inflammatory TME and pro-inflammatory setting in the lung could be the basis for lymphocyte migration from the tumour to the lung upon infection. In agreement with this, an increased population of tetramer-binding

tumour-specific CD8$^+$ T cells was detected (Figure 3-11). Therefore, the following section focuses on the direct analysis of migration of the lymphocytes.

3.8.1 Egress from lymphocytic organs.

Fingolimod (FTY720) prevents egress from lymphoid organs as described in section 2.3.2.5. We could already show the importance of CD8$^+$ T cells for tumour growth inhibition. Next, FTY720 application was used to distinguish between the requirement for CD8$^+$ T cell activation within the tumour or *de novo* infiltration of activated CD8$^+$ T cells from lymphoid organs into the tumour. When inhibiting infiltration during IAV infection of tumour bearing mice, a decrease in tumour growth inhibition was observed (Figure 3-18).

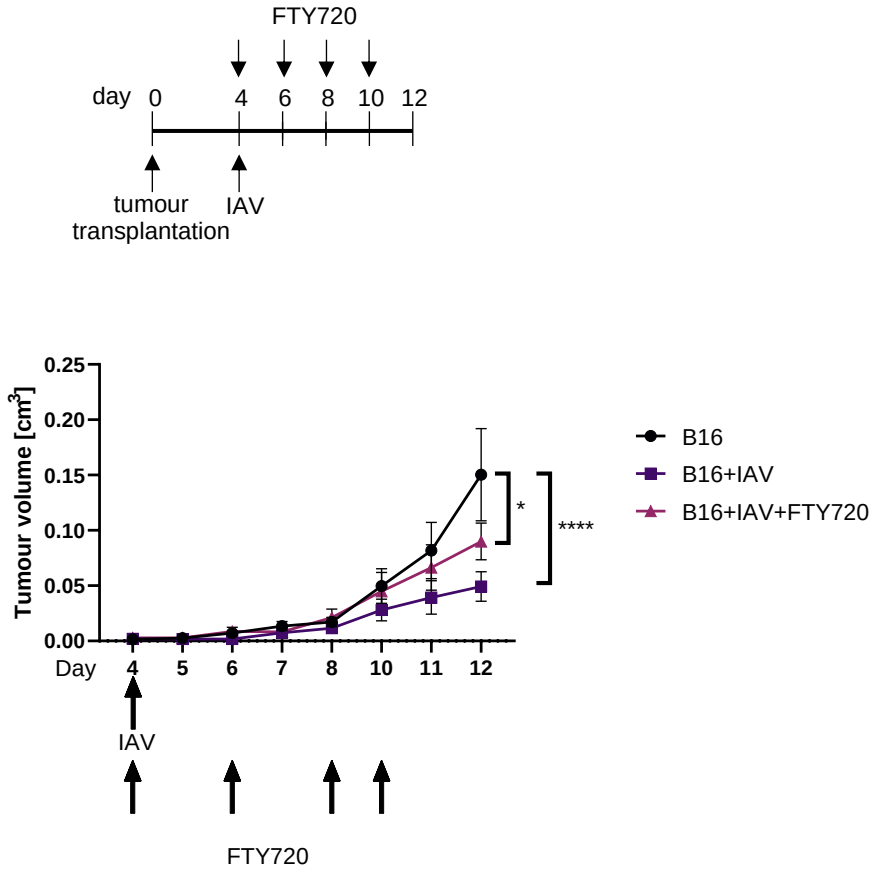

Figure 3-18 Fingolimod treatment impairs tumour growth inhibition.

B16F1 tumour cells were transplanted subcutaneously into C57BL/6 mice. Mice were i.n. infected with IAV 4 days post tumour transplantation. 1 mg/kg body weight FTY720 was applied i.p. every other day, as indicated. Tumours were measured and the volume was calculated as described in section 2.3.2.1 following formula (2). Data from 2 individual experiments are shown. Mean tumour sizes ± SEM are plotted. Statistical analysis was performed by 2way ANOVA, followed by Tukey's multiple comparisons test. * = p≤0.05, **** = p ≤ 0.0001.

3.8.2 Tumour CD8$^+$ T cells migrate from the tumour to the lung.

To characterise migration in more detail, endogenously marked CD8$^+$ T cells were used to track their migration in infected mice. Briefly, CD8$^+$ T cells were isolated from tumours of Thy1.1$^+$ mice and adoptively transferred into wildtype mice, which are Thy1.1$^-$ (Figure 3-19, A). Thy1.1$^+$ cell numbers were compared in infected and non-infected mice in different organs: Lung and tumour as sites of the two immunological challenges of interest and the spleen as a lymphoid organ that is independent of direct affection of both challenges. In the spleen, there was no difference in Thy1.1$^+$ CD8$^+$ T cells with or without infection, neither in absolute (Figure 3-19 B) nor in relative populations (Figure 3-19 C). Both, tumour and lung showed more Thy1.1$^+$ cells in infected mice compared to non-infected mice. In infected lungs, this effect was even stronger than in the respective tumours. So transferred tumour-derived CD8$^+$ T cells (Thy1.1$^+$) do not only migrate to the tumour but upon infection also to the lung. This is in line with the detection of CD8$^+$ T cells specific for the gp100 tetramer in the infected lung.

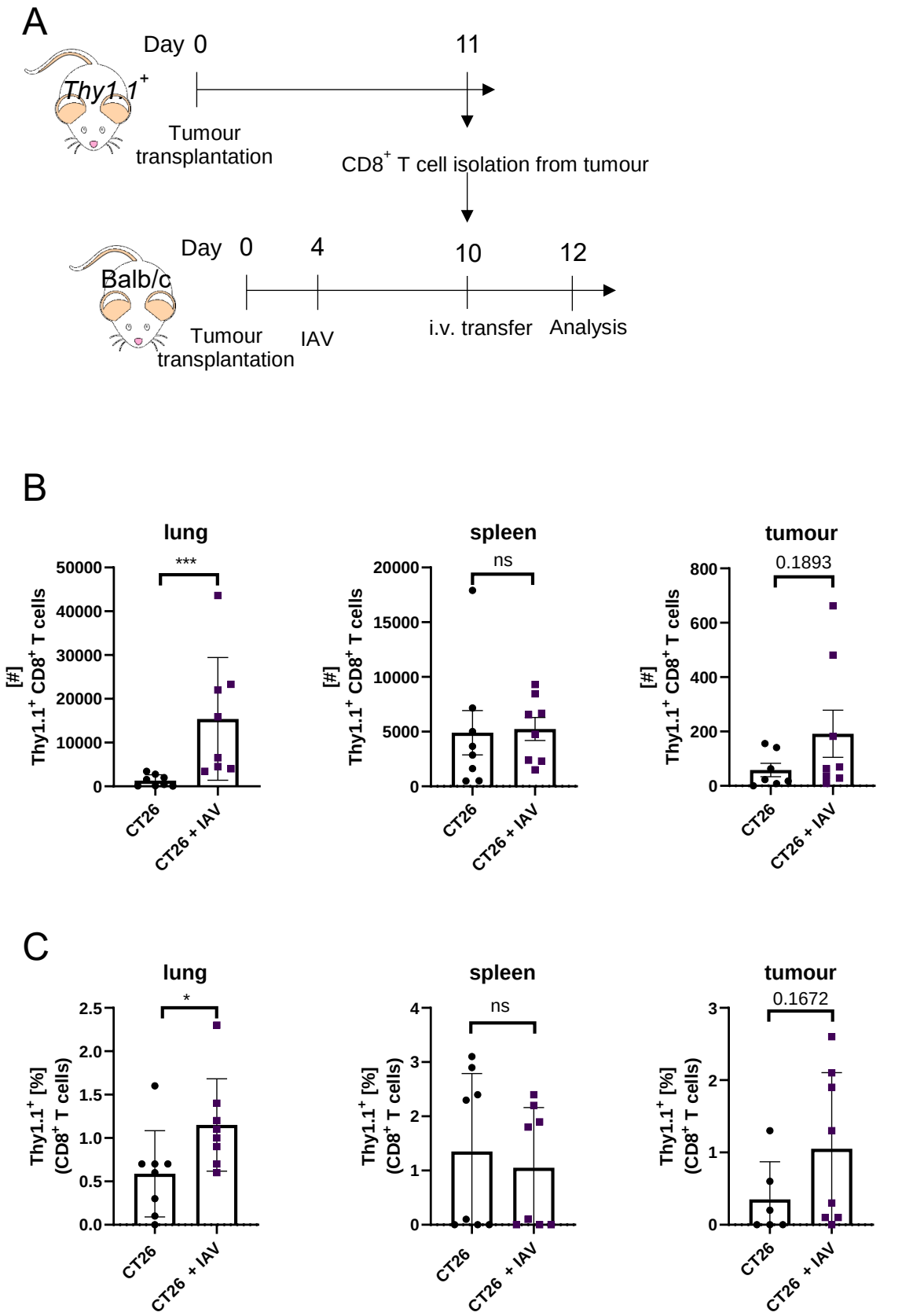

Figure 3-19: Tumour CD8⁺ T cells migrate in the lung in adoptive cell transfer.

CT26 tumour cells were transplanted subcutaneously into *Thy1.1*⁺ mice. 11 days post tumour transplantation, CD8⁺ T cells were isolated from these tumours *via* MACS and adoptively transferred into Balb/c mice. Recipient mice had

CT26 tumour cells subcutaneously transplanted 10 days prior to cell transfer and were i.n. infected with IAV 4 days post tumour transplantation. 12 days post tumour transplantation in Balb/c mice, corresponding with 2 days post adoptive cell transfer, cell numbers and frequencies of Thy1.1$^+$ CD8$^+$ T cells were determined in lung, spleen and tumour. A: Experimental setup. B: Absolute cell numbers of Thy1.1$^+$ CD8$^+$ T cells in the indicated organs. B: Cell frequencies of Thy1.1$^+$ CD8$^+$ T cells in the indicated organs Data from 2 individual experiments are shown. Statistical analysis was performed by Mann-Whitney test. * = p≤0.05, *** = p≤0.001.

3.8.3 CXCR3 is required for migration and tumour growth inhibition.

Since migration of CD8$^+$ T cells was shown to be important for tumour growth inhibition, chemokines responsible for recruitment were analysed in more detail. As shown in section 3.7, serum and lung cytokine levels of CXCL10 were increased in infected mice at 8 days post infection compared to non-infected mice. CXCL10 is one of three known ligands for C-X-C motif chemokine receptor 3 (CXCR3) and acts as a chemoattractant for CXCR3-expressing immune cells [108]. Apart from CXCL10, also CXCL9 and CXCL11 are known ligands.

For IAV, an active recruitment of CXCR3$^+$ NK-cells has been described [109, 110]. Interestingly, CXCR3 expression was elevated on melanoma-specific CD8$^+$ T cells in the tumour in our model (Figure 3-20 A, B). This may suggest a basis for T cell migration, following the CXCL10 gradient, especially with decreased CXCL10 levels in tumours of infected mice compared to those without infection (Figure 3-14). Therefore, the requirement for CXCR3 was tested by blocking this factor in our experimental setup. Indeed, this blockade did reverse tumour growth inhibition upon infection (Figure 3-20 C). In line, CXCR3 seems to be involved in recruiting melanoma-specific CD8$^+$ T cells from the tumour to the lung: As described previously, infection leads to an increase of gp100-specific CD8$^+$ T cells in the lung (Figure 3-11). Upon CXCR3 blockade, there was a clear decrease of this CD8$^+$ T cell population in the infected lungs, indicating an impaired recruitment and thus an important role for CXCR3-mediated migration (Figure 3-20 D).

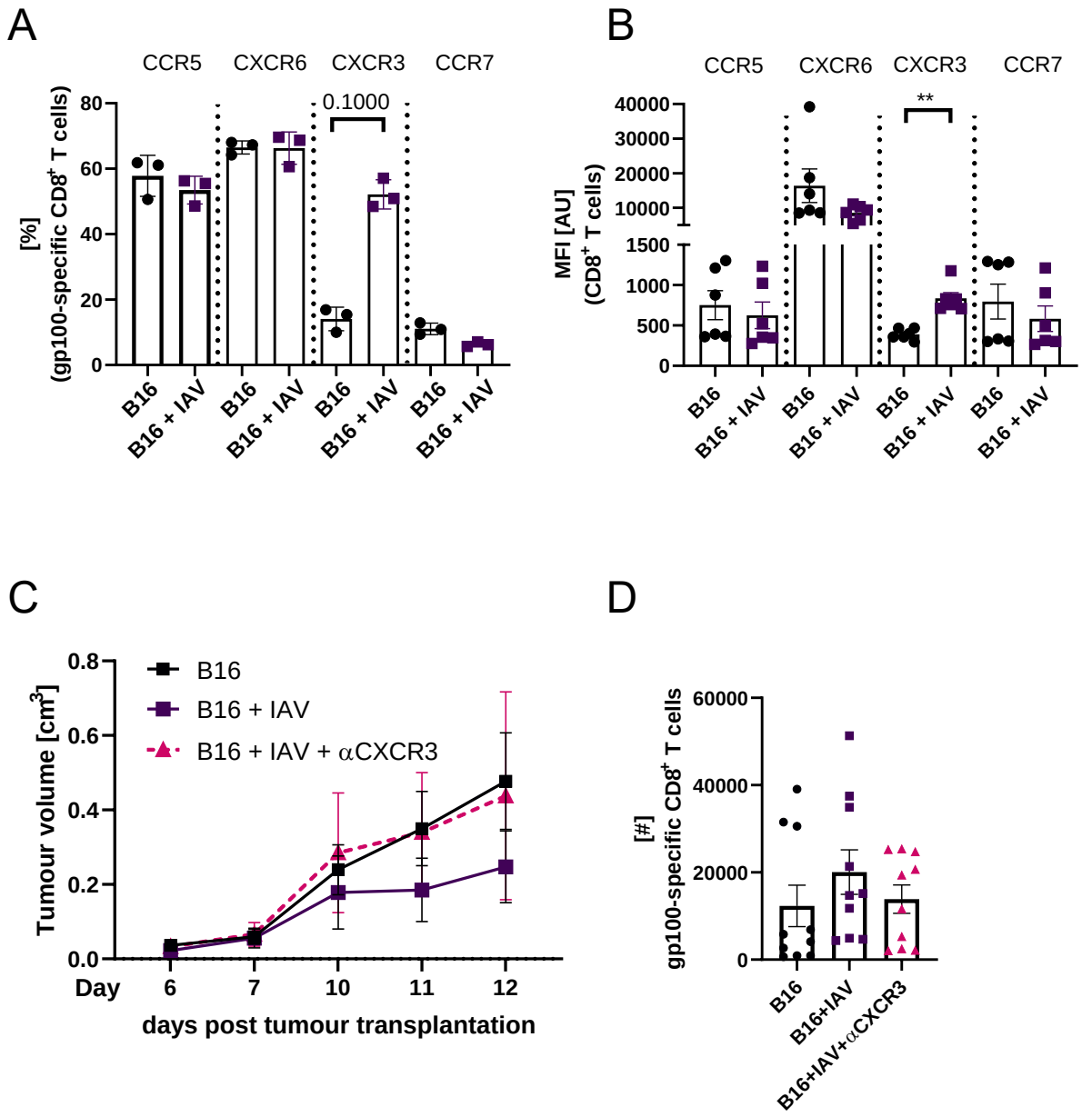

Figure 3-20 The CXCL10-CXCR3 axis is altered in infected mice and CXCR3 is required for tumour growth inhibition and tumour CD8⁺ T cell migration.

B16F1 tumour cells were transplanted subcutaneously into C57BL/6 mice. Mice were i.n. infected with IAV 4 days post tumour transplantation. A,B: Tumours were analysed 12 days post transplantation *via* flow cytometry. Indicated cell populations were calculated with respect to viable gp100-specific CD8⁺ T cells or MFI was measured with respect to viable CD8⁺ T cells. Data from 1-2 experiments are shown. C: Antibodies were applied i.p. at the indicated days. Tumours were measured and the volume was calculated as described in section 2.3.2.1 following formula (2). Data from one experiment are shown. Mean tumour sizes ± SD are plotted. D: Cell numbers of gp100-specific CD8⁺ T cells in the lung at day 12 of the experiment indicated in C. Data from one or two experiments are shown. Mean frequencies ± SD are plotted. Statistical analysis was performed by Mann-Whitney test (A, B and D) and by 2way ANOVA, followed by Tukey's multiple comparisons test (C). * = p≤0.05, ** = p≤0.01. MFI = Median fluorescence intensity, AU = Arbitrary units.

3.9 Contribution of Influenza-specific CD8$^+$ T cells.

So far, an increased activation of CD8$^+$ T cells in general and of gp100-specific CD8$^+$ T cells specifically was detected in the tumour in our infection setup. In the following, the impact of influenza-specific CD8$^+$ T cells on tumour development was defined.

3.9.1 NP-specific CD8$^+$ T cells in the TME.

An MHC tetramer specific for the influenza nucleoprotein (NP) was chosen to focus on IAV-specific CD8$^+$ T cells. NP-specific T cells were detectable in the TME (Figure 3-21 A). A deeper characterisation of these cells showed that they were strongly activated as shown by expression of CD43 and Granzyme B (Figure 3-21 B). Interestingly, the activation level did not depend on the organ: In IAV-infected lungs, the strongly activated NP-specific T cells are expected; but remarkably, also in the tumour, these cells still showed a comparable activation and proliferation (Figure 3-21 B). Also when comparing the activation status of the NP-specific CD8$^+$ T cells to that of tumour antigen gp100-specific CD8$^+$ T cells, they are on similar levels (Figure 3-11).

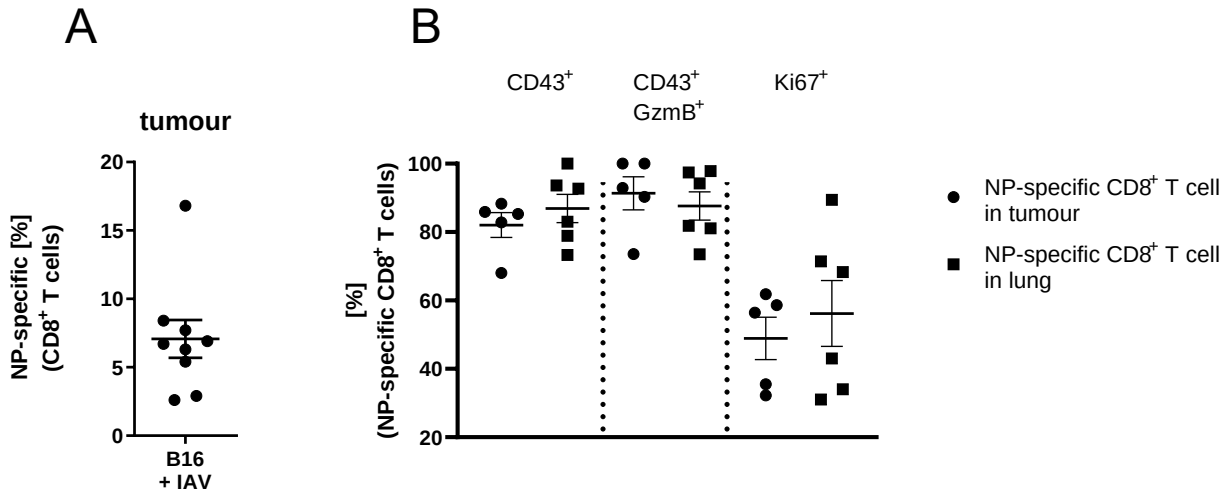

Figure 3-21 Identification and characterization of NP-specific CD8$^+$ T cells.

B16F1 tumour cells were transplanted subcutaneously into C57BL/6 mice. Mice were i.n. infected with IAV 4 days post tumour transplantation. Tumours and lungs were analysed 12 days post transplantation *via* flow cytometry. A: NP-specific CD8$^+$ T cells were calculated with respect to all viable CD8$^+$ T cells. B: Frequencies of indicated activation markers on NP-specific CD8$^+$ T cells in tumour and lung. Data from 2 or 3 experiments are shown. Mean frequencies ± SEM are plotted. GzmB = Granzyme B, NP = Nucleoprotein.

3.9.2 Influenza CD8⁺ T cells do not perform a "bystander" effect in controlling tumour growth.

Influenza infection induces specific T cell responses. Additionally, levels of cross-protection or heterologous immunity have also been observed when patients [111, 112] or mice [113] were previously infected with different types of IAV, due to cross-reactive T cells against conserved proteins. Also, T cells can be activated due to pro-inflammatory cytokines, including IFNs or TLR agonists. This effect is referred to as "bystander effect" which also evokes T cell cross-reactivity, for example against a different virus which is unrelated to the initial viral infection [114]. In this way, an influenza infection could potentially evoke non-specific T cell responses against the tumour. Indeed, this effect has been observed for orthotopic 3LL mouse lung tumour [115]. Therefore, we tested if in the present model, influenza CD8⁺ T cells alone would perform tumour growth inhibition to any degree. For this purpose, CD8⁺ T cells from influenza infected lungs were isolated 8 days post infection and intravenously transferred into tumour bearing mice. As depicted in Figure 3-22, this transfer was not sufficient to inhibit tumour growth. The timing for adoptive cell transfer as 7 days post tumour transplantation reflects a time where the adaptive immune response would arise when mice are infected at day 4 after tumour cell transplantation. Transfer did not facilitate tumour inhibition, hence the influenza CD8⁺ T cells do not perform a bystander effect in tumour growth inhibition. Still, future studies should clarify this further for example in *CD8*$^{-/-}$ or *Rag2*$^{-/-}$ mice.

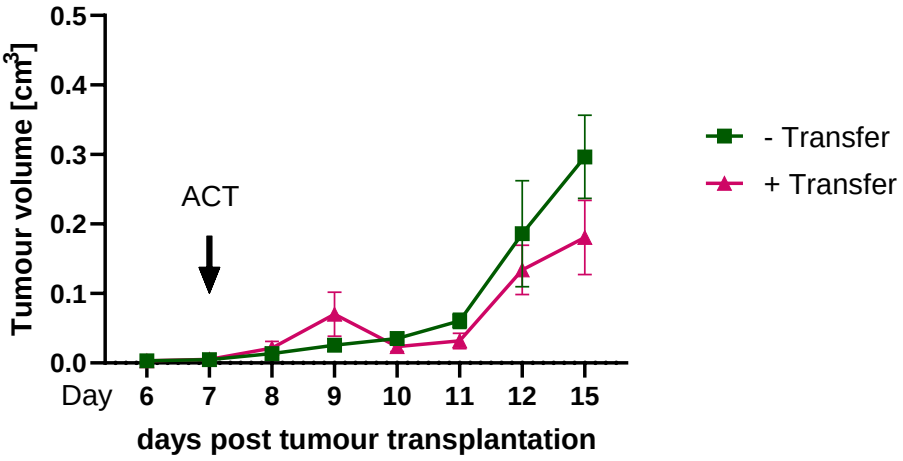

Figure 3-22 IAV CD8⁺ T cells alone do not perform tumour growth inhibition.

B16F1 tumour cells were transplanted subcutaneously into C57BL/6 mice. 7 days post tumour transplantation, mice received 5 × 10^5 CD8⁺ T cells i.v. from infected lungs at 8 days post their infections. Tumours were measured and the volume was calculated as described in section 2.3.2.1 following formula (2). Data from 2 individual experiments

are shown. Mean tumour sizes ± SEM are plotted. Tumour sizes were not significantly different based on a 2way ANOVA followed by Tukey's multiple comparisons test. ACT = Adoptive cell transfer.

3.10 Succession, but not the absolute timing of infection is decisive for tumour growth inhibition.

The so far established tumour models focused on an early infection during tumour development. An infection however can occur at any time during the course of cancer. Additionally, the treatment for cancer is not only based on the type of cancer but also on the stadium of the disease. Therefore, it is important to study the impact of the timing of infection onset.

3.10.1 Infection at a later time still leads to tumour growth control.

Four days post tumour transplantation, the tumours usually become palpable. Hence, this mirrors an early timing in the course of tumorigenesis. Clinically, this would be the earliest possible treatment start. Stochastically, more tumours will be discovered at a later time. In order to test whether the inhibitory effect of an IAV infection is also effective in more advanced tumours, tumour-bearing mice were infected with IAV 10 days after transplantation (Figure 3-23 A). Figure 3-23 B shows significantly smaller tumours after 8 days of infection in both scenarios, infection after 4 days and infection after 10 days post tumour transplantation. Tumours of mice that were infected on day 10 showed an average size of 0.150 cm^3 after 18 days of tumour growth, whereas non-infected mice had tumours of an average size of 0.546 cm^3 on day 18. This shows that the previously observed effect is not dependent on an early infection.

In agreement with the tumour size development, cell characterisation likewise showed a stronger $CD8^+$ T cell activation upon additional infection, in both, early and late infection. As observed in the early infection model, increases in $CD43^+$ and Granzyme B^+ $CD8^+$ T cell populations were observed in the late infection model (Figure 3-23 C).

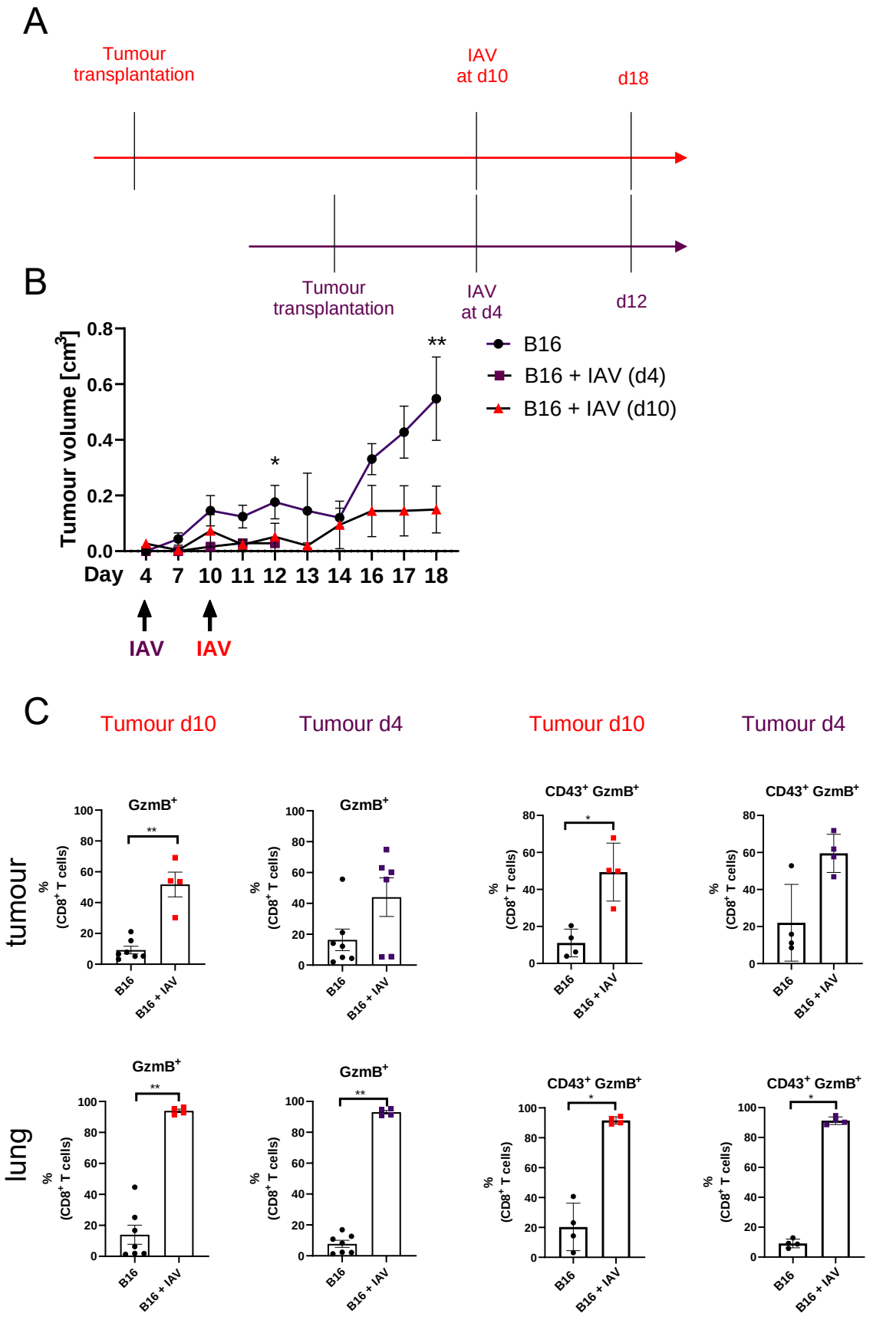

Figure 3-23 IAV infection at a later time still leads to tumour growth inhibition.

B16F1 tumour cells were transplanted subcutaneously into C57BL/6 mice. Mice were i.n. infected with IAV 4 days post tumour transplantation or 10 days post tumour transplantation. A: Experimental setup. B: Tumours were measured and the volume was calculated as described in section 2.3.2.1 following formula (2). Data from 2 individual experiments are shown. Mean tumour sizes ± SEM are plotted. Statistical analysis was performed by 2way ANOVAs for early or late infection, followed by Tukey's multiple comparisons test. C: Frequencies of indicated activation markers on $CD8^+$ T cells in tumour and lung. Data from 1 or 2 individual experiments are shown. Mean frequencies ± SEM are plotted for Granzyme B and mean frequencies ± SD for CD43 Granzyme B. Statistical analysis was performed by Mann-Whitney test. * = p≤0.05, ** = p≤0.01. GzmB = Granzyme B.

3.10.2 Prior infection results in enhanced tumour growth.

A previous study by Kohlhapp *et al*. investigated the effect of IAV infection on survival of tumour bearing mice. They showed that mice that had an IAV infection prior to tumour transplantation had a more severe tumour development than non-infected mice [88]. This disadvantageous tumour development is in contrast to the finding of this thesis. To reproduce these findings, mice were also infected with IAV 3 days before tumour transplantation (Figure 3-24 A). Interestingly, tumour growth was significantly increased compared to mice infected 4 days after tumour transplantation (Figure 3-24 B).

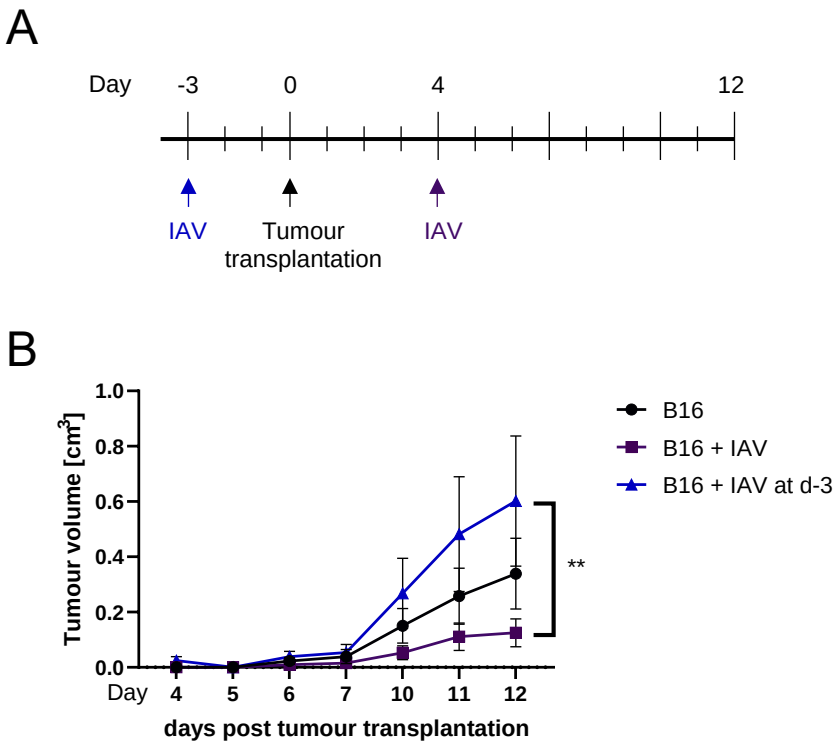

Figure 3-24 Preceding IAV infection enhances tumour growth.

B16F1 tumour cells were transplanted subcutaneously into C57BL/6 mice. Mice were i.n. infected with IAV either 3 days prior to tumour transplantation or 4 days post tumour transplantation. Tumours were measured and the volume was calculated as described in section 2.3.2.1 following formula (2). Data from 2 individual experiments are shown. Mean tumour sizes ± SEM are plotted. Statistical analysis was performed by 2way ANOVA, followed by Tukey's multiple comparisons test. ** = p≤0.01.

3.11 Tumours do not influence the immune response against infection.

So far, the present study focused on changes in the immunology of a solid tumour in case of a viral respiratory infection. Since the applied model involves two immunological challenges, the tumour and the infection, the following section will describe the impact of tumour transplantation on lung immunology during influenza infection.

3.11.1 Virus levels are not changed by the presence of a distal tumour.

To study possible changes in the immune response against IAV infection, viral titres were determined with or without a subcutaneously transplanted tumour. Viral titres were determined by qPCR (Figure 3-25 A) or by Plaque Assay (Figure 3-25 B). Neither detection method revealed changes in viral titres in infected mice with or without a B16 tumour. Likewise, the tumour did not significantly affect the body weight development upon infection (Figure 3-25 C). So, IAV titres are not affected by tumour transplantation.

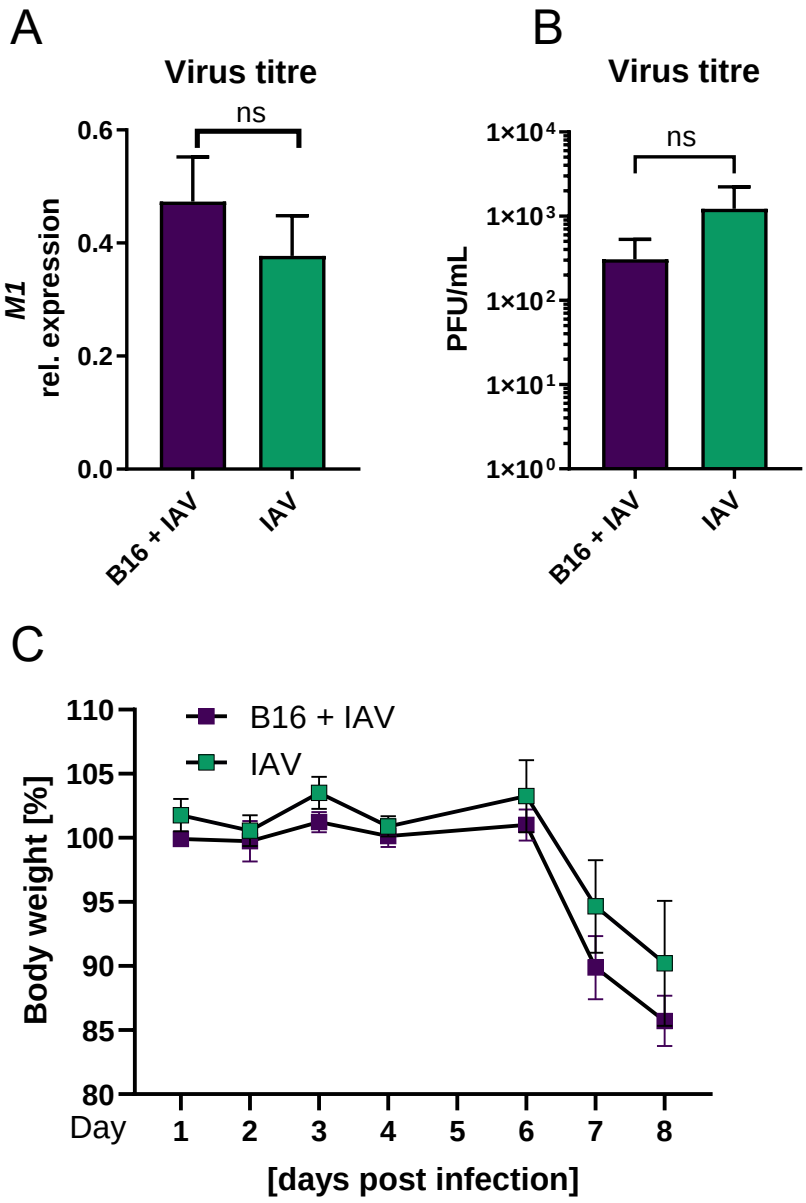

Figure 3-25 Viral titres in lungs and body weight development of IAV infected mice is not altered with or without distal tumour transplantation.

B16F1 tumour cells were transplanted subcutaneously into C57BL/6 mice. Mice were i.n. infected with IAV 4 days post tumour transplantation. Lungs were analysed 12 days post tumour transplantation, corresponding to 8 days post infection. Viral levels without a tumour were measured 8 days post infection A: Viral loads as determined by qPCR. Relative *M1* expression was calculated with respect to *Rps9* expression. B: Viral loads as determined by Plaque Assay. Data from 2-4 mice are shown. Statistical analysis was performed by Mann-Whitney test. C: Body weight development of infected mice. Data from 2 individual experiments are shown. Mean body weights ± SEM are plotted. PFU = Plaque forming units.

3.11.2 Lung cytokine levels are not changed by the presence of a distal tumour.

As expected, a very strong pro-inflammatory milieu could be detected in the infected lung, i.e. cytokine and chemokine levels were significantly increased compared to non-infected mice (Figure 3-26). Most levels were similar in infected lungs with or without

a tumour (“B16+IAV” or “IAV” respectively). Only IL-17 showed differences: With a tumour, levels were decreased in infected lungs compared to non-infected, tumour bearing mice, whereas only an infection without an additional distal tumour led to increased IL-17 levels. Although this results in a significant difference between infected lungs with or without a tumour, IL-17 levels are generally low so that the absolute difference is small compared to most other cytokines and chemokines where an absolute higher difference results in non-significant changes. Overall, cytokine/chemokine levels were increased upon infection and were generally not affected by the presence of a distal tumour.

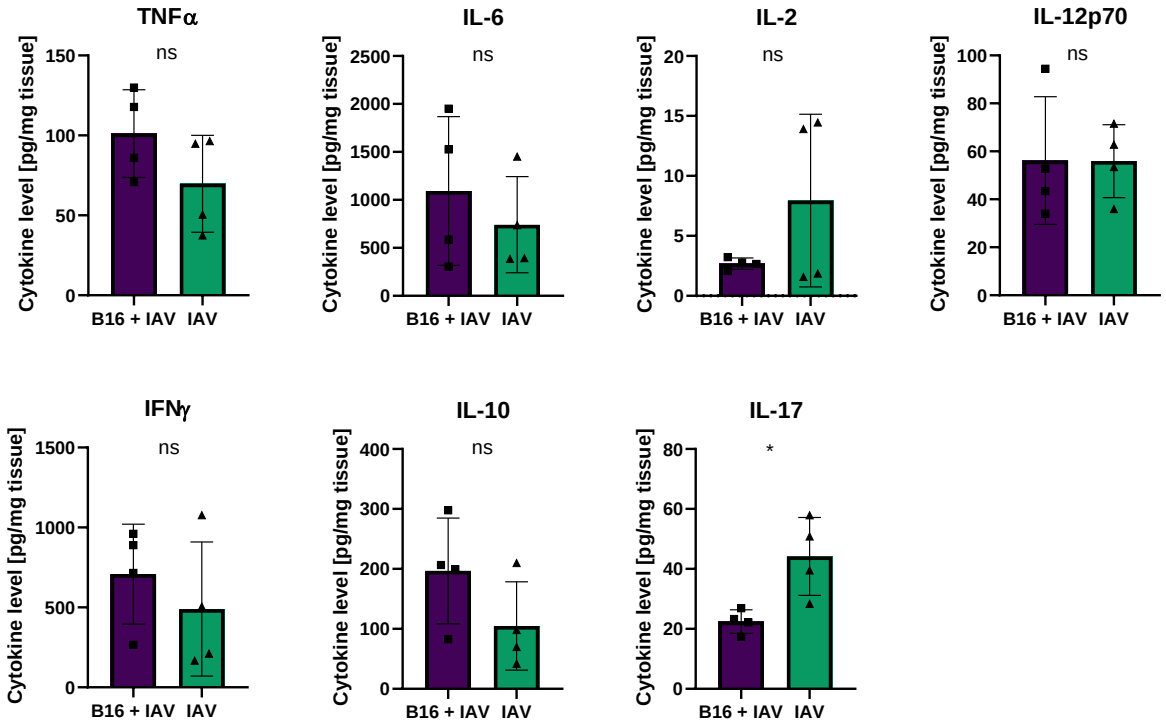

Figure 3-26 Lung cytokine levels of IAV infected mice with or without tumour transplantation.

B16F1 tumour cells were transplanted subcutaneously into C57BL/6 mice. Mice were i.n. infected with IAV 4 days post tumour transplantation. Lungs were analysed 12 days post transplantation, corresponding with 8 days post influenza infection. Viral levels without a tumour were measured 8 days post infection. Lung biopsies were homogenized and supernatants were analysed by Luminex. Cytokine levels were normalised to biopsy weight to obtain cytokine level per tissue-mass. Values of 1 experiment are shown. Mean levels ± SD are plotted. Significance was calculated by Mann Whitney test. * = p≤0.005.

3.12 Friend virus infection does not limit tumour growth

The results of the present study suggest that IAV-related inflammation in the lung leads to recruitment and activation of tumour-specific $CD8^+$ T cells. To assess whether this

effect is exclusively applicable to the lung and IAV infection, the influence of a systemic infection on tumour control was investigated.

The Friend Virus (FV) is a murine leukaemia retrovirus. The target cells of FV infection are nucleated erythroid precursors, therefore leading to a systemic infection with the spleen as a central organ of infection due to its role in blood filtration and the hence high blood flow rate.

To study the effect of a systemic infection on tumour growth, mice were infected with FV 4 days after tumour transplantation in accordance with the IAV experiments. Importantly, no smaller tumour sizes were observed any more but on the contrary, tumours were significantly bigger: ⌀ 0.857 cm^3 without infection and ⌀ 1.366 cm^3 upon FV infection (Figure 3-27).

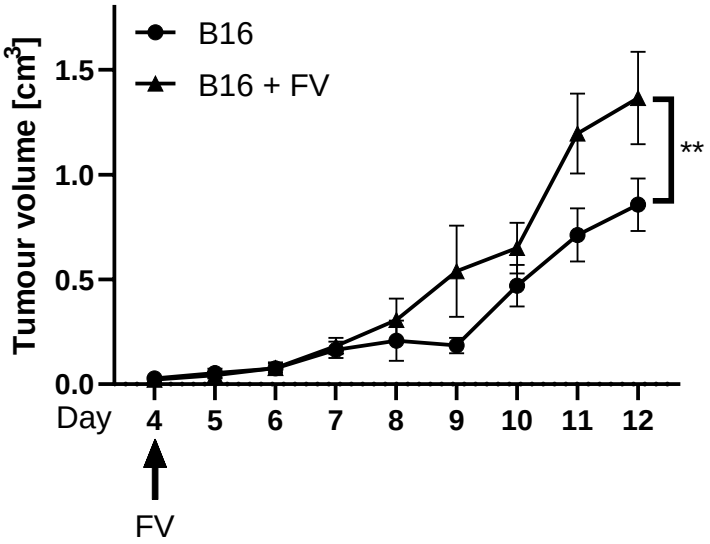

Figure 3-27 Friend virus infection enhances tumour growth.

B16F1 tumour cells were transplanted subcutaneously into C57BL/6 mice. Mice were i.v. infected with FV 4 days post tumour transplantation. Tumours were measured and the volume was calculated as described in section 2.3.2.1 following formula (2). Data from 4 individual experiments are shown. Mean tumour sizes ± SEM are plotted. Statistical analysis was performed by 2way ANOVA, followed by Tukey's multiple comparisons test. ** = p≤0.01.

4 Discussion

The immunological response towards a tumour or cancer is a complex process in which a multitude of different cell types and other immunologically active factors interact. In this regard, a solid tumour can be infiltrated by immune cells, among others, even of distal origin. Therefore, another immunological challenge, such as an infection, can alter the response in the TME, even if locally separated. In general, it is often assumed that infections have a negative effect on the outcome of cancer patients, like cancer is assumed a risk factor for influenza infection [116]. In fact, the present study was able to show that infections can definitely have a positive influence on the T cell response to tumours. To date, this field of how an infection alters tumour immunology is highly understudied and hence not yet understood. For the present thesis, an influenza A virus infection was used to analyse this interaction. An influence of this infection of the respiratory tract on a locally distinct tumour was demonstrated. The infection enables a tumour growth inhibition due to enhanced $CD8^+$ T cell activation in immunocompetent mice. A better understanding of this interplay of a tumour with other immunological challenges is the initial basis that is required at an early stage in the development of improved therapeutic options so that insights into possible interactions can be directly considered or even used. A previous study showed that lung cancer patients that were additionally hospitalized because of an influenza infection during their course of cancer indeed showed reduced mortality [117]. This supports the findings of this thesis in the human situation empirically.

4.1 The impact of IAV infection on distal tumours: Model and T cell contribution

Based on the experiments described, this thesis suggests the following model (Figure 4-1). The generally immunosuppressive TME in melanoma shows only few strongly activated $CD8^+$ T cells. In case of an influenza infection, $CD8^+$ T cells follow the inflammatory gradient to the infected lung in a CXCR3-dependent manner. In the highly pro-inflammatory milieu in the lung, $CD8^+$ T cells are strongly activated, including the recruited tumour $CD8^+$ T cells. These activated $CD8^+$ T cells might then migrate back to the tumour, for example “following” the antigenic epitope which they are primed for (discussed in [118]) or *via* other means. With their increased activation, these $CD8^+$ T cells perform tumour growth inhibition more effectively.

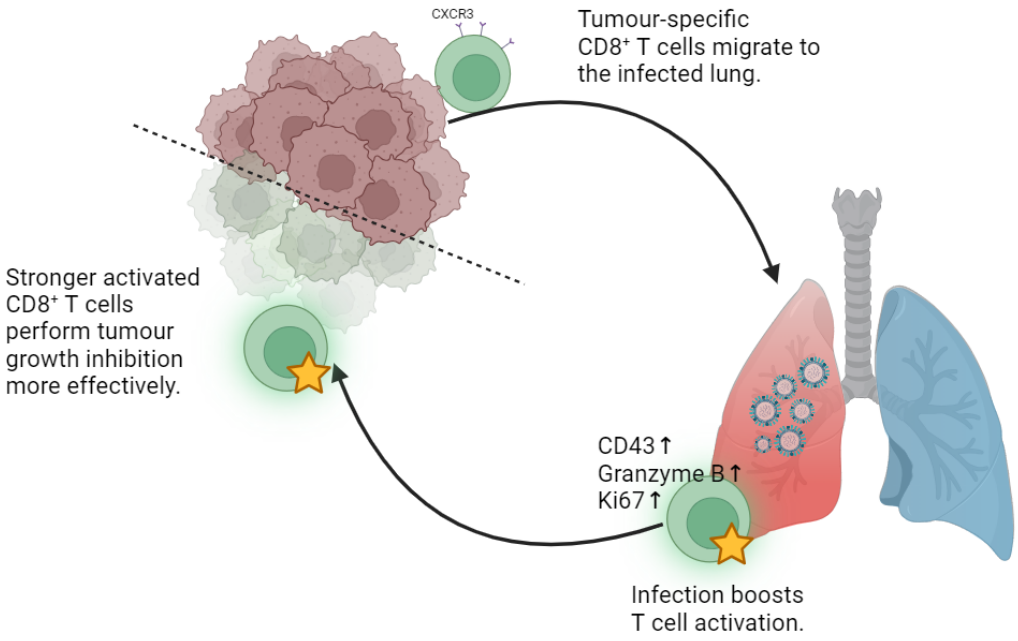

Figure 4-1 Viral respiratory infection induces CD8⁺ T cell activation and thereby induces tumour growth inhibition.

Upon viral lung infection with IAV, CD8⁺ T cells migrate from a distal tumour to the infected lung. In the highly pro-inflammatory milieu, the CD8⁺ T cells are boosted in their activation and express more activation and proliferation markers. Therefore, these CD8⁺ T cells are able to fight the tumour more efficiently upon migration back to the TME.

Importantly, the observed tumour growth inhibition is not dependent on a specific type of tumour or mouse strain but is indeed dependent on viral replication, whereas an inactivated virus is not sufficient for the described effect. Previous studies focused on an anti-tumoural effect of the influenza vaccine when it was directly injected into the TME [117]. Newman *et al*. describe that this injection provokes a TME development from an anti-inflammatory, “cold” tumour towards a pro-inflammatory, “hot” tumour if the vaccine was injected intratumourally but not when applied intramuscularly as performed in the normal process of vaccination. Like in the present thesis, the authors used the B16 melanoma model.

In vitro, B16 cells are permissive for infection by IAV, although not ideal since the addition of trypsin appears to be necessary to maintain the replication cycle [89, 119]. In search for an oncolytic virus against B16, Chen *et al*. tested different viruses for their oncolytic effects *in vitro* and finally decided against IAV due to comparably low cell lysis [89]. However, this effect has been described *in vivo* for an influenza infection

during non-small cell lung cancer (NSCLC) [87]. Like melanoma, NSCLC comprises a highly anti-inflammatory TME. IAV infection leads to NSCLC tumour cell lysis, however, this also requires support by macrophages which help in remodelling the TME towards a more pro-inflammatory milieu. The tumour type, i.e. the cellular origin determines the receptor expression. Lung cancer patients show elevated levels of sialic acids [120]. NSCLC cells indeed express sialoglycoproteins [121], i.e. the receptors required for influenza infection. The skin on the other hand lacks the targets for influenza infection so that melanoma is no target of influenza cell lysis [117]. One further difference apart from the type of tumour is the distance between infection and tumour: NSCLC is a lung tumour, therefore IAV infection and tumour are in direct proximity and the virus does not have to migrate but can directly reach the tumour cells. In the presented model in this thesis, the virus is not found in the tumour or replicates there. Therefore, the observed tumour growth inhibition is not the result of direct cell lysis by the virus, as also this thesis shows no detection of viral RNA in the tumour. Instead, the tumour is fought by modulating the immune response, most likely by $CD8^+$ T cell activation.

Of the tested ones in this thesis, the depletion of no other immune cell population but $CD8^+$ T cells led to diminished tumour growth inhibition. The previously mentioned study of an IAV-induced anti-tumour effect on NSCLC identified macrophages to be a main driver of this effect [87].

It is well established that an influenza infection evokes a strong $CD8^+$ T cell response. These CTLs migrate to the infected lung as the site of infection. To clear the viral infection, they target and kill infected epithelial cells in the lung [76]. The outcome of both diseases, tumour and influenza infection, has been shown to be improved with the abundance of more or pre-existing $CD8^+$ T cells [73, 122]. In this thesis, also tumour-specific $CD8^+$ T cells showed increased activation as well as decreased exhaustion phenotypes in the tumours of infected mice compared to non-infected mice. Both indicate more functional $CD8^+$ T cells upon infection.

With respect to T cell specificity, an antigen overlap between influenza and melanoma cannot be completely excluded. Also other diseases than cancer can induce a repertoire of tumour-associated antigens (TAAs). These are self-antigens with an abnormal high abundance on tumour cells and can therefore serve as a potentially known target in the immune response against the tumours. Examples for such

diseases that elicit TAAs are asthma, allergies, infections or autoimmune disorders [123]. Influenza infection indeed produces tumour-associated antigens for 3LL mouse lung tumour [115]. Infection with LCMV can produce TAAs, especially the acute infection enabled mice to control LLC tumours [124]. Studies in healthy individuals revealed a repertoire of already existing TAAs, including TAAs associated with melanoma as reviewed in [123]. In this sense, influenza infection could produce TAAs that support the observed tumour growth inhibition. On the other hand, the observed effect of tumour growth inhibition was consistent in all tested tumour models. This makes an antigen overlap as underlying mechanism rather unlikely.

The present work suggests that tumour-specific $CD8^+$ T cells also migrate to the lungs by processes similar to the recruitment of influenza-specific $CD8^+$ T cells to the lungs. It is well studied that a pro-inflammatory milieu enhances $CD8^+$ T cell function [19]. The sensitivity for antigen, proliferation and trafficking of $CD8^+$ T cells can be modulated by cytokines [125-127]. Concerning specific factors, this study could show that IFNγ is required for tumour growth inhibition. In this regard, it is not clear whether IFNγ is required for its direct effect on tumour cells or for its indirect effect *via* T cell activation. Direct effects of IFNγ on tumour cells include inhibition of proliferation and angiogenesis and enhancement of apoptosis [128]. However, opposite effects of tumour-promoting functions of IFNγ have also been reported [129]. Despite the effects on tumour cells and on T cells, IFNγ can also act on further players of the immune system: In an anti-tumour manner, e.g. immune cells of the innate immune system can be recruited and tumoricidal factors by macrophages are enhanced. However, also Treg and MDSC development is increased by IFNγ [129]. This thesis showed clear anti-tumour effects of IFNγ. IFNα and IFNβ levels were increased in tendency in the tumours of mice infected with IAV 8 dpi but in contrast to IFNγ, type I IFNs were not required for tumour growth inhibition. Although required for full tumour growth inhibition, tumour IFNγ levels were not increased in infected mice 8 dpi but strongly increased in the infected lung 8 dpi. Since IFNγ is likely involved in $CD8^+$ T cell activation, this also indicates that the activation or boosting takes place outside the TME in the infected lung. Interestingly, type I IFNs seem to enhance granzyme B expression in CTLs [130] whereas this has not (yet?) been described for IFNγ.

The detected increased proportion of cytotoxic $CD8^+$ T cells expressing granzyme B in IAV-infected tumour-bearing mice could have a direct effect on tumour growth. CTLs are crucial for an anti-tumour response. In this regard, even a small amount of

peptide:MHC complexes is sufficient to trigger cytotoxicity [131, 132]. Once in the target cell, granzyme B activates cascading processes that lead to induction of apoptosis. It cleaves specific proteins, particularly caspase-3, which is a key protein in the apoptosis signalling pathway. Upon recognition, target cell killing can occur quickly within minutes [133].

To prevent tissue damage, CTLs gain a dysfunctional phenotype upon constant antigen exposure, as also seen in the current model. These dysfunctional $CD8^+$ T cells on the one hand do not perform target cell killing anymore and on the other hand even create or sustain an immunosuppressive environment in melanoma [134]. In fact, this thesis was able to show that the proportion of highly exhausted $CD8^+$ T cells indicated by high PD-1 and TIM3 expression was significantly reduced in the tumour when the tumour-bearing mice were infected with IAV. This fits with the idea that tumour-specific T cells in the lung, i.e. outside the tumour and the high antigen concentration, are activated under strongly pro-inflammatory conditions.

Studies in human patients showed that also vaccination with the seasonal influenza vaccine induces a cytokine response [135]. However, the conventional inactivated vaccine, which is predominantly used in Western countries, induces an immune response which is mainly antibody-driven [136] whereas T cell-driven immune responses are difficult to achieve with inactivated vaccines in humans [137]. In agreement to this, the experiments with inactivated virus did not show the effect of tumour growth inhibition. The background here could be that on the one hand, the immune response towards the inactivated IAV is also in this model not T cell-driven and on the other hand, that the process of viral replication and distribution is missing and hence the longer lasting immune activation due to the infection. During the process of virus replication, PRRs are repeatedly activated, which are responsible for the induction of further immune cascades [138].

As shown in this study, the specific timing of infection of tumour-bearing mice is not decisive for the suggested model: Both, an early and a late infection after tumour onset lead to the observed tumour growth inhibition. In contrast, infection prior to tumour onset showed more severe tumour development as shown in previous studies [88]. The authors explained this by increased exhaustion of $CD8^+$ T cells in this setup as indicated by stronger PD-1 abundance. These higher PD-1 levels were found specifically on anti-melanoma $CD8^+$ T cells compared to anti-influenza specific

$CD8^+$ T cells which were both found in the infected lung. Interestingly, this is consistent with this thesis in which likewise, tumours demonstrated accelerated growth upon infection prior to tumour cell transplantation. Immunobiochemical modelling showed in a previous study that the antigen abundance seems to determine the PD-1 expression [139]. The PD-1:PD-L1 interaction determines the motility of $CD8^+$ T cells: Higher interaction results in lower motility and lower interaction results in higher $CD8^+$ T cell motility [139]. Indeed, Kohlhapp *et al*. measured increased PD-1 levels in infection, enabling in turn increased PD-1:PD-L1 interactions. However, in this model, PD-1 levels were not elevated, which may facilitate a decrease in PD-1:PD-L1 interaction and therefore also less dysfunctional $CD8^+$ T cells were detected. The higher or lower PD-1 expression is in well agreement with the observation described by Kohlhapp *et al.* that in their model, the tumour $CD8^+$ T cells are stuck in the lung, which is in agreement with decreased motility. However, in the present model, the tumour $CD8^+$ T cells migrate back to the tumour, in agreement with the higher motility. That indeed the CTL motility is required for tumour growth inhibition is supported by the FTY720 experiment in this thesis in which the restricted migration likewise showed a clear decrease in tumour growth inhibition, as discussed in the next section. The main difference in the study by Kohlhapp *et al*. to this thesis is that the tumour was transplanted after infection. The results of the current work thus indicate that infection during a tumour event does not negatively affect this migration of $CD8^+$ T cells. In the clinics, an acute infection of patients during ongoing progression of tumour growth is presumably the more common case compared to tumour manifestation during an acute infection. However, previous virus contacts or cross-immunities could potentially reverse the observed effects in humans.

In general, the smaller tumours upon infection may also be the result of a lack of supply due to impaired angiogenesis as shown in this thesis. Yet, it could also be the other way round, that the smaller tumours do not need as much nutrition due to their smaller sizes and therefore induce less angiogenetic factors.

4.2 The requirement of T cell migration

The herein suggested model is based on $CD8^+$ T cell migration from the anti-inflammatory milieu in the tumour to the pro-inflammatory milieu in the infected lung. One possibility to study migration is its manipulation. FTY720 leads to the

internalisation of S1P which is a receptor required for egress from lymphoid organs. This treatment can indicate whether the observed tumour growth inhibition in this model requires *de novo* lymphocyte infiltration or if the pre-existing $CD8^+$ T cells in the tumour are sufficient. At the same time, it also suggests where the actual activation of the T cells takes place. Application of FTY720 abrogated the influenza-induced tumour growth inhibition showing the necessity of migration or in this case of egress from lymphoid organs. In the clinics, FTY720 is used under the name fingolimod for treatment of multiple sclerosis [140]. Indeed, fingolimod treatment of patients seems to be associated with increasing skin diseases including several cancer types like melanoma [141]. Also there, this is explained with a general immunosuppression as lymphocyte egress from lymphoid organs is suppressed.

In the herein presented model, migration to the lung seems to happen in a CXCR3-dependent manner. The role of CXCR3 in both diseases, tumour and influenza infection, has been previously studied. Indeed, knock-out of CXCR3 led to impaired $CD8^+$ T cell infiltration into the lung in influenza infection [142]. In the same study, transfer experiments with $Thy1.1^+$ mice similar to the experiments in this work showed a clear impairment but not full loss of migration upon CXCR3 deficiency. Likewise, in the present work, tumour-specific $CD8^+$ T cells are reduced but not abolished upon antibody-mediated CXCR3-blockade. Interestingly, the inhibition of CXCR3 expression on T cells and thereby limiting their migration to tumours seems to be one mechanism of TGFβ-mediated immunosuppression [143]. Indeed, *Tgfb* mRNA levels in this model were decreased in the tumour 8 days post IAV infection compared to tumours of non-infected mice. CXCR3 deficiency did not impair IFNγ levels in the lungs of influenza-infected mice [142] whereas others showed a T cell activating role of CXCR3. Concerning CXCR3 ligands, an attractant function and also T cell activating effect of CXCL10 was observed previously. CXCL10 expression in tumours is associated with a better prognosis [144]. In melanoma, among other tumours, the expression of CXCL9, which is another ligand for CXCR3, correlates with high $CD8^+$ T cell infiltration, at least in co-expression with CCL5 [145, 146]. In this regard, CXCR3 has also been shown to be required for successful anti-PD-1 therapy, specifically the interaction with its ligand CXCL9 [146]. This chemokine expression could also be one reason for the migration of $CD8^+$ T cells back into the tumour. Tumour-specific $CD8^+$ T cells may follow the antigen gradient for which they are primed into the tumour. However, this thesis showed that not only tumour specific $CD8^+$ T cells migrate back into the tumour,

but the observation that also NP-specific, i.e. influenza-specific $CD8^+$ T cells are found in the TME indicates that $CD8^+$ T cells in general may migrate into the tumour. As described above, CXCL9 is a good candidate that could be responsible for this observed migration. The exact mechanisms of attraction of $CD8^+$ T cells to the lung and back to the tumour remain to be deciphered. Ongoing experiments determine CXCL9 levels in tumours of infected and non-infected mice.

4.3 Does T cell activation occur in the lung?

The lung itself is a highly immunogenic organ. Due to its exposure to various kinds of environmental or infectious factors upon breathing, it bears a wide variety of immune cells, including cells of the innate and of the adaptive immune system [147]. The present thesis suspects the lung to be the place for the boosting of tumour-derived $CD8^+$ T cells. In fact, the data on Friend Virus show that an infection that is not localized in the lungs but is present systemically can have the opposite effect and promote tumour growth.

One characteristic of the lung is the presence of alveolar macrophages. Indeed, influenza infection induces a strong response of alveolar macrophages [148, 149]. Recently it has been shown that IAV-infection trained alveolar macrophages show anti-tumoural activities in the lung [150]. This aforementioned study focused on alveolar macrophages fighting local tumours in the lung. Tumour-associated macrophages however can have beneficial or detrimental effects on the tumour. Tumour-promoting properties include the production of angiogenetic factors [151] and anti-tumour activities are the release of pro-inflammatory cytokines and direct tumour cell phagocytosis among others [152]. In this thesis, the depletion of macrophages did not impair tumour growth. Since tumour growth inhibition was still present, they do not seem to be the driver for boosting activity. (Alveolar) macrophages therefore seem to be important for local anti-tumour effects in the lung but not at distal sites.

Macrophages do not only act as phagocytes directly but also as APCs and are therefore directly linked to $CD8^+$ T cell immunity. Other professional APCs are DCs which perform most of the antigen presentation. Also DCs are strongly activated upon IAV infection in the lung [153]. If tumour antigen carrying DCs should be present in the infected lung, lung lymph nodes or mucosa-associated lymphoid tissue (MALT), the DCs there could potentially also prime $CD8^+$ T cells tumour-specifically. In this study,

DCs were not further investigated but future experiments could indeed focus on the place of initial T cell priming and potential roles of DCs in CTL boosting.

The results presented in this thesis indicate the importance of the lung for the observed tumour growth inhibition. However, the contribution of other lymphoid organs to tumour growth inhibition cannot be excluded. The tumour-derived $CD8^+$ T cells could potentially be activated on their route to the lung, for example in lymph nodes. The enhanced tumour growth in the FV infection model indicates the importance of a distinct organ for tumour growth inhibition. IAV infection shows that the lung is such an organ, yet it remains elusive if it is the only one or if for instance infections of specifically the liver would show similar effects. One hallmark of the lung is the mucosa comprising the MALT [2]. If this should be vital, tumour inhibition could also benefit e.g. from gut, nose or genital tract infections among others since these organs likewise comprise a MALT. Independent of the specific organ, this thesis showed that $CD8^+$ T cells can be boosted not in the tumour but distally, in the periphery.

The question remains: How important is the lung as the initiating organ? In the FV infection model, there is no tumour growth inhibition but on the contrary, tumour growth was even accelerated. This points towards the importance of the lung – or at least a distinct organ – as the place for infection as the Friend Virus infection is of systemic nature. Therefore, infection models targeting other distinct organs could help in clarifying the role of specific organs like the lung. Others have shown, that in cytomegalovirus (CMV)-infected mice the immune response can be directed against the tumour by intra-tumoural application of viral peptides [154]. However, intra-tumoural application of viral peptides is not directly comparable to this study as it does not show the effect of infection. Like influenza, a CMV infection is attributed to organs, however there, multiple organs are targeted. Interestingly, one of these organs is the lung, meaning that this is also in agreement with the presented model.

Although viral infections generally trigger TLR sensing and responses, different viral infections trigger different TLRs which in turn raises different pro-inflammatory milieus. The infection with influenza is sensed by the intracellular TLRs TLR3, which senses dsRNA and TLR7 which senses ssRNA [155]. Interestingly, also acute FV infection is sensed by TLR3 [156]. TLR7 seems to induce a B cell driven immune response at a later time during infection [83] but seems dispensable for $CD8^+$ T cell induction [157]. This also seems to be the case for an influenza infection, for which a previous study

showed similar levels of NP-specific lysis in TLR7-KO mice [158]. If the observed effect of this thesis should be TLR-driven, this could indeed mean that the TLR-immune response in the lung is important.

Still, the boosting of $CD8^+$ T cells could also occur in the lymph node. This thesis indicates that tumour-specific $CD8^+$ T cells migrate from the tumour to the infected lung and that in the end, more highly activated CTLs are found in the tumour. However, the lung as the place for boosting is only indicated, other sites like the lymph node should not be ignored.

Different cancer types have different preferences in the organ they invade for metastases. Indeed, melanoma tends to spread to the lung [159]. It has been observed that primary tumours send systemic signals, which influence distant organs and form pre-metastatic niches. In this regard, B16 melanoma and LLC tumours act similarly [160]. CT26 acts *via* slightly different means but similar in the way that it “prepares” target organs for metastasis [160].

4.4 Clinical relevance and outlook

Many cancer therapy options are based on T cell manipulation [161]. For example, the most widely used therapy for solid tumours has become immune checkpoint blockade, which has revolutionized immunotherapy of cancer, including that of melanoma [162]. However, the clinical results still do not have the desired impact since too many patients do not respond to a satisfactory level [163]. Therefore, further developments in this area are highly mandatory. In this regard, identifying the pathways leading to $CD8^+$ T cell activation within this model may drive advancements in T cell manipulation strategies. It is important to note that the results of this thesis, in its current form, do not directly translate into clinical therapeutic applications involving infectious influenza virus. Therefore, the identification of the underlying pathway remains essential for therapeutic translation and this could indeed contribute to the development of new techniques to affect T cells for therapy.

One example of how the research on the infection-tumour-axis can be translated to the clinics is a clinical trial which started in 2021, in which the influenza vaccine is injected into the tumour prior to surgery (ClinicalTrials.gov Identifier: NCT04697576). The aim of this trial is to boost the patient’s immune response against the tumour. This

intralesional injection is in the direction of a previously mentioned study [117]. Although this is not the scope of this work, it shows the need to understand the interactions of immunological responses and even more importantly the potential we gain from this knowledge.

The results presented here may be used to provide a new therapeutic approach to tackle melanoma from a different angle. As discussed above, this thesis showed that these pathways include the CXCR3-CXCL10 axis as a basis for T cell migration to the site of inflammation and IFNγ, which could be involved in the boosting of the recruited $CD8^+$ T cells. The gained understanding from this research opens doors to potential applications in tumour therapy, where patients may benefit from treatments involving attenuated or modified viruses or the targeted application of specific factors. CXCL10 emerges as a promising candidate, particularly in combination with IFNγ and tumour derived antigens, to enhance the activation profile of recruited T cells. In this regard, triggering TLRs and their respective signalling using TLR ligands in combination with antigen could also potentiate the induced anti-tumour response. The accessibility of the lung through inhalers or nasal sprays adds an intriguing dimension to these prospects.

One common problem in melanoma and for example in ICB is the exhaustion of $CD8^+$ T cells. This emphasizes the necessity to identify pathways that prevent or reverse exhaustion. The results of the present work could also contribute to this aim. In summary, this thesis could show the substantial impact of a viral respiratory infection on distal tumour immunology. It demonstrated that several diseases clearly affect each other even if the organs are located separately. In this case, chemokine expressions were altered in tumour and lung, recruiting CTLs from the tumour to the lung, where they were boosted in activation so that upon migration back to the tumour, tumour growth inhibition was more efficient. Possible applications of the gained understanding here can be used in tumour therapy.

In conclusion, the influence of influenza virus infection on tumour immunology should find consideration in novel therapeutic approaches and the enhancement of CTL-mediated tumour treatments. This thesis highlights the complex interaction between infections and cancer, providing conceivable advances in the therapy of cancer patients.

5 References

1. Murphy, K.P., C. Weaver, L. Seidler, and C. Janeway, *Janeway Immunologie*. Immunologie. 2018, Berlin: Springer Spektrum.
2. Kindt, T.J., B.A. Osborne, and R.A. Goldsby, *Kuby immunology*. 6th ed. 2006, New York: W.H. Freeman & Company. 574.
3. DeFranco, A.L., *Signaling Pathways Downstream of TLRs and IL-1 Family Receptors*, in *Encyclopedia of Immunobiology*, M.J.H. Ratcliffe, Editor. 2016, Academic Press: Oxford. p. 106-114.
4. Siegal, F.P., et al., *The nature of the principal type 1 interferon-producing cells in human blood.* Science, 1999. **284**(5421): p. 1835-7.
5. McNab, F., et al., *Type I interferons in infectious disease.* Nature Reviews Immunology, 2015. **15**(2): p. 87-103.
6. Boehm, U., T. Klamp, M. Groot, and J.C. Howard, *CELLULAR RESPONSES TO INTERFERON-γ.* Annual Review of Immunology, 1997. **15**(1): p. 749-795.
7. Klein, U. and R. Dalla-Favera, *Germinal centres: role in B-cell physiology and malignancy.* Nature Reviews Immunology, 2008. **8**(1): p. 22-33.
8. Hwang, J.-R., Y. Byeon, D. Kim, and S.-G. Park, *Recent insights of T cell receptor-mediated signaling pathways for T cell activation and development.* Experimental & Molecular Medicine, 2020. **52**(5): p. 750-761.
9. Anthony A. Gaspari, S.K.T., Daniel H. Kaplan, *Clinical and Basic Immunodermatology*. 2 ed. 2017, Dordrecht ; New York: Springer. XVI, 895 p.
10. Gutcher, I. and B. Becher, *APC-derived cytokines and T cell polarization in autoimmune inflammation.* The Journal of Clinical Investigation, 2007. **117**(5): p. 1119-1127.
11. Schmitt, E. and C. Williams, *Generation and Function of Induced Regulatory T Cells.* Frontiers in Immunology, 2013. **4**.
12. Liu, C.-C., C.M. Walsh, and J.D.-E. Young, *Perforin: structure and function.* Immunology Today, 1995. **16**(4): p. 194-201.
13. Darmon, A.J., T.J. Ley, D.W. Nicholson, and R.C. Bleackley, *Cleavage of CPP32 by Granzyme B Represents a Critical Role for Granzyme B in the Induction of Target Cell DNA Fragmentation*.* Journal of Biological Chemistry, 1996. **271**(36): p. 21709-21712.
14. Strasser, A., P.J. Jost, and S. Nagata, *The many roles of FAS receptor signaling in the immune system.* Immunity, 2009. **30**(2): p. 180-92.
15. Tanaka, T., *Leukocyte Adhesion Molecules*, in *Encyclopedia of Immunobiology*, M.J.H. Ratcliffe, Editor. 2016, Academic Press: Oxford. p. 505-511.
16. Sperling, A.I., et al., *CD43 is a murine T cell costimulatory receptor that functions independently of CD28.* J Exp Med, 1995. **182**(1): p. 139-46.
17. Park, J.K., et al., *Enhancement of T-cell activation by the CD43 molecule whose expression is defective in Wiskott–Aldrich syndrome.* Nature, 1991. **350**(6320): p. 706-709.
18. Gerdes, J., et al., *Cell cycle analysis of a cell proliferation-associated human nuclear antigen defined by the monoclonal antibody Ki-67.* J Immunol, 1984. **133**(4): p. 1710-5.
19. Condotta, S.A. and M.J. Richer, *The immune battlefield: The impact of inflammatory cytokines on CD8+ T-cell immunity.* PLoS Pathog, 2017. **13**(10): p. e1006618.
20. Frebel, H., et al., *Programmed death 1 protects from fatal circulatory failure during systemic virus infection of mice.* J Exp Med, 2012. **209**(13): p. 2485-99.

21. Alfei, F., et al., *TOX reinforces the phenotype and longevity of exhausted T cells in chronic viral infection.* Nature, 2019. **571**(7764): p. 265-269.
22. Schietinger, A. and P.D. Greenberg, *Tolerance and exhaustion: defining mechanisms of T cell dysfunction.* Trends Immunol, 2014. **35**(2): p. 51-60.
23. Wherry, E.J., *T cell exhaustion.* Nature Immunology, 2011. **12**(6): p. 492-499.
24. Blank, C.U., et al., *Defining 'T cell exhaustion'.* Nature Reviews Immunology, 2019. **19**(11): p. 665-674.
25. Zander, R. and W. Cui, *Exhausted CD8+ T cells face a developmental fork in the road.* Trends in Immunology, 2023. **44**(4): p. 276-286.
26. Mann, T.H. and S.M. Kaech, *Tick-TOX, it's time for T cell exhaustion.* Nature Immunology, 2019. **20**(9): p. 1092-1094.
27. Pauken, K.E., et al., *Epigenetic stability of exhausted T cells limits durability of reinvigoration by PD-1 blockade.* Science, 2016. **354**(6316): p. 1160-1165.
28. Ghoneim, H.E., et al., *De Novo Epigenetic Programs Inhibit PD-1 Blockade-Mediated T Cell Rejuvenation.* Cell, 2017. **170**(1): p. 142-157.e19.
29. Deng, S., et al., *Targeting tumors with IL-21 reshapes the tumor microenvironment by proliferating PD-1intTim-3–CD8+ T cells.* JCI Insight, 2020. **5**(7).
30. Knuschke, T., et al., *A Combination of Anti-PD-L1 Treatment and Therapeutic Vaccination Facilitates Improved Retroviral Clearance via Reactivation of Highly Exhausted T Cells.* mBio, 2021. **12**(1).
31. National-Cancer-Institute. *malignant*. 14.05.2023]; Available from: https://www.cancer.gov/publications/dictionaries/cancer-terms/def/malignant.
32. National-Cancer-Institute. *tumor*. 02.07.2023]; Available from: https://www.cancer.gov/publications/dictionaries/cancer-terms/def/tumor.
33. Cooper, G.M., *The Cell: A Molecular Approach. 2nd edition*. 2000: Sinauer Associates 2000.
34. Hanahan, D. and R.A. Weinberg, *The hallmarks of cancer.* Cell, 2000. **100**(1): p. 57-70.
35. Hanahan, D. and R.A. Weinberg, *Hallmarks of cancer: the next generation.* Cell, 2011. **144**(5): p. 646-74.
36. Hanahan, D., *Hallmarks of Cancer: New Dimensions.* Cancer Discovery, 2022. **12**(1): p. 31-46.
37. Khazen, R., et al., *Melanoma cell lysosome secretory burst neutralizes the CTL-mediated cytotoxicity at the lytic synapse.* Nature Communications, 2016. **7**(1): p. 10823.
38. Siegel, R.L., K.D. Miller, and A. Jemal, *Cancer statistics, 2017.* CA: A Cancer Journal for Clinicians, 2017. **67**(1): p. 7-30.
39. National-Health-Service. *Melanoma skin cancer*. 19.09.2022]; Available from: https://www.nhs.uk/conditions/melanoma-skin-cancer/.
40. Siegel, R.L., K.D. Miller, H.E. Fuchs, and A. Jemal, *Cancer Statistics, 2021.* CA: A Cancer Journal for Clinicians, 2021. **71**(1): p. 7-33.
41. Wang, J., et al., *Exploring Tumor Immune Microenvironment and Its Associations With Molecular Characteristics in Melanoma.* Frontiers in Oncology, 2022. **12**.
42. Falcone, I., et al., *Tumor Microenvironment: Implications in Melanoma Resistance to Targeted Therapy and Immunotherapy.* Cancers (Basel), 2020. **12**(10).
43. Fridman, W.H., F. Pagès, C. Sautès-Fridman, and J. Galon, *The immune contexture in human tumours: impact on clinical outcome.* Nat Rev Cancer, 2012. **12**(4): p. 298-306.

44. de Visser, K.E. and J.A. Joyce, *The evolving tumor microenvironment: From cancer initiation to metastatic outgrowth.* Cancer Cell, 2023. **41**(3): p. 374-403.
45. Dermani, F.K., et al., *PD-1/PD-L1 immune checkpoint: Potential target for cancer therapy.* J Cell Physiol, 2019. **234**(2): p. 1313-1325.
46. Aegerter, H., et al., *Influenza-induced monocyte-derived alveolar macrophages confer prolonged antibacterial protection.* Nature Immunology, 2020. **21**(2): p. 145-157.
47. World-Health-Organization. *Influenza (Seasonal)*. 30.09.2022]; Available from: https://www.who.int/news-room/fact-sheets/detail/influenza-(seasonal).
48. Robert-Koch-Institut. *Influenza (Teil 1): Erkrankungen durch saisonale Influenzaviren/Infektionsweg*. 26.01.2023]; Available from: https://www.rki.de/DE/Content/Infekt/EpidBull/Merkblaetter/Ratgeber_Influenza_saisonal.html#doc2382022bodyText5.
49. Robert-Koch-Institut. *Influenza (Teil 1): Erkrankungen durch saisonale Influenzaviren*. 26.01.2023]; Available from: https://www.rki.de/DE/Content/Infekt/EpidBull/Merkblaetter/Ratgeber_Influenza_saisonal.html.
50. Sekiya, T., et al., *Selecting and Using the Appropriate Influenza Vaccine for Each Individual.* Viruses, 2021. **13**(6).
51. Modrow, S., *Molekulare Virologie*. 2010, Heidelberg: Spektrum Akad. Verl.
52. Samji, T., *Influenza A: understanding the viral life cycle.* Yale J Biol Med, 2009. **82**(4): p. 153-9.
53. AbuBakar, U., et al., *Avian Influenza Virus Tropism in Humans.* Viruses, 2023. **15**(4): p. 833.
54. Gu, Y., et al., *Role of the Innate Cytokine Storm Induced by the Influenza A Virus.* Viral Immunol, 2019. **32**(6): p. 244-251.
55. Palese, P., *Influenza: old and new threats.* Nat Med, 2004. **10**(12 Suppl): p. S82-7.
56. Boulo, S., H. Akarsu, R.W. Ruigrok, and F. Baudin, *Nuclear traffic of influenza virus proteins and ribonucleoprotein complexes.* Virus Res, 2007. **124**(1-2): p. 12-21.
57. Atkin-Smith, G.K., M. Duan, W. Chen, and I.K.H. Poon, *The induction and consequences of Influenza A virus-induced cell death.* Cell Death & Disease, 2018. **9**(10): p. 1002.
58. Damjanovic, D., et al., *Immunopathology in influenza virus infection: uncoupling the friend from foe.* Clin Immunol, 2012. **144**(1): p. 57-69.
59. Doherty, P.C., S.J. Turner, R.G. Webby, and P.G. Thomas, *Influenza and the challenge for immunology.* Nat Immunol, 2006. **7**(5): p. 449-55.
60. Teijaro, J.R., et al., *Endothelial cells are central orchestrators of cytokine amplification during influenza virus infection.* Cell, 2011. **146**(6): p. 980-91.
61. Tisoncik, J.R., et al., *Into the eye of the cytokine storm.* Microbiol Mol Biol Rev, 2012. **76**(1): p. 16-32.
62. Liu, Q., Y.H. Zhou, and Z.Q. Yang, *The cytokine storm of severe influenza and development of immunomodulatory therapy.* Cell Mol Immunol, 2016. **13**(1): p. 3-10.
63. Wang, J., et al., *Differentiated human alveolar type II cells secrete antiviral IL-29 (IFN-lambda 1) in response to influenza A infection.* J Immunol, 2009. **182**(3): p. 1296-304.
64. Xiao, H., et al., *The human interferon-induced MxA protein inhibits early stages of influenza A virus infection by retaining the incoming viral genome in the cytoplasm.* J Virol, 2013. **87**(23): p. 13053-8.

65. Kochs, G. and O. Haller, *Interferon-induced human MxA GTPase blocks nuclear import of Thogoto virus nucleocapsids.* Proc Natl Acad Sci U S A, 1999. **96**(5): p. 2082-6.
66. Grant, E.J., S.M. Quiñones-Parra, E.B. Clemens, and K. Kedzierska, *Human influenza viruses and CD8+ T cell responses.* Current Opinion in Virology, 2016. **16**: p. 132-142.
67. Kirby, A.C., M.C. Coles, and P.M. Kaye, *Alveolar macrophages transport pathogens to lung draining lymph nodes.* J Immunol, 2009. **183**(3): p. 1983-9.
68. Legge, K.L. and T.J. Braciale, *Accelerated migration of respiratory dendritic cells to the regional lymph nodes is limited to the early phase of pulmonary infection.* Immunity, 2003. **18**(2): p. 265-77.
69. Chen, X., et al., *Host Immune Response to Influenza A Virus Infection.* Front Immunol, 2018. **9**: p. 320.
70. Brincks, E.L., et al., *CD8 T cells utilize TRAIL to control influenza virus infection.* J Immunol, 2008. **181**(7): p. 4918-25.
71. Hufford, M.M., T.S. Kim, J. Sun, and T.J. Braciale, *Antiviral CD8+ T cell effector activities in situ are regulated by target cell type.* J Exp Med, 2011. **208**(1): p. 167-80.
72. Braciale, T.J., J. Sun, and T.S. Kim, *Regulating the adaptive immune response to respiratory virus infection.* Nature Reviews Immunology, 2012. **12**(4): p. 295-305.
73. Sridhar, S., et al., *Cellular immune correlates of protection against symptomatic pandemic influenza.* Nature Medicine, 2013. **19**(10): p. 1305-1312.
74. Brown, D.M., A.M. Dilzer, D.L. Meents, and S.L. Swain, *CD4 T cell-mediated protection from lethal influenza: perforin and antibody-mediated mechanisms give a one-two punch.* J Immunol, 2006. **177**(5): p. 2888-98.
75. Graham, M.B., V.L. Braciale, and T.J. Braciale, *Influenza virus-specific CD4+ T helper type 2 T lymphocytes do not promote recovery from experimental virus infection.* J Exp Med, 1994. **180**(4): p. 1273-82.
76. Spitaels, J., K. Roose, and X. Saelens, *Influenza and Memory T Cells: How to Awake the Force.* Vaccines, 2016. **4**(4): p. 33.
77. Snelgrove, R.J., A. Godlee, and T. Hussell, *Airway immune homeostasis and implications for influenza-induced inflammation.* Trends Immunol, 2011. **32**(7): p. 328-34.
78. Campbell, D.J. and M.A. Koch, *Phenotypical and functional specialization of FOXP3+ regulatory T cells.* Nat Rev Immunol, 2011. **11**(2): p. 119-30.
79. Myers, M.A., et al., *Dynamically linking influenza virus infection kinetics, lung injury, inflammation, and disease severity.* eLife, 2021. **10**: p. e68864.
80. Rangel-Moreno, J., et al., *B Cells Promote Resistance to Heterosubtypic Strains of Influenza via Multiple Mechanisms1.* The Journal of Immunology, 2008. **180**(1): p. 454-463.
81. Christensen, J.P., P.C. Doherty, K.C. Branum, and J.M. Riberdy, *Profound Protection against Respiratory Challenge with a Lethal H7N7 Influenza A Virus by Increasing the Magnitude of CD8⁺ T-Cell Memory.* Journal of Virology, 2000. **74**(24): p. 11690-11696.
82. David, P., et al., *Combination immunotherapy with anti-PD-L1 antibody and depletion of regulatory T cells during acute viral infections results in improved virus control but lethal immunopathology.* PLoS Pathog, 2020. **16**(3): p. e1008340.

83. Dittmer, U., et al., *Friend retrovirus studies reveal complex interactions between intrinsic, innate and adaptive immunity.* FEMS Microbiol Rev, 2019. **43**(5): p. 435-456.
84. abcam. *Introduction to flow cytometry*. 23.04.2023]; Available from: https://www.abcam.com/protocols/introduction-to-flow-cytometry.
85. World-Health-Organization. *Cancer*. 04.05.2023]; Available from: https://www.who.int/news-room/fact-sheets/detail/cancer.
86. Our-World-in-Data. *Cancer*. 02.10.2022]; Available from: https://ourworldindata.org/cancer#the-number-of-cancer-deaths-is-increasing-as-the-world-population-is-growing-and-aging.
87. Masemann, D., et al., *Oncolytic influenza virus infection restores immunocompetence of lung tumor-associated alveolar macrophages.* Oncoimmunology, 2018. **7**(5): p. e1423171.
88. Kohlhapp, F.J., et al., *Non-oncogenic Acute Viral Infections Disrupt Anti-cancer Responses and Lead to Accelerated Cancer-Specific Host Death.* Cell Rep, 2016. **17**(4): p. 957-965.
89. Chen, T., et al., *IL-21 arming potentiates the anti-tumor activity of an oncolytic vaccinia virus in monotherapy and combination therapy.* J Immunother Cancer, 2021. **9**(1).
90. Lugano, R., M. Ramachandran, and A. Dimberg, *Tumor angiogenesis: causes, consequences, challenges and opportunities.* Cell Mol Life Sci, 2020. **77**(9): p. 1745-1770.
91. Cabral-Pacheco, G.A., et al., *The Roles of Matrix Metalloproteinases and Their Inhibitors in Human Diseases.* Int J Mol Sci, 2020. **21**(24).
92. Shibuya, M., *Vascular Endothelial Growth Factor (VEGF) and Its Receptor (VEGFR) Signaling in Angiogenesis: A Crucial Target for Anti- and Pro-Angiogenic Therapies.* Genes Cancer, 2011. **2**(12): p. 1097-105.
93. Fenton, S.E., D. Saleiro, and L.C. Platanias, *Type I and II Interferons in the Anti-Tumor Immune Response.* Cancers, 2021. **13**(5): p. 1037.
94. Yu, R., B. Zhu, and D. Chen, *Type I interferon-mediated tumor immunity and its role in immunotherapy.* Cell Mol Life Sci, 2022. **79**(3): p. 191.
95. Basham, T.Y. and T.C. Merigan, *Recombinant interferon-gamma increases HLA-DR synthesis and expression.* J Immunol, 1983. **130**(4): p. 1492-4.
96. Benci, J.L., et al., *Tumor Interferon Signaling Regulates a Multigenic Resistance Program to Immune Checkpoint Blockade.* Cell, 2016. **167**(6): p. 1540-1554.e12.
97. Lazear, H.M., T.J. Nice, and M.S. Diamond, *Interferon-λ: Immune Functions at Barrier Surfaces and Beyond.* Immunity, 2015. **43**(1): p. 15-28.
98. Lasfar, A., et al., *IFN-λ cancer immunotherapy: new kid on the block.* Immunotherapy, 2016. **8**(8): p. 877-88.
99. Killip, M.J., E. Fodor, and R.E. Randall, *Influenza virus activation of the interferon system.* Virus Res, 2015. **209**: p. 11-22.
100. Hussell, T. and T.J. Bell, *Alveolar macrophages: plasticity in a tissue-specific context.* Nat Rev Immunol, 2014. **14**(2): p. 81-93.
101. Schultz-Cherry, S., *Role of NK cells in influenza infection.* Curr Top Microbiol Immunol, 2015. **386**: p. 109-20.
102. Singh, A., et al., *Role of lymphocytes, macrophages and immune receptors in suppression of tumor immunity.* Prog Mol Biol Transl Sci, 2023. **194**: p. 269-310.

103. Modak, M., et al., *Engagement of distinct epitopes on CD43 induces different co-stimulatory pathways in human T cells.* Immunology, 2016. **149**(3): p. 280-296.
104. McLane, L.M., M.S. Abdel-Hakeem, and E.J. Wherry, *CD8 T Cell Exhaustion During Chronic Viral Infection and Cancer.* Annu Rev Immunol, 2019. **37**: p. 457-495.
105. Alvarez Mde, L., et al., *Cross-talk between IFN-alpha and TGF-beta1 signaling pathways in preneoplastic rat liver.* Growth Factors, 2009. **27**(1): p. 1-11.
106. Guerin, M.V., et al., *TGFβ blocks IFNα/β release and tumor rejection in spontaneous mammary tumors.* Nature Communications, 2019. **10**(1): p. 4131.
107. Zarkoob, H., et al., *Modeling SARS-CoV-2 and influenza infections and antiviral treatments in human lung epithelial tissue equivalents.* Communications Biology, 2022. **5**(1): p. 810.
108. Wang, X., et al., *The role of CXCR3 and its ligands in cancer.* Front Oncol, 2022. **12**: p. 1022688.
109. Scharenberg, M., et al., *Influenza A Virus Infection Induces Hyperresponsiveness in Human Lung Tissue-Resident and Peripheral Blood NK Cells.* Front Immunol, 2019. **10**: p. 1116.
110. Carlin, L.E., et al., *Natural Killer Cell Recruitment to the Lung During Influenza A Virus Infection Is Dependent on CXCR3, CCR5, and Virus Exposure Dose.* Front Immunol, 2018. **9**: p. 781.
111. Lee, L.Y.-H., et al., *Memory T cells established by seasonal human influenza A infection cross-react with avian influenza A (H5N1) in healthy individuals.* The Journal of Clinical Investigation, 2008. **118**(10): p. 3478-3490.
112. Hayward, A.C., et al., *Natural T Cell–mediated Protection against Seasonal and Pandemic Influenza. Results of the Flu Watch Cohort Study.* American Journal of Respiratory and Critical Care Medicine, 2015. **191**(12): p. 1422-1431.
113. Schulman, J.L. and E.D. Kilbourne, *Induction of Partial Specific Heterotypic Immunity in Mice by a Single Infection with Influenza A Virus.* Journal of Bacteriology, 1965. **89**(1): p. 170-174.
114. Kim, T.S. and E.C. Shin, *The activation of bystander CD8(+) T cells and their roles in viral infection.* Exp Mol Med, 2019. **51**(12): p. 1-9.
115. Iheagwara, U.K., et al., *Influenza virus infection elicits protective antibodies and T cells specific for host cell antigens also expressed as tumor-associated antigens: a new view of cancer immunosurveillance.* Cancer Immunol Res, 2014. **2**(3): p. 263-73.
116. Ramahi, R.E. and A. Freifeld, *Epidemiology, Diagnosis, Treatment, and Prevention of Influenza Infection in Oncology Patients.* Journal of Oncology Practice, 2019. **15**(4): p. 177-184.
117. Newman, J.H., et al., *Intratumoral injection of the seasonal flu shot converts immunologically cold tumors to hot and serves as an immunotherapy for cancer.* Proc Natl Acad Sci U S A, 2020. **117**(2): p. 1119-1128.
118. Krummel, M.F., F. Bartumeus, and A. Gérard, *T cell migration, search strategies and mechanisms.* Nat Rev Immunol, 2016. **16**(3): p. 193-201.
119. Sitnik, S., et al., *PD-1 IC Inhibition Synergistically Improves Influenza A Virus-Mediated Oncolysis of Metastatic Pulmonary Melanoma.* Mol Ther Oncolytics, 2020. **17**: p. 190-204.
120. Krolikowski, F.J., et al., *Serum Sialic Acid Levels in Lung Cancer Patients.* Pharmacology, 2008. **14**(1): p. 47-51.

121. Kumari, M., et al., *Identification and characterization of non-small cell lung cancer associated sialoglycoproteins.* J Proteomics, 2021. **248**: p. 104336.
122. Paijens, S.T., A. Vledder, M. de Bruyn, and H.W. Nijman, *Tumor-infiltrating lymphocytes in the immunotherapy era.* Cellular & Molecular Immunology, 2021. **18**(4): p. 842-859.
123. Jacqueline, C. and O.J. Finn, *Antibodies specific for disease-associated antigens (DAA) expressed in non-malignant diseases reveal potential new tumor-associated antigens (TAA) for immunotherapy or immunoprevention.* Semin Immunol, 2020. **47**: p. 101394.
124. Jacqueline, C., et al., *LCVM infection generates tumor antigen-specific immunity and inhibits growth of nonviral tumors.* Oncoimmunology, 2022. **11**(1): p. 2029083.
125. Starbeck-Miller, G.R., H.-H. Xue, and J.T. Harty, *IL-12 and type I interferon prolong the division of activated CD8 T cells by maintaining high-affinity IL-2 signaling in vivo.* Journal of Experimental Medicine, 2013. **211**(1): p. 105-120.
126. Richer, Martin J., Jeffrey C. Nolz, and John T. Harty, *Pathogen-Specific Inflammatory Milieux Tune the Antigen Sensitivity of CD8+ T Cells by Enhancing T Cell Receptor Signaling.* Immunity, 2013. **38**(1): p. 140-152.
127. Richer, M.J., et al., *Inflammatory IL-15 is required for optimal memory T cell responses.* The Journal of Clinical Investigation, 2015. **125**(9): p. 3477-3490.
128. Fisher, P.B., A.F. Miranda, and L.E. Babiss, *[80] Measurement of the effect of interferons on cellular differentiation in murine and human melanoma cells*, in *Methods in Enzymology*. 1986, Academic Press. p. 611-618.
129. Zaidi, M.R. and G. Merlino, *The Two Faces of Interferon-γ in Cancer.* Clinical Cancer Research, 2011. **17**(19): p. 6118-6124.
130. Lu, C., et al., *Type I interferon suppresses tumor growth through activating the STAT3-granzyme B pathway in tumor-infiltrating cytotoxic T lymphocytes.* J Immunother Cancer, 2019. **7**(1): p. 157.
131. Sykulev, Y., et al., *Evidence that a single peptide-MHC complex on a target cell can elicit a cytolytic T cell response.* Immunity, 1996. **4**(6): p. 565-71.
132. Purbhoo, M.A., D.J. Irvine, J.B. Huppa, and M.M. Davis, *T cell killing does not require the formation of a stable mature immunological synapse.* Nat Immunol, 2004. **5**(5): p. 524-30.
133. Raskov, H., A. Orhan, J.P. Christensen, and I. Gögenur, *Cytotoxic CD8+ T cells in cancer and cancer immunotherapy.* British Journal of Cancer, 2021. **124**(2): p. 359-367.
134. Li, H., et al., *Dysfunctional CD8 T Cells Form a Proliferative, Dynamically Regulated Compartment within Human Melanoma.* Cell, 2019. **176**(4): p. 775-789.e18.
135. Athale, S., et al., *Influenza vaccines differentially regulate the interferon response in human dendritic cell subsets.* Sci Transl Med, 2017. **9**(382).
136. Lee, J., et al., *Molecular-level analysis of the serum antibody repertoire in young adults before and after seasonal influenza vaccination.* Nature Medicine, 2016. **22**(12): p. 1456-1464.
137. Isakova-Sivak, I., et al., *Influenza vaccine: progress in a vaccine that elicits a broad immune response.* Expert Rev Vaccines, 2021. **20**(9): p. 1097-1112.
138. Yu, J., X. Sun, J.Y.G. Goie, and Y. Zhang, *Regulation of Host Immune Responses against Influenza A Virus Infection by Mitogen-Activated Protein Kinases (MAPKs).* Microorganisms, 2020. **8**(7).

139. Nikolaev, E.V., A. Zloza, and E.D. Sontag, *Immunobiochemical Reconstruction of Influenza Lung Infection-Melanoma Skin Cancer Interactions.* Front Immunol, 2019. **10**: p. 4.
140. Gajofatto, A., M. Turatti, S. Monaco, and M.D. Benedetti, *Clinical efficacy, safety, and tolerability of fingolimod for the treatment of relapsing-remitting multiple sclerosis.* Drug Healthc Patient Saf, 2015. **7**: p. 157-67.
141. Velter, C., et al., *Melanoma during fingolimod treatment for multiple sclerosis.* European Journal of Cancer, 2019. **113**: p. 75-77.
142. Fadel, S.A., S.K. Bromley, B.D. Medoff, and A.D. Luster, *CXCR3-deficiency protects influenza-infected CCR5-deficient mice from mortality.* Eur J Immunol, 2008. **38**(12): p. 3376-87.
143. Gunderson, A.J., et al., *TGFβ suppresses CD8(+) T cell expression of CXCR3 and tumor trafficking.* Nat Commun, 2020. **11**(1): p. 1749.
144. Karin, N. and H. Razon, *Chemokines beyond chemo-attraction: CXCL10 and its significant role in cancer and autoimmunity.* Cytokine, 2018. **109**: p. 24-28.
145. Dangaj, D., et al., *Cooperation between Constitutive and Inducible Chemokines Enables T Cell Engraftment and Immune Attack in Solid Tumors.* Cancer Cell, 2019. **35**(6): p. 885-900.e10.
146. Dolina, J.S., N. Van Braeckel-Budimir, G.D. Thomas, and S. Salek-Ardakani, *CD8+ T Cell Exhaustion in Cancer.* Frontiers in Immunology, 2021. **12**.
147. Kawasaki, T., M. Ikegawa, and T. Kawai, *Antigen Presentation in the Lung.* Frontiers in Immunology, 2022. **13**.
148. Tate, M.D., et al., *Critical Role of Airway Macrophages in Modulating Disease Severity during Influenza Virus Infection of Mice.* Journal of Virology, 2010. **84**(15): p. 7569-7580.
149. Tumpey, T.M., et al., *Pathogenicity of Influenza Viruses with Genes from the 1918 Pandemic Virus: Functional Roles of Alveolar Macrophages and Neutrophils in Limiting Virus Replication and Mortality in Mice.* Journal of Virology, 2005. **79**(23): p. 14933-14944.
150. Wang, T., et al., *Influenza-trained mucosal-resident alveolar macrophages confer long-term antitumor immunity in the lungs.* Nature Immunology, 2023. **24**(3): p. 423-438.
151. Jahandideh, A., et al., *Macrophage's role in solid tumors: two edges of a sword.* Cancer Cell International, 2023. **23**(1): p. 150.
152. Wang, H., et al., *Targeting macrophage anti-tumor activity to suppress melanoma progression.* Oncotarget, 2017. **8**(11).
153. Waithman, J. and J.D. Mintern, *Dendritic cells and influenza A virus infection.* Virulence, 2012. **3**(7): p. 603-8.
154. Çuburu, N., et al., *Harnessing anti-cytomegalovirus immunity for local immunotherapy against solid tumors.* Proceedings of the National Academy of Sciences, 2022. **119**(26): p. e2116738119.
155. Girkin, J.L.N., S. Maltby, and N.W. Bartlett, *Toll-like receptor-agonist-based therapies for respiratory viral diseases: thinking outside the cell.* Eur Respir Rev, 2022. **31**(164).
156. Gibbert, K., et al., *Friend retrovirus drives cytotoxic effectors through Toll-like receptor 3.* Retrovirology, 2014. **11**(1): p. 126.
157. Browne, E.P., *Toll-like Receptor 7 Controls the Anti-Retroviral Germinal Center Response.* PLOS Pathogens, 2011. **7**(10): p. e1002293.
158. Koyama, S., et al., *Differential Role of TLR- and RLR-Signaling in the Immune Responses to Influenza A Virus Infection and Vaccination.* The Journal of Immunology, 2007. **179**(7): p. 4711-4720.

159. Sundararajan, S., A.M. Thida, S. Yadlapati, and S. Koya, *Metastatic Melanoma*, in *StatPearls*. 2022, Treasure Island (FL): StatPearls Publishing.
160. Liu, Y. and X. Cao, *Characteristics and Significance of the Pre-metastatic Niche.* Cancer Cell, 2016. **30**(5): p. 668-681.
161. Oliveira, G. and C.J. Wu, *Dynamics and specificities of T cells in cancer immunotherapy.* Nature Reviews Cancer, 2023. **23**(5): p. 295-316.
162. Sharma, P. and J.P. Allison, *The future of immune checkpoint therapy.* Science, 2015. **348**(6230): p. 56-61.
163. Aris, M. and M.M. Barrio, *Combining immunotherapy with oncogene-targeted therapy: a new road for melanoma treatment.* Front Immunol, 2015. **6**: p. 46.

6 Appendix

6.1 List of abbreviations

AEC	Alveolar epithelial cell
AF488	Alexa Fluor 488
ANOVA	Analysis of Variance
APC	Allophycocyanin
APC	Antigen presenting cell
BCR	B cell receptor
BSA	Bovine serum albumine
BV510	Brillian Violet 510
CCL	CC-chemokine ligand
CCR	C-C chemokine receptor type 5
CD	Cluster of differentiation
cDNA	Complementary DNA
CMV	cytomegalovirus
CTL	Cytotoxic T lymphocyte
CXCR	C-X-C motif chemokine receptor
CXCL	C-X-C motif chemokine ligand
DAMP	Danger-associated molecular patterns
DC	Dendritic cell
DMEM	Dulbecco's Modified Eagle Medium
DMSO	Dimethylsulfoxid
DNA	Deoxyribonucleic acid
DNase	Deoxyribonuclease
dNTP	Deoxynucleotide Triphosphate
EDTA	Ethylendiamintetraacetat
ELISA	Enzyme-linked Immunosorbent Assay
FACS	Fluorescent activated cell sorting
FasL	Fas ligand
FCS	Fetal calf serum
FITC	Fluoresceinisothiocyanat
F-MulV	Friend murine leukaemia virus

FoxP3	Forkhead box P3
FSC	Forward scatter
FV	Friend Virus
FVD	Fixable viability dye
GC	Germinal centre
HA	hemagglutinin
HBV	Hepatitis B virus
HCV	Hepatitis C virus
HIV	Human immunodeficiency virus
IAV	Influenza A virus
ICB	Immune checkpoint blockade
IFN	Interferon
IFNAR	IFN alpha receptor
IFNLR1	IFN lambda receptor 1
IgG	Immunoglobulin G
IL	Interleukin
IMDM	Iscove's Modified Dulbecco's Medium
i.n.	intranasal
i.p.	intraperitoneal
ISG	Interferon stimulated gene
i.t.	intratumoural
i.v.	intravenous
IVC	Individually ventilated cage
JAK-STAT	Janus kinase-signal transducer and activator of transcription
LANUV	*Landesamt für Natur-, Umwelt- und Verbraucherschutz*
LCMV	lymphocytic choriomeningitis virus
LDV	lactate dehydrogenase virus
LED	light-emitting diode
LLC	Lewis lung carcinoma
MACS	Magnetic cell separation
MALT	mucosa-associated lymphoid tissue
MDCK	Madin-Darby canine kidney
MHC	major histocompatibility complex

MML V-RT	Moloney Murine Leukemia reverse transcriptase
MMP9	Matrix metallopeptidase 9
NA	neuraminidase
NK-cell	Natural killer cell
NOD	nucleotide-binding oligomerization domain
NP	nucleoprotein
NSCLC	non-small cell lung cancer
PAMP	pathogen-associated molecular patterns
PB	Pacific Blue
PBS	Phosphate buffered saline
PCR	Polymerase chain reaction
PD-1	Programmed cell death protein 1
PD-L1	Programmed cell death 1 ligand 1
PE	Phycoerythrin
PE-Cy7	Phycoerythrin-Cyanine 7
PerCP	Peridinin-Chlorophyll-Protein Complex
PerCP-Cy5.5	PerCP-Cyanine5.5
PFA	Paraformaldehyde
PFU	Plaque forming units
PMA	Phorobol 12-myristate 13-acetate
PRR	pattern recognition receptors
pH	*potentia hydrogenii*
qPCR	Quantitative PCR
Rag	Recombination activating gene
RIG-I	retinoic acid-inducible gene I
RNA	Ribonucleic acid
RPMI	Roswell Park Memorial Institute
RPS9	Ribosomal Protein S9
RT	Reverse transcriptase
RT	Room temperature
S1PR	sphingosine-1-phosphate receptors
SA	Sialic acid
s.c.	subcutaneous
SFFU	spleen focus-forming units

SFFV	spleen focus forming virus
SPF	Specific pathogen free
SSC	Side scatter
TAA	Tumour-associated antigens
TCR	T cell receptor
TGF-β	Transforming growth factor-β
T_H	T-helper cell
TIL	Tumour infiltrating lymphocytes
TIM-3	T cell immunoglobulin mucin-3
TLR	Toll-like receptor
TME	Tumour microenvironment
TNF	Tumour necrosis factor
TOX	Thymocyte Selection Associated High Mobility Group Box
Treg	Regulatory T cell
UV	ultraviolet
VEGF	Vascular Endothelial Growth Factor

6.2 List of figures

6.3 List of tables

6.4 Acknowledgements/Danksagung

Die Danksagung ist in der Online-Version nicht enthalten.

6.5 Curriculum vitae

Der Lebenslauf ist in der Online-Version aus Gründen des Datenschutzes nicht enthalten.

Presentations at Scientific Meetings, Awards and Scholarships and peer-reviewed publications

Presentations at Scientific Meetings

2023	Poster presentation: “Influenza virus infections strengthens tumour specific CD8+ T-cell activation and facilitates tumour control via CXCR3-mediated migration.”, Conference of the International Union of Immunological Societies (IUIS), Cape Town, South Africa
2023	Poster presentation: “Respiratory but not systemic viral infection induces tumour growth inhibition through CD8+ T-cell activation.”, Annual meeting held by the German and French Immunology Societies DGfI and SFI, Strasbourg, France
2023	Poster presentation: “Influenza virus infection elicits $CD8^+$ T cell activation to perform tumour growth inhibition.”, Deutsches Konsortium für Translationale Krebsforschung (DKTK) Oncology Symposium, Essen
2022	Poster presentation: “Viral respiratory infection facilitates tumour control by strengthening $CD8^+$ T cell immunity”, Annual meeting held by the German and Austrian Immunology Societies DGfI and ÖGAI, Hannover
2022	Poster presentation: “Viral respiratory infection facilitates tumour control by strengthening $CD8^+$ T cell immunity”, 17th Spring School on Immunology, held by the DGfI, Ettal
2021	Oral online presentation: “Respiratory influenza virus infection strengthens cancer specific $CD8^+$ T cell immunity and impedes tumour growth”, 20th Day of Research, University Hospital Essen
2021	Oral online presentation: “Viral respiratory infection strengthens tumour-specific $CD8^+$ T cell immunity and suppresses tumour growth”, NDI3 online conference held by Research Center Borstel: Leibniz Lung Center
2020	Oral online presentation: “The impact of Thrombospondin-1 on CD47 regulated immune responses during influenza virus infection”, 19th Day of Research, University Hospital Essen

Awards and Scholarships

2023	Scientific Excellence Award by the RTG1949 for outstanding success during the PhD project
2022	Poster prize at the joint annual meeting held by the German and Austrian societies for immunology (DGfI and ÖGAI) in Hannover, Germany
2022	2nd prize for Poster Presentation at 17th Spring School on Immunology, held by the DGfI in Ettal, Germany
2021	Poster Prize at the 20th Day of Research, University Hospital Essen
2021	Best oral presentation award at the online conference on New Developments in Immunology, Inflammation and Infection (NDI3) by Research Center Borstel
2017 – 2018	Scholarship of the Deutschlandstipendium by the Federal Government
2015	RISE Worldwide fellowship of the German Academic Exchange Service (Deutscher Akademischer Austauschdienst, DAAD)

Peer-reviewed publications

Steinbach P, Pastille E, Kaumanns L, Adamczyk A, Sutter K, Hansen W, Dittmer U, Buer J, Westendorf AM, Knuschke T. Influenza virus infection enhances tumour-specific CD8+ T-cell immunity, facilitating tumour control. PLOS Pathogens, 2024 Jan 25; 20(1): e1011982.

Wenzek C, **Steinbach P**, Wirsdöfer F, Sutter K, Boehme JD, Geffers R, Klopfleisch R, Bruder D, Jendrossek V, Buer J, Westendorf AM, Knuschke T. CD47 restricts antiviral function of alveolar macrophages during influenza virus infection. iScience, 2022 Nov 11;25(12):105540.

Knuschke T, Kollenda S, Wenzek C, Zelinskyy G, **Steinbach P**, Dittmer U, Buer J, Epple M, Westendorf AM. A Combination of Anti-PD-L1 Treatment and Therapeutic Vaccination Facilitates Improved Retroviral Clearance via Reactivation of Highly Exhausted T Cells. mBio. 2021 Feb 2;12(1):e02121-20.

Killinger K, Böhm M, **Steinbach P**, Hagemann G, Blüggel M, Jänen K, Hohoff S, Bayer P, Herzog F, Westermann S. Auto-inhibition of Mif2/CENP-C ensures centromere-dependent kinetochore assembly in budding yeast. EMBO J. 2020 Jul 15;39(14):e102938.

Erklärung:

Hiermit erkläre ich, gem. § 7 Abs. (2) d) + f) der Promotionsordnung der Fakultät für Biologie zur Erlangung des Dr. rer. nat., dass ich die vorliegende Dissertation selbständig verfasst und mich keiner anderen als der angegebenen Hilfsmittel bedient, bei der Abfassung der Dissertation nur die angegeben Hilfsmittel benutzt und alle wörtlich oder inhaltlich übernommenen Stellen als solche gekennzeichnet habe.

Essen, den _____ _____
Philine Steinbach

Erklärung:

Hiermit erkläre ich, gem. § 7 Abs. (2) e) + g) der Promotionsordnung der Fakultät für Biologie zur Erlangung des Dr. rer. nat., dass ich keine anderen Promotionen bzw. Promotionsversuche in der Vergangenheit durchgeführt habe und dass diese Arbeit von keiner anderen Fakultät/Fachbereich abgelehnt worden ist.

Essen, den _____ _____
Philine Steinbach

Erklärung:

Hiermit erkläre ich, gem. § 6 Abs. (2) g) der Promotionsordnung der Fakultät für Biologie zur Erlangung der Dr. rer. nat., dass ich das Arbeitsgebiet, dem das Thema *„Analysis of the influence of influenza virus infection on tumour progression and $CD8^+$ T cell immunity“* zuzuordnen ist, in Forschung und Lehre vertrete und den Antrag von Philine Steinbach befürworte und die Betreuung auch im Falle eines Weggangs, wenn nicht wichtige Gründe dem entgegenstehen, weiterführen werde.

Essen, den _____ _____
Prof. Dr. Jan Buer

DOI: 10.17185/duepublico/81786
URN: urn:nbn:de:hbz:465-20240402-082627-2